Collisionally Activated Mass

Spectra of

Selected Negative Ions.

A thesis presented for the degree of

Doctor of Philosophy

by

Mark James Raftery BSc. (Hons.),

Department of Organic Chemistry,

University of Adelaide,

July 1988.

Contents

List of Figures

List of Tables

Abstract.

This thesis deals with the collisionally activated mass spectra of a number of classes of deprotonated organic compounds. Mechanisms are proposed to explain the major fragmentation processes and a set of rules given in the final chapter.

The enolate ion $MeOCO\bar{C}HCH_2CO_2Me$ fragments through the intermediacy of two complexes $[MeO\bar{C}O(CH_2=CHCO_2Me)]$ and $[MeO^-(O=C=CHCH_2CO_2Me)]$. The major fragmentation of these two ion complexes produce; $CH_2=C=C(OMe)O^-$ + HCO_2Me and $O=C=CHCH=C(OMe)O^-$ + $HOMe$. Similar ion complexes are formed from methyl substituted succinates, but their fragmentations are often different from those outlined above. In contrast, evidence is presented which indicates the ester enolate of dimethyl adipate eliminates MeOH *via* a gas phase Dieckmann reaction.

The enolates of a number of substituted cyclohexanones have also been studied. All show a characteristic retro reaction involving the specific loss of an alkene, except for the 3 substituted derivatives which show two competitive retro processes, the major of which involves the loss of the larger alkene. The major loss from the deprotonated cyclohexanones is the loss of H_2. There are two losses of H_2. These originate from the 3,4 and 3,6 positions: the former being the more pronounced. 3-Alkylcyclohexanone enolates also lose RH (R is the 3-alkyl substituent): there are two discrete mechanisms directly analogous to the losses of H_2. 3-Substituted cyclohexanone enolates undergo a unique reaction which involves two specific proton transfers. The 2-substituted cyclohexanone ions also undergo retro reactions and loss of H_2, but when the substituent$\geq$Et, characteristic elimination of an olefin (with proton transfer from the 1' position) occurs from the side chain.

The ion $PhCH_2O^-$ undergoes competitive losses of $H\cdot$, H_2, CH_2O and C_6H_6 upon collisional activation. The loss of H_2 occurs mainly to form $(C_6H_4)^-CHO$, and *ab initio* calculations suggest the reaction proceeds by a stepwise mechanism. Ion $Ph(CH_2)_3O^-$ undergoes many fragmentations including the losses of H_2O, CH_2O and H_2. The loss of H_2 occurs by both 1,2 and 1,3 eliminations. A number of minor fragmentations occur after partial interchange of phenyl hydrogens and hydrogens at position 2.

The deprotonation of unsubstituted and N-substituted amides occur on the nitrogen, whereas deprotonation of N,N-disubstituted amides occurs on the α carbon. It is proposed that fragmentations are of four types; i) loss of a radical to form a stabilized radical anion, ii) direct formation of a radical to form an anion complex which may then undergo competitive reactions, iii) initial proton transfer to form a new anion which fragments in turn through anion complexes and iv) reactions which involve skeletal rearrangement.

Deprotonation of simple primary and secondary amines followed by collision activation generally leads to the formation of simple ion complex; viz a major fragmentation of deprotonated ethylamine is $MeCH_2NH^- \longrightarrow [Me^-(CH_2NH)] \longrightarrow CH_2N^- + CH_4$. The secondary amines studied also fragment via solvated ion complex intermediates. The fragmentation of cyclic and aromatic amines were also studied. Cyclic amines may undergo retro reactions analogous to those observed for cyclohexanone enolates, whereas $PhNH^-$ undergoes specific loss of CNH to yield $C_5H_5^-$.

Statement

This thesis contains no material which has been accepted for the award of any other degree or diploma in any University and that to the best of my knowledge and belief, this thesis contains no material previously published or written by any other person, except where due reference is made in the text of this thesis. This thesis is also available for photocopying and loan from the library if it is accepted for the award of the degree.

Mark J. Raftery.

Acknowledgement

I would like to thank my supervisor Professor John Bowie for his help and encouragement during the period of this work. I would also like to thank Tom Blumenthal and Lee Paltridge for the operation and maintenance of the mass spectrometers in the department.

I would like to thank all the other members of the department for their friendship and also my family for their support over the years.

Chapter 1

Introduction.

1.1 Mass Spectrometry.

Over the past 30 years mass spectrometry has been used as a tool to investigate gas phase organic reactions[1] as well as being a very sensitive analytical technique[2] for determining trace amounts of compounds. One of the major reasons for its sensitivity is the small amount of compound required to obtain a characteristic spectrum.

A mass spectrometer is an instrument that produces ions by the interaction of a molecule with an electron beam in the gas phase (other methods of ionization are also used, see below). These ions are then accelerated in an electrostatic field to a predetermined energy (typically 7-8 kV). The first mass spectrometers[3,4] produced had only one sector, often a magnetic sector. The magnetic sector separates charged ions by deflecting their path by interaction with the magnetic field (B). The ions are forced into a circular flight path with a radius (r) *(equation 1.1)*.

$$r = \frac{mv}{eB} = \frac{J}{eB} \tag{1.1}$$

J=momentum

This equation shows that the radius is proportional to the momentum. It can also be shown that the ions with different mass (m) to charge (e) ratios will have different flight path radii (r) *(equation 1.2)*.

i.e.

$$r = \frac{1}{B} \cdot \sqrt{\frac{2mV}{e}} \tag{1.2}$$

1

Ions which have the same kinetic energy and mass are brought to a common focus after leaving the magnetic sector. These ions can then be analysed and a spectrum drawn. The addition of an electric sector[5] after the magnetic sector has the effect of improving the resolution of the m/e of the ions in the spectrum. The electric sector also focusses the ions according to their m/e ratio, by passing the ion between to two charged plates of opposite charge, with a total potential (E).

$$r = \frac{1}{2}mv^2 \cdot \frac{2}{eE} \qquad (1.3)$$

The radius of an ion of charge (e) in the electric field (E) is then proportional to its initial kinetic energy *(equation 1.3)*. The equation can be rearranged to exclude the mass (m) and the charge (e) terms, this means all ions of the same kinetic energy have the same radius of flightpath and are brought to a common focus *(equation 1.3)*. The electric sector is a kinetic energy analyser. The ions are then separated according to their mass to charge ratio in either the magnetic or electric sector, depending on the geometry of the instrument. The normal arrangement of the sectors is to have the electric sector first, followed by the magnetic sector. In reversed geometry instruments the magnetic sector precedes the electric sector. This latter arrangement has a number of advantages that will be discussed in detail later.

1.2 Types of Ionization Processes.

1.2.1 Electron Impact.

The most widely used ionization technique in mass spectrometry is electron impact, and both positive and negative ions can be formed by this method[6]. Approximately 90% of all organic molecules can be ionized by this technique. The sample is introduced into the instrument, vapourised, and bombarded with a beam of electrons. The energy of the electron beam is typically between 5 and 100 eV, but generally 70 eV is used. A molecule loses an electron by interaction with the electron beam and a positively charged species is formed *(equation 1.4)*.

$$M + e^- \longrightarrow M^{+\cdot} + 2e^- \qquad\qquad (1.4)$$

The minimum energy required to remove one electron from the highest occupied molecular orbital of a molecule is called the ionization potential[7]. A second or even a third electron can be removed but with decreasing probability due to the increasing energy required.

1.2.2 Field desorption.

In examples where there is no molecular ion formed by electron impact and where molecular weight information is required, another method must be found to ionize the molecule[8]. This may be done by use of field desorption as the ionization technique. The sample is coated onto the surface of the anode and placed in the ionization source. A large voltage (typically 10 kV) is applied and the molecule ionized in this manner. The ions formed by this technique have less energy than when formed by electron impact, and are therefore less likely to fragment. These type of spectra contain very large $M^{+\cdot}$ peaks and few daughter ions. This method is very useful in studying biological molecules where often no molecular ion is observed by electron impact.

1.2.3 Chemical Ionization.

This technique can also used when electron impact fails to give a molecular ion and will be discussed in detail later in the next chapter.

1.2.4 Fast atom bombardment.

Ionization by fast atoms is a relatively new ionization method which was first introduced in the late 1970's. It is primarily used for high molecular weight compounds which give no molecular ion by other ionization techniques. This technique will be discussed in detail later.

1.3   The VG ZAB 2HF Mass Spectrometer.

The ZAB is a double focussing reverse geometry magnetic sector type instrument; it incorporates both a magnetic sector and an electric sector in such a way that the combined sectors have the property of being both angular (or directional) focussing and energy (or velocity) focussing, and the order of analysis is magnetic sector first and electric sector second. This is the reverse of what is generally considered the conventional geometry and it enables the instrument to be used for MIKES[9] (Mass Analysed Ion Kinetic Energy Spectrometry). The ZAB is also equipped with a variable potential gas cell which allows collisionally induced decompositions to be observed (*Figure 1.1*[10]).

The geometry[11] of the ZAB is similar to that derived by originally by Hintenberger and König[11] in that it is angular and energy focussing not only to the first order but also to the second order without need to recourse to special field shaping technology. The aberrations which are due to second order effects of angular spread and energy spread and to the combined angular magnetic and electric fields are both homogeneous and the magnetic sector pole boundaries are straight and normal to the ion beam trajectory. The choice of sources that may be fitted include a combined electron impact and chemical ionization (EI/CI) source, and a fast atom bombardment (FAB) source. Each source may be operated at up to ± 8 kV for the production of positive or negative ions. In each source the ions are extracted from the source and focussed and centred onto the source slit by an immersion lens. This incorporates two half plates in which the mean and differential voltages can be separately adjusted from the control panel.

To obtain a MIKE spectrum, the ion of interest is selected by tuning to the right magnetic field strength *(cf. equation 1.2)* to "mass select" the ion of interest, the electric sector is then scanned[9,12]. Gas is introduced into the collision cell and the electric sector scanned again to obtain a collisionally activated MIKE spectrum. Collisionally activated peaks can be distinguished from the unimolecular peaks by applying a voltage to the collision cell in which case the collisionally induced daughter ions will be displaced within the MIKE spectrum[12].

Figure 1.1: *Schematic diagram of a VG ZAB 2HF Mass spectrometer*[10].

GAS CELL
Z-RESTRICTOR
(VARIABLE)

TOTAL ION
MONITOR'1

CURVATURE &
ROTATION PLATES

α-SLIT

ALIGNMENT &
FOCUS PLATES

SOURCE SLIT(VARIABLE)

ION EXIT(VARIABLE)

EI-CI ION SOURCE

ION REPELLER

MAGNETIC
ANALYSER

B-SLIT
(VARIABLE)

TOTAL ION
MONITOR'2

ELECTRON
MULTIPLIER'1

GAS CELL

α-SLIT'2

ELECTROSTATIC
ANALYSER

CURVATURE
PLATES

Z-RESTRICTOR
(VARIABLE)

BEAM
DEFLECTOR

ALIGNMENT &
FOCUS PLATES

COLLIMATION
SLITS(VARIABLE)

ALIGNMENT
PLATES

COLLECTOR
SLIT(VARIABLE)

Z-RESTRICTOR
(VARIABLE)

BEAM
DEFLECTOR

FARADAY
CUP

ELECTRON
MULTIPLIER'2

ION OPTICS
VG MICROMASS
ZAB-2F

1.4 Introduction to Isotope Effects.

Isotope effects have been used to determine the mechanism of both solution and gas phase[13] reactions. Isotope effects are caused by the substitution of (for example) a hydrogen atom for one of its isotopes (e.g. deuterium or tritium). The largest isotope effects observed, are seen when the substituted atom is involved in the bond making or breaking step of the chemical reaction [these are termed primary isotope effects]. Smaller isotope effects are observed when the substituted atom is next to the bond making or breaking site [these are called secondary isotope effects[14]].

Isotope effects can be divided into two types; i) equilibrium isotope effects, which occur when the reaction is under thermodynamic control (i.e. K_1/K_2, the ratio of equilibrium constants), ii) kinetic isotope effects, these occur when there is a change in the rate of a reaction due to the isotopic substitution of an atom by an isotope. Kinetic isotope effects are expressed in terms of the isotopic rate constants of the reaction (i.e. k_H/k_D). Isotope effects can be observed whenever an atom is substituted by an isotope; e.g. H/D, $^{12}C/^{13}C$, $^{16}O/^{18}O$, and others[15].

1.4.1 Kinetic Isotope Effects.

Kinetic isotope effects are expressed by the following equation,

$$k_H/k_D = MMI \times EXE \times TUN \times \exp^{\frac{(\Delta\varepsilon_o^r - \Delta\varepsilon_o^\ddagger)}{2kT}} \qquad (1.4)$$

Where;

MMI- masses and moment of inertia contribution to the translational and rotational partition functions,

EXE- vibrational partition function which takes account of the thermal excitation of low frequency vibrations,

TUN- tunnelling quantum mechanical correction to the reaction coordinate.

$\Delta\varepsilon_o^r$ and $\Delta\varepsilon_o^\ddagger$ are the zero point energy differences of the reactant and transition state. The contribution of MMI and EXE partition function terms is generally small, however the TUN term can be large. The Born Oppenheimer

6

approximation[16] states that the potential energy surface for a reaction is not a function of isotopic substitution (i.e. the quantum mechanics of molecules can be separated into electronic motion with a fixed nuclei).

Zero Point Energy.

Isotope effects are caused by the difference in the zero point energy (ZPE) of different isotopically substituted compounds.

$$\varepsilon_o = \frac{1}{2}h\nu_o \tag{1.5}$$

$$\nu_o = \frac{1}{2\pi}\sqrt{\frac{f}{m^*}} \tag{1.6}$$

where f = the force constant and m* is the effective mass.

$$\varepsilon_o = \frac{h}{4\pi}\sqrt{\frac{f}{m^*}} \tag{1.7}$$

Equation 1.7 shows that the ZPE is related to the force constant (which is a measure of the stiffness of a chemical bond) and the effective mass.

For small displacements Δr from the equilibrium bond distance, the PE curve approximates a parabolic curve *(see Figure 1.2)*.

$$\Delta V = V - V_o = \frac{1}{2}f\Delta r^2 \tag{1.8}$$

where

$$f = (\frac{\partial^2 V}{\partial r^2})_{ro} \tag{1.9}$$

The changes in the ZPE upon isotopic substitution are due to: *i*) the PE and the force constant which are unaffected by isotopic substitution (*cf.* the Born Oppenheimer approximation[16]), *ii*) the effective mass. This implies that the changes

7
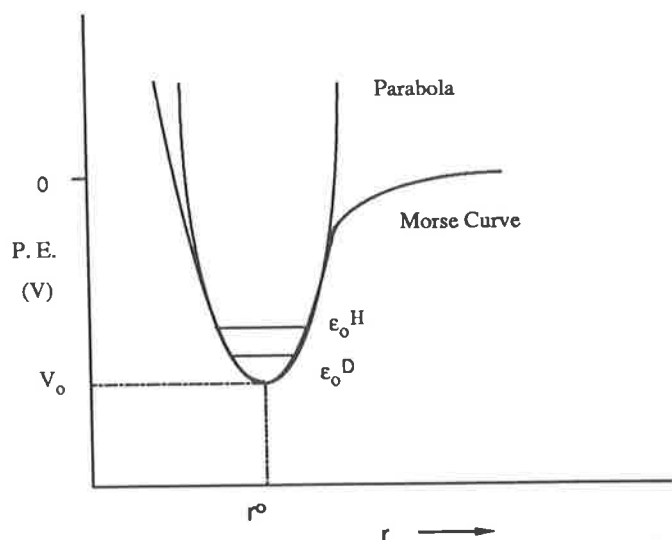
Figure 1.2: *Potential Energy vs r plot for a Diatomic system A–H (D).*

in ZPE after isotopic substitution are due to only a change in the effective mass. For a diatomic system (A—H) where $m_A \gg m_H$

$$m^* = \frac{m_A m_H}{m_A + m_H} \qquad (1.10)$$

i.e.

$$\frac{1}{u} = \frac{1}{m_A} + \frac{1}{m_H} \qquad (1.11)$$

The effective mass m^* equals the reduced mass u when $m_A \gg m_H$. The reduced mass approximately equals the mass of hydrogen (m_H), or the mass of deuterium when deuterium is substituted (m_D). Substituting in *equation 1.7*;

$$\Delta \varepsilon_o(H, D) = (\frac{f^{\frac{1}{2}} h}{4\pi})(1 - \frac{1}{\sqrt{2}}) \qquad (1.12)$$

From *equation 1.12* it can be seen that the $ZPE \propto f^{\frac{1}{2}}$. The isotope effect is a function of the difference between the ZPE of the reactant and the transition state.

$$\Delta \varepsilon^{\ddagger} - \Delta \varepsilon_r \simeq \frac{h}{4\pi}(f^{\ddagger \frac{1}{2}} - f_r^{\frac{1}{2}})(1 - 2^{\frac{1}{2}}) \qquad (1.13)$$

8
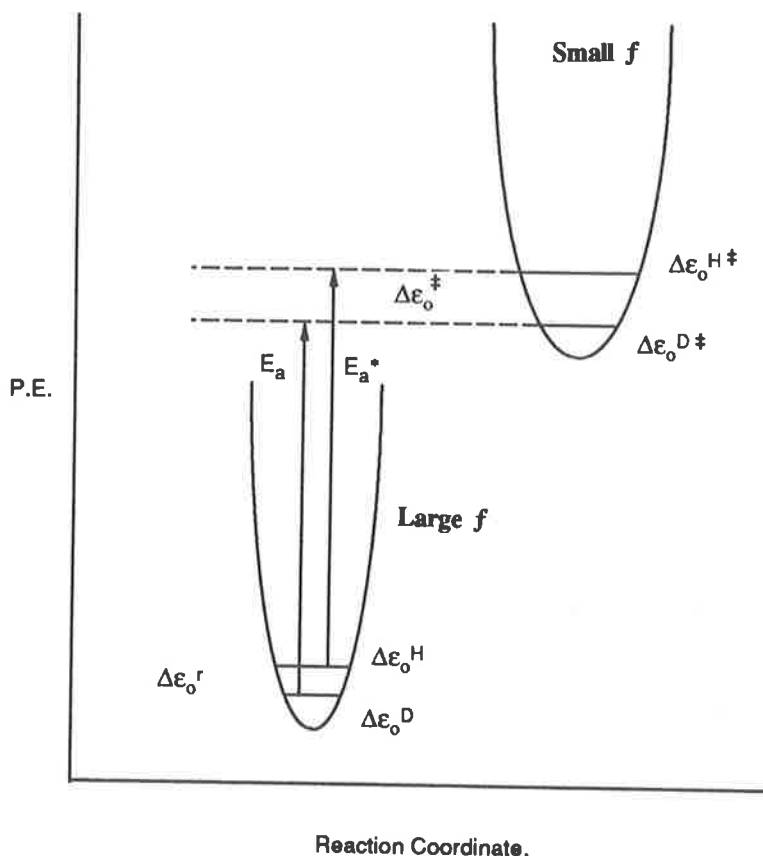
Figure 1.3: *PE plot for Reactant and Transition state.*

The force constants determine the difference in ZPE between A—H and A—D *(equation 1.13, Figure 1.3)*. The difference in force constants between *i*) reactant and transition state determine primary and secondary isotope effects, *ii*) reactant and product determine equilibrium isotope effects.

Rotational and Vibrational Partition Functions.

The following equations *(equations 1.14–1.16)* describe the contributions the isotope effects from the MMI and EXE terms. In general these only contribute a small amount to the overall isotope effect.

$$MMI = (\frac{m_H}{m_D})^{\frac{3}{2}}(\frac{I_H}{I_D})^{\frac{3}{2}} \tag{1.14}$$

$$MMI \times \prod_{3n-6} \frac{\nu_D}{\nu_H} = (\frac{m_H}{m_D})^{\frac{3}{2}} \tag{1.15}$$

9

$$EXE = \prod_{3n-6} \frac{(1 - e^{\frac{-u_H}{kT}})}{(1 - \exp^{\frac{-u_D}{kT}})} \qquad (1.16)$$

The above explanation of kinetic isotope effects is a summary of classical isotope effect theory when the species which undergo reaction have a Maxwell Boltzmann distribution[17] (i.e. in most condensed phase reactions). In gas phase reactions Maxwell Boltzmann conditions are not always achieved. Thus the simple classical isotope theory does not always predict the correct isotope effect value in the gas phase. This has been discussed in a recent review by Derrick[18], and in the particular case of the McLafferty rearrangement[19]. Nevertheless, the basic concepts of the classical isotope effect theory still pertain in gas phase ion chemistry, and these concepts are used in a qualitative fashion throughout this thesis.

Chapter 2

Negative Ion Mass Spectrometry.

2.1 Introduction.

Negative ion mass spectrometry has in the past been used little compared to positive ion mass spectrometry, in both analytical and mechanistic studies. This was due to: *i)* an early report that many organic molecules gave poor ion yields on electron impact[20] and *ii)* the lack of suitable instruments in the 1960's and 1970's available for the production and detection[10] of negative ions. The introduction of negative ion chemical ionization[21,22] and negative ion fast atom bombardment[23] as means of producing negative ions has been a major reason for the resurgence of interest in negative ions in the 1980's. In addition, the availability of commercial mass spectrometers which are able to operate in the negative ion mode has also contributed to recent advances in negative ion chemistry.

2.2 Early Studies.

Almost all the early work on negative ions was done by the use of electrons to form the negative ion[20,24]. The energy of the electron determines the type of ionization process. For example,

i) Resonance capture, $AB + e^- \longrightarrow AB^{-\cdot}$
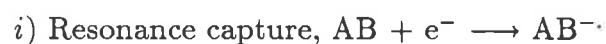
ii) Dissociative resonance capture,

$AB + e^- \longrightarrow A^- + B^\cdot$

or

$AB + e^- \longrightarrow A^\cdot + B^-$
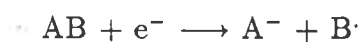
iii) Ion pair formation,

$$AB + e^- \longrightarrow A^- + B^+ + e^-$$

or

$$AB + e^- \longrightarrow A^+ + B^- + e^-$$

Process *i*) occurs with an electron energy close to 0 eV, process *ii*) occurs in the range 0 to 15 eV, and *iii*) occurs above 1 eV. When using electron energies of around 70 eV, ions formed from several different processes may be observed, in addition, the molecular anion can be formed by secondary electron capture. Secondary (or thermal) electrons are produced by the ionization process which forms the molecular cation, or alternatively from electrode surfaces[20,24].

Molecular anions are not detected for most aliphatic compounds due to the low electron affinity of such compounds (the electron affinity of a compound is defined as the amount of energy given out when an atom or molecule gains an electron). Aromatic compounds with their extended π systems, and other compounds with at least one electron withdrawing group (e.g. NO_2, CN etc.) often produce molecular anions formed by secondary (or thermal) electron capture[25,26,27]. Molecular anions may also show unimolecular or collisionally induced fragmentations which can be used to aid structure determination. An example of a unimolecular spectrum is shown in *Figure 2.1*. It is the ion kinetic energy spectrum of phenyl (4-nitrophenyl) acetate[28], the major fragmentations are shown in *Figure 2.1*.

Due to the low internal energy of the molecular anion formed by this process, fragmentation is often minimal. Fragmentation may be achieved if the molecular ion is collisionally activated by the use of a collision gas such as helium or argon in a field free region of the mass spectrometer. The CA mass spectrum of 4-nitroacetanilide is given in *Figure 2.2*[29], the major fragmentations are: *A*) loss of NO$\cdot$ and *B*) loss of $MeCO\overset{\bullet}{}$.

Compounds most likely to give a molecular anion under secondary (or thermal) electron capture conditions, are compounds which contain fluorine[30], some dicarboxylic acids[31] and some sulphur compounds[32,33]. The nitrophenyl group has been extensively studied, and it is a reasonable electron acceptor. This is due to; *i*) the electron withdrawing capability of the nitro group and *ii*) the low energy
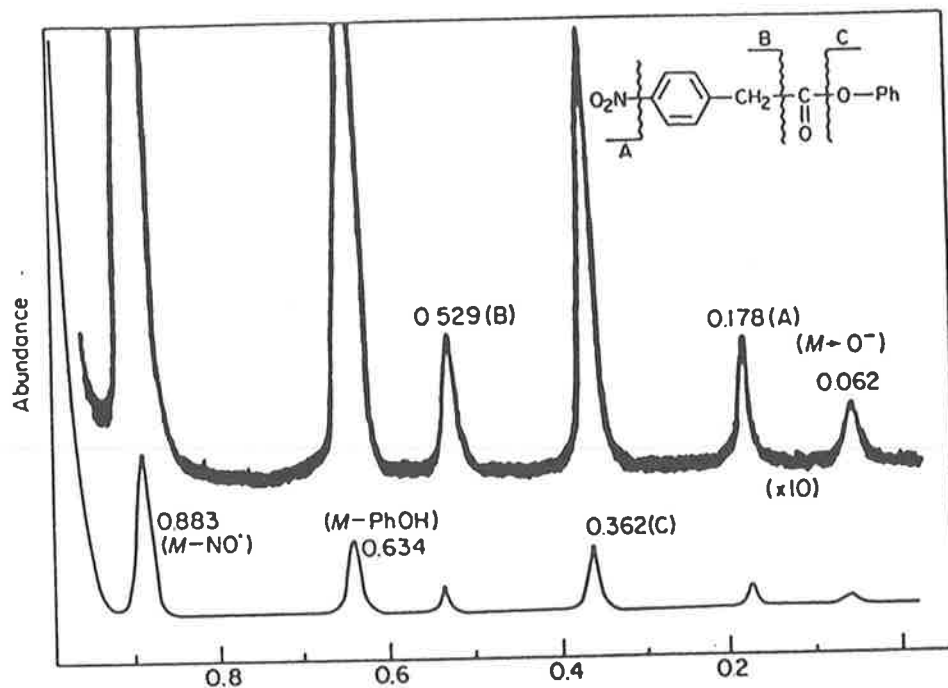
Figure 2.1: *Negative Ion Mass Spectrum of Phenyl (4-nitrophenyl) acetate. Reverse sector Hitachi Perkin Elmer RMU 7D instrument*[28].
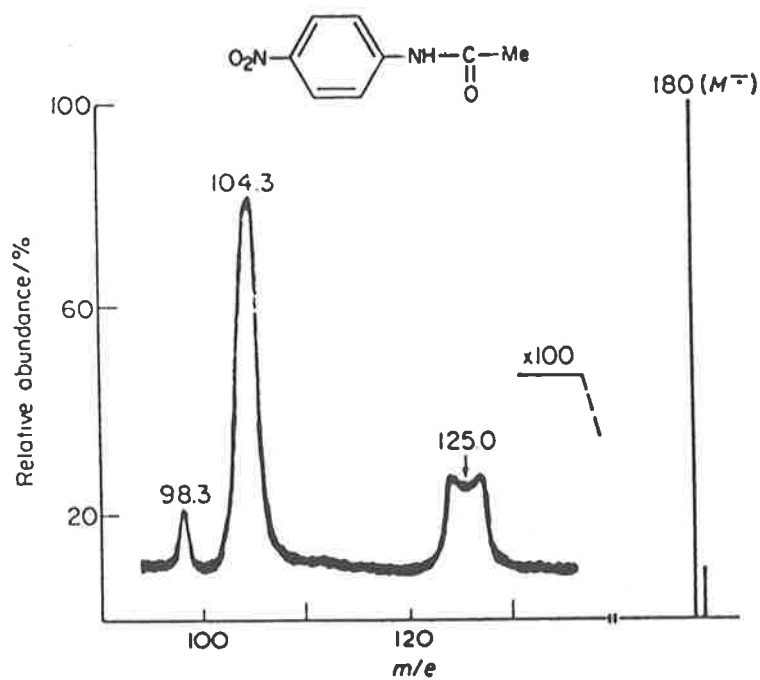
Figure 2.2: *CA Mass Spectrum of 4-nitroacetanilide. Sample pressure 1×10^{-5} Torr, electron energy 70 eV, accelerating voltage 3.6 kV. Reverse sector Hitachi Perkin Elmer RMU 7D instrument. Collision gas (helium) in second field free region, pressure 1×10^{-6} Torr*[29]

vacant π molecular orbital which can accept the electron. For example, nitrobenzene will produce molecular radical anions with the electron beam at less than 1 eV by electron capture[27], or at 70 eV by secondary electron capture. The major fragmentations of the molecular ions of many aromatic nitro compounds are the formation of NO_2^- and $[M^- \cdot - NO\cdot]^-$ ions. The latter process involves rearrangement to the nitrite ester which may eliminate $NO\cdot$ to form the phenoxide anion[34,35]. 2-Substituted benzenes show a number of ortho rearrangement reactions. An example of this process can be seen in the mass spectrum of 2-nitroacetanilide[35]. The $[M^- \cdot - NO\cdot]^-$ ion from this compound eliminates ketene. The hydrogens on the methyl group are statistically scrambled with the nitrogen hydrogen, as shown by deuterium labelling. It is suggested that hydrogen transfer occurs to a nitro oxygen, followed by hydrogen equilibration through a four centre intermediate, then loss of ketene[35] *(Scheme 2.1)*.

Scheme 2.1
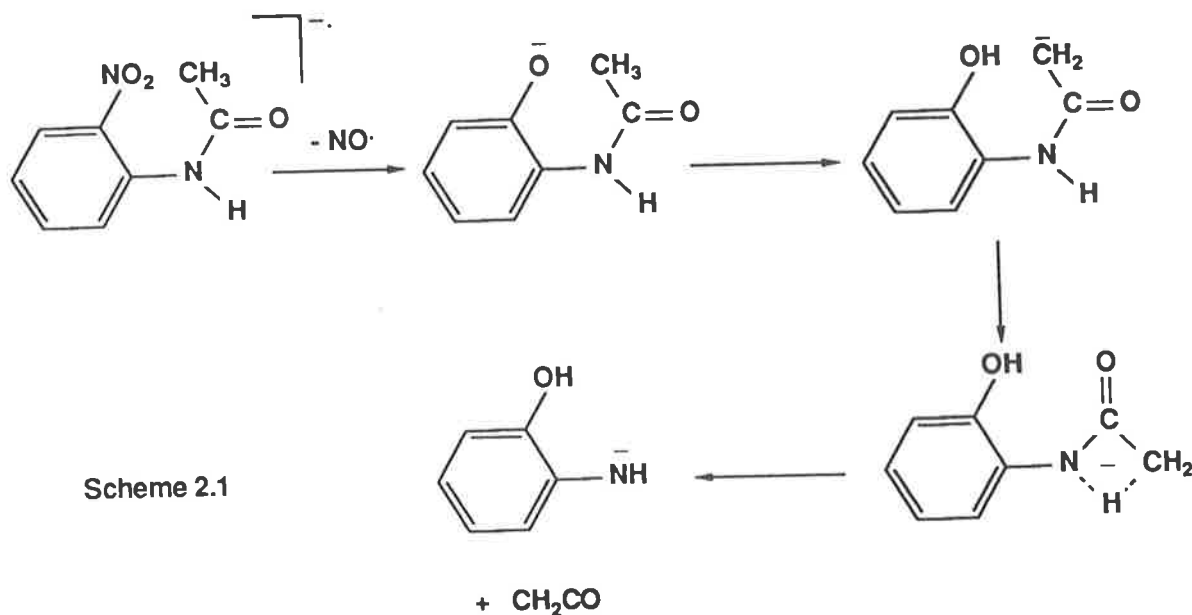
The negative ion mass spectra of many aliphatic carboxylic acids formed by electron impact have been studied and contain large $[M^- \cdot - H\cdot]^-$ peaks; this is generally the base peak of the spectrum[31,36,37]. A number of other peaks are also present in the 70 eV spectra but the molecular anion is generally very small or absent. Some of the other peaks that are observed are due to the elimination of H_2O and HCO_2^-. Rearrangement reactions are also observed for 2-substituted benzoic acids; these are similar to those of the nitro compounds already cited. The
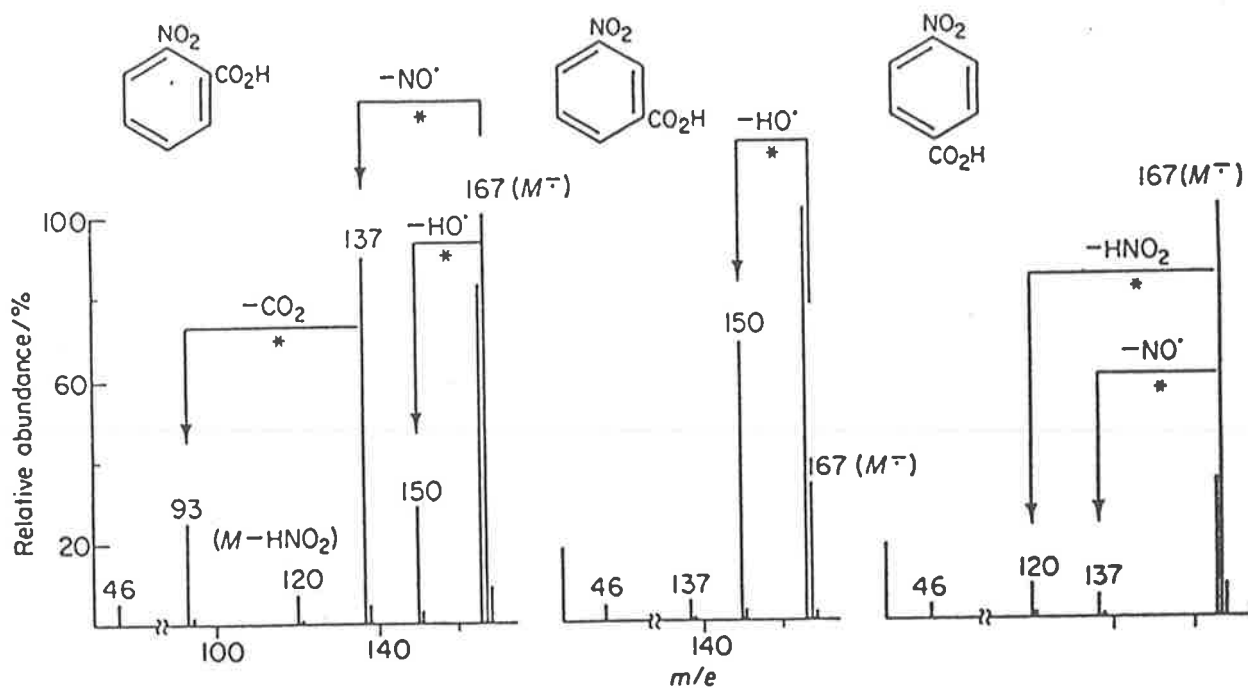
Figure 2.3: *Negative Ion Mass Spectra of 2-, 3- and 4- Nitrobenzoic Acids, Reverse sector Hitachi Perkin Elmer RMU 7D instrument*[37].

spectra of 2, 3, and 4 substituted nitrobenzoic acids are shown in *Figure 2.3*[37]. These spectra were measured under the same conditions; i.e. at 70 eV and at a measured source pressure of 1×10^{-6} Torr. All show large $M^{-\cdot}$ and $[\, M^{-\cdot} - H\cdot \,]^-$ peaks and characteristic fragmentations. The molecular anion of the 2-substituted derivative loses NO· and then CO_2 *(Figure 2.3)*. The 3-nitrobenzoic acid analogue loses OH· and 4-nitrobenzoic acid loses HNO_2 by a two step process.

As a general rule, fragmentation of a molecular anion may occur by two different paths; *i*) simple cleavage which often occurs α to the negative charge or α to an atom which is in conjugation to the charge, *ii*) by a process involving rearrangement of a hydrogen or another group within the molecule. If a rearrangement process can occur, the resulting product peak is generally more abundant than that arising by direct cleavage. This is due to the low internal energy of the parent ion, and the relatively low energy required for a rearrangement reaction to occur.

2.3   Other Ionization Techniques.

2.3.1   Negative Ion Chemical Ionization [NICI].

This is a technique where a reagent gas interacts with the electron beam to form a negative ion which in turn can react with a neutral molecule to form an ionized species[22]. A typical example is the formation of OH^- by the processes outlined in *equations 2.1* and *2.2*[38] below.

$$H_2O + e^- \longrightarrow H^- + OH \cdot \qquad (2.1)$$

$$H^- + H_2O \longrightarrow H_2 + OH^- \qquad (2.2)$$
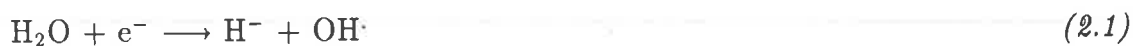
When hydroxide ion is formed in the gas phase it is a particularly strong base ($\triangle H_{acidH_2O}=391$ kcal.mol^{-1})[39] which can deprotonate acidic hydrogens that may be present in an organic molecule. For example, if the molecule to be studied is a ketone, the most acidic proton is adjacent to the carbonyl functionality. Deprotonation forms an enolate anion. Enolate anions formed by deprotonation of ketones, esters, ketoesters etc. can be represented by <u>A</u> in *Scheme 2.2*. The enolate fragmentations considered throughout this thesis are drawn as proceeding through the carbanion form, purely for convenience of representation.

Such anions are formed by thermal ion molecule reactions, and undergo little fragmentation. Collisional activation is generally required in order to effect fragmentation[40].

Scheme 2.2

16
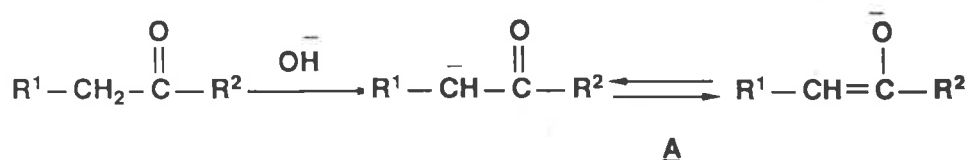
Hydroxide ion can also be formed in the gas phase by the interaction of methane and nitrous oxide[41] (or any other hydrocarbon such as isobutane and cyclohexane) in the source (see *equations 2.3* and *2.4* below).

$$N_2O + e^- \longrightarrow O^{-\cdot} + N_2 \qquad\qquad (2.3)$$

$$O^{-\cdot} + CH_4 \longrightarrow OH^- + CH_3^{\cdot} \qquad\qquad (2.4)$$

In this technique, OH^- is produced either from CH_4/N_2O at 1 eV or H_2O at 5 eV; this reagent then reacts with the molecule of interest to produce a $[M - H^+]^-$ species. The mass spectrometer must have a chemical ionization source (see earlier) where the reagent gas and the molecule to be studied are injected. The typical pressure in this source is between 10^{-3} and 1 torr, and since the ion is formed by thermal ion molecule reactions the internal energy of the $[M - H^+]^-$ ion is low. Consequently if there are fragmentations, the resultant peaks will be of low abundance. To overcome this problem, collisionally induced spectra can be obtained (see earlier). If a reversed geometry instrument is used, the ion of interest (for example, the $[M-H^+]^-$ parent ion) can be selected using the magnetic sector. The electric sector is scanned thus producing the CA MIKE[9,12] spectrum. Use of hydroxide ion NICI has been reported for a number of organic molecules; these include for example, alcohols[38,42,43], ketones[44,45], and carboxylic acids[46]. Other bases may be used in cases where OH^- is not sufficiently strong to remove a proton. Some examples would be aldehydes which contain no α hydrogens, and aliphatic amines. In these cases, NH_2^- is the reagent ion of choice; it is formed from ammonia in the chemical ionization source of the instrument[47].

Hydroxide ion negative ion chemical ionization has been used for analytical purposes; many different types of compound have been studied, some recent examples include; andosine diols[48], pyrrolizidine alkaloids[49] *(Figure 2.4)* and penicillins[49]. The spectra can give molecular weight information, and collisional activation may produce a characteristic mass spectrum of the daughter ions. As an example, the

17
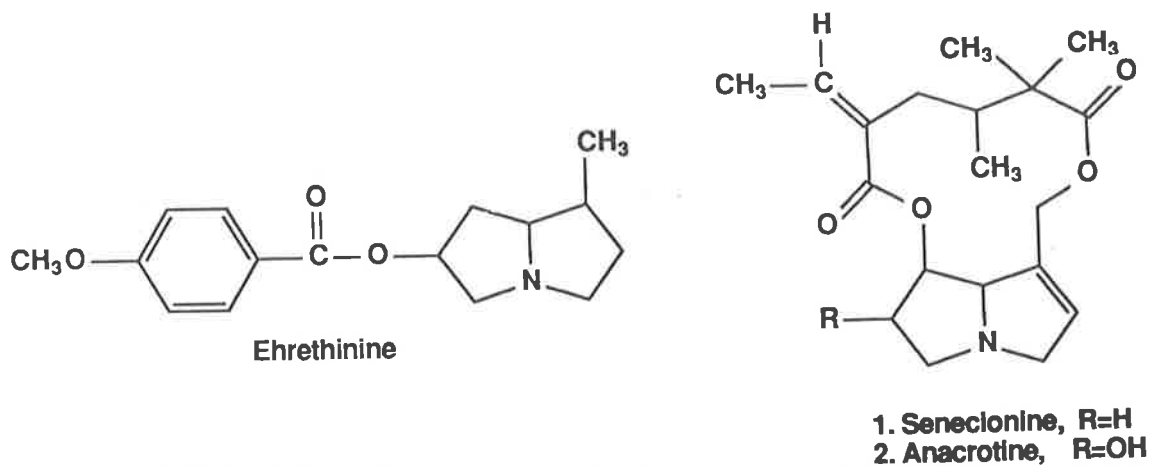
Figure 2.4: *Examples of some Pyrrolizidine Alkaloids*[49].

$OH^-/NICI$ mass spectrum of pyrrolizidine alkaloids (*e.g. Senecione, Figure 2.5*) have been studied. These macrocyclic diesters and noncyclic monoesters gave abundant $[M - H^+]^-$ ions which show a number of characteristic fragmentations. The characteristic ion from senecionine occurs at m/e 154 (*Figure 2.5*).

The technique of $OH^-/NICI$ has also been used for a limited number of mechanistic studies by Hunt[44,45]. He investigated a number of different compounds, including esters, ketones and nitrophenols. Formation of $[M - H^+]^-$ was favourable. The gas phase Dieckmann condensation of dimethyl suberate and dimethyl adipate have been studied by Hunt[44] and Cooks[50] respectively. $[M - H^+]^-$ and ([M $- H^+]^- -$ MeOH) ions were observed, and it was proposed that the latter was a cyclic β-ketoester formed by a gas phase Dieckmann reaction. Deprotonation of the diester is followed by an intramolecular displacement of methoxide which then abstracts a proton from the neutral β-ketoester *(see Chapter 3)*.

During the late 1970's negative ion chemical ionization was used mainly in analytical studies. The types of compounds studied range from polyhalogenated hydrocarbons[51] (*Figure 2.6*) to flurazepam[52,53] (*Figure 2.7*) in human plasma, at concentrations as low as 12 pg/ml. Methane/NICI is a very sensitive technique for the determination of polyhalogenated aromatic compounds. The information obtained is generally only the molecular weight (by formation and detection of the M^- anion), fragmentations of the parent anion are seldom observed.
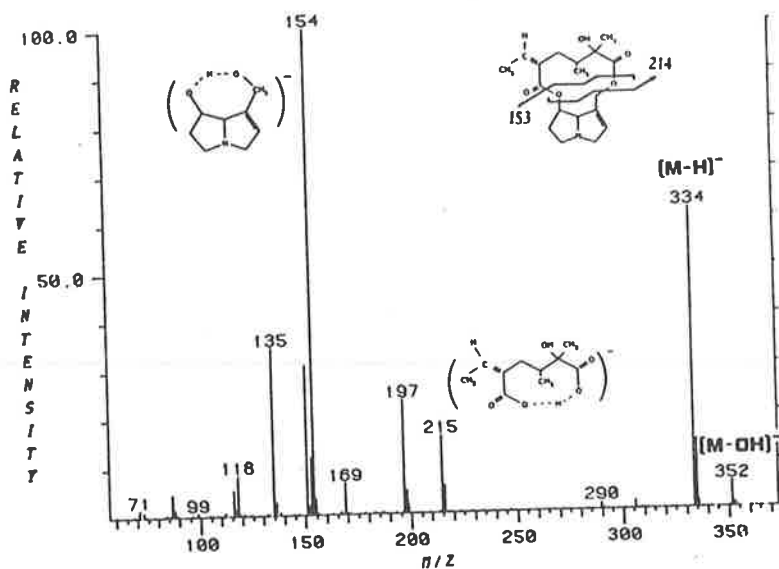
Figure 2.5: *OH⁻ Negative Ion Chemical Ionization Mass Spectrum of Senecionine*[49].

The types of compound required to produce the $M^{-\cdot}$ anion are compounds with a high electron affinity, which generally means the presence of electron withdrawing atoms or groups such as oxygen, fluorine and chlorine etc. Polychlorodiphenyls, naphthalenes and specifically dibenzofurans and dibenzodioxins[54], which are very toxic even at low concentrations, have been found in fish from various lakes and rivers in the USA. These compounds have also been detected in turtles and in grey seals in Sweden. Aflatoxin B_1 found in peanut oil and corn and aflatoxin M_1[55] found in milk have also been detected at levels as low as 10 p.p.b.

Dibenzofurans   **Dibenzodioxins**
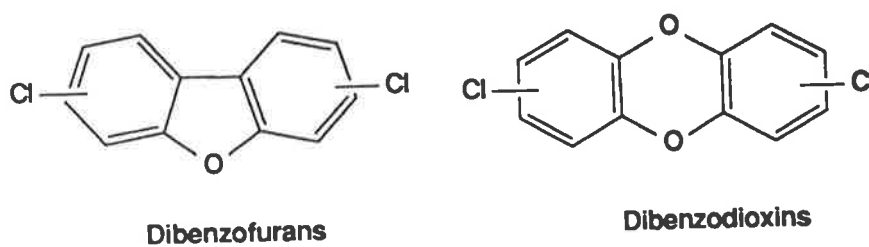
Figure 2.6: *Polychlorodiphenyls*[51].

N(Et)$_2$

CH$_2$

CH$_2$

N

O

Cl

N

F
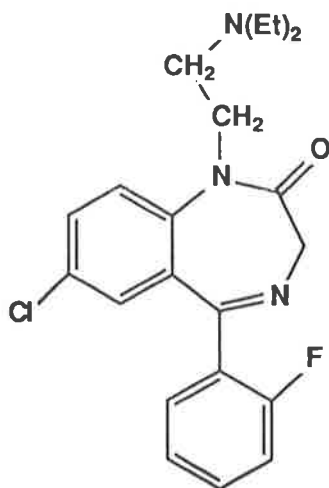
Figure 2.7: *Flurazepam*[52,53].

2.3.2 Negative Ion FAB Mass Spectrometry.

Fast atom bombardment spectrometry[23,56,57,58] is a relatively new ionization technique and is most appropriate in the study of non volatile compounds of high molecular weight, or thermally labile and also polar compounds including salts. The compound of interest is placed on the end of a metal probe and placed in the source of a mass spectrometer. A beam of fast atoms *(equation 2.5)* produced by the exchange of electrons between fast ions and slow atoms (usually argon or xenon) impinges on the surface of the probe sputtering the ions away from the probe. The energy of the beam is between 3-10 KeV.

$$\underline{Ar^+_\alpha} + Ar_\beta \longrightarrow \underline{Ar_\alpha} + Ar^+_\beta \qquad\qquad (2.5)$$

This process can last only a few seconds before all the compound has been consumed. However the life time of a spectrum can be increased to several hours if the compound is dissolved in a suitable matrix (or solvent). This matrix (often glycerol) is an involatile compound which increases both the life of the spectrum and the sensitivity. Both positive $[M + H^+]^+$ and negative $[M - H^+]^-$ ions are produced but the exact mechanism of formation of the ions is not known with certainty. However, it is believed that the fast atom beam interacts with the matrix to effect an ion molecule reaction forming the $[M + H^+]^+$ by proton transfer

AcTrp-Ile-Glu-Iva-Ile-Thr-Aib-Leu-Aib-Hyp-Glu-Aib-Hyp-Aib-
-Pro-Phol
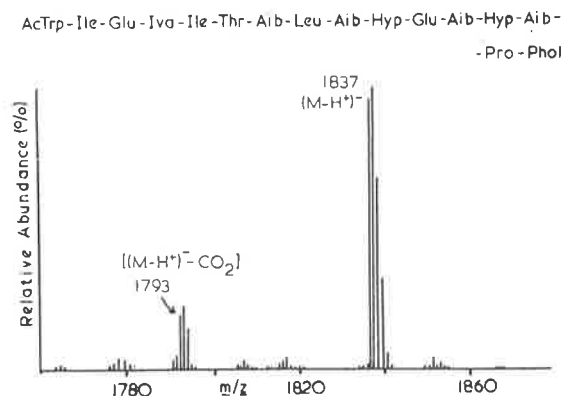
Figure 2.8: *FAB/MS of Zervamycin IC*[61].

from the matrix. Deprotonation of the matrix (ROH) yields RO^- which may interact with the substrate to form an $[M - H^+]^-$ ion. The use of both negative and positive ions is useful because of the $[M - H^+]^-$ ions show few fragmentations and can be used to determine the molecular weight of a compound, whereas the positive $[M + H^+]^+$ ion generally has various fragmentations which can be used to determine the structure of the compound. The two ions provide complementary information. Molecular weights of up to approximately 10,000 are routinely available and on nanograms of substrate. The most obvious use of this technique is for large molecular weight molecules of biological origin. A number of FAB mass spectra of biological molecules[59] have been reported and also large molecular weight organometallic compounds[60]. The structures of several zervamycin peptide antibiotics were determined with the aid of FAB mass spectrometry. After purifying the crude zervamycin using reverse phase HPLC the major component zervamycin C was obtained (several minor components were also obtained). The molecular ion region of the negative ion FAB/MS is shown in *Figure 2.8*. The molecular weight was determined from the $[M - H^+]^-$ peak at 1837. The sequence of the amino acids were determined from the positive ion FAB/MS[61].

21
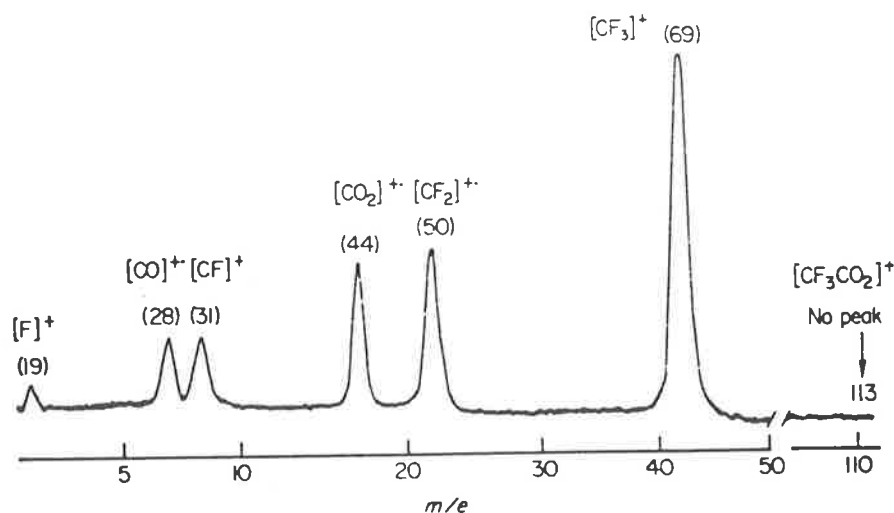
Figure 2.9: *Dissociative charge-inversion spectrum derived from* $CF_3CO_2^-$. *Decompositions occurring in the second field free region ; magnetic field scan. Peaks are shown with the conventional masses in brackets (Hitachi Perkin-Elmer R.M.U. mass spectrometer)*[62].

2.4 Charge Reversal Mass Spectrometry.

It has been shown[63] that non decomposing negative ions may be converted into decomposing positive ions by interaction with a neutral molecule (*equation 2.6*).

$$A^- + N \longrightarrow A^+ + N + 2e^- \qquad (2.6)$$

The ions A^+ that are formed within 10^{-12} seconds of the collision process are generally not stable and are generally only observed in small abundance. The decomposing forms of A^+ fragment in less than 10^{-8} of a second to produce an intense spectrum of daughter cations. A typical charge reversal spectrum is shown in *Figure 2.9*.

Chapter 3

CA Mass Spectra of Deprotonated Dimethyl Succinate and Related Molecules.

3.1 Introduction.

Over the last several years there have been a number of reports dealing with the CA mass spectra of ester enolates[64,65]. Some of the compounds studied include: i) deprotonated secondary and tertiary alkyl malonates[64]: the major fragmentation of deprotonated secondary alkyl malonates is outlined in *equation 3.1*.

$$\bar{C}H(CO_2Me)_2 \longrightarrow \begin{array}{c} \overset{\bar{O}}{\underset{MeO}{\diagdown}} C{=}C{=}C{=}O \end{array} + \ MeOH \qquad \textbf{3.1}$$

$$\bar{C}Me(CO_2Me)_2 \longrightarrow MeOCOCH(Me)\bar{C}{=}O \ + \ CH_2O \qquad \textbf{3.2}$$

$$\bar{C}Me(CO_2Me)_2 \longrightarrow CH_2{=}C{=}C\overset{\diagup \overset{\bar{O}}{}}{\underset{OMe}{\diagdown}} + \ CH_4 \ + \ CO_2 \qquad \textbf{3.3}$$
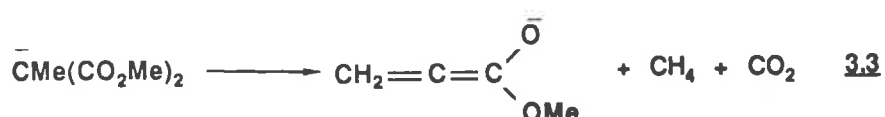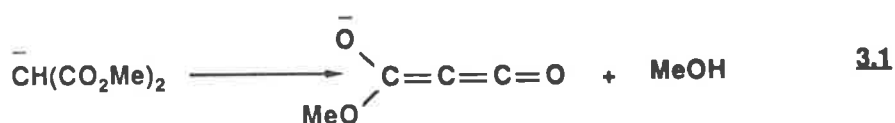
The major fragmentations of deprotonated tertiary alkyl malonates are shown in *equations 3.2* and *3.3*. ii) tertiary alkyl ester enolates[65] $R^1R^2\bar{C}CO_2R^3$ (R^1, R^2 and R^3 are alkyl) show a variety of competitive fragmentations including the losses of H_2, $R^3\cdot$ and (R^3O+H) together with the formation of R^3O^- and $R^1C_2O^-$ (*see Figure 3.1*). The major loss from deprotonated $Et_2CHCO_2CD_3$ is loss of CD_3OH. Deuterium labelling indicated the hydrogen came from the terminal position exclusively. iii) Hunt[44] and Cooks[50] have proposed that deprotonated dimethyl adi-

23
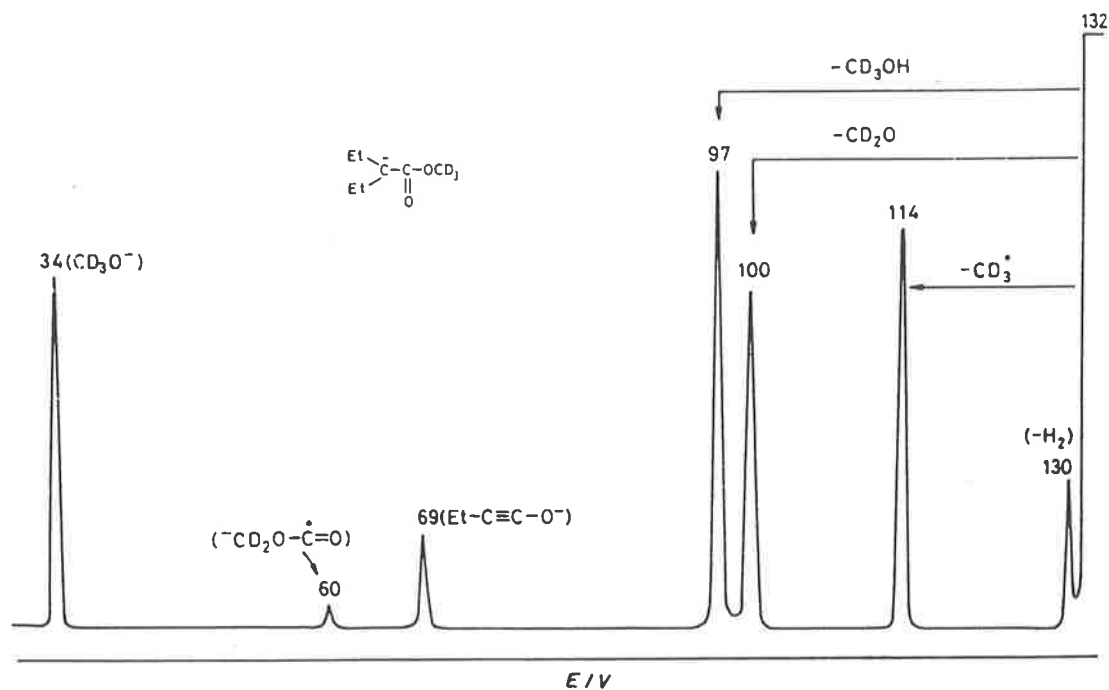
Figure 3.1: *CA Mass Spectrum of the enolate ion of* $Et_2CHCO_2CD_3$.

pate undergoes a gas phase Dieckmann condensation with loss of methanol *(equation 3.4)*.
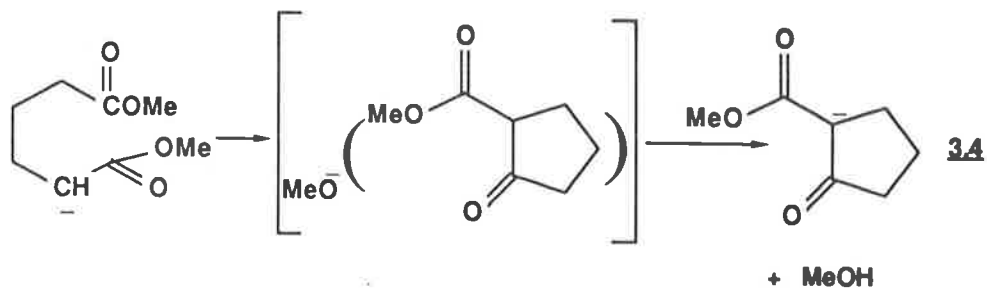
3.2 Results and Discussion.

3.2.1 The CA Fragmentations of the Enolate Anion of Dimethyl Succinate.

Compounds used in this section are listed in *Table 3.1*. Full details of the syntheses are given in the experimental section, but a selection are shown in *equations 3.5-3.7*.

	R^1	R^2	R^3	R^4	R^5
(I)	MeO	H	H	H	H
(II)	CD_3O	H	H	H	H
(III)	MeO	D	D	D	D
(IV)	MeO	D	H	D	H
(V)	MeO	Me	D	Me	D
(VI)	MeO	Me	Me	H	H
(VII)	MeO	Me	Me	D	D
$(VIII)$	MeO	Me	Me	Me	D
(IX)	CD_3O	Me	Me	Me	H
(X)	MeO	Me	Me	CD_3	H
(XI)	MeO	CD_3	Me	Me	H
(XII)	Me	H	H	H	H
$(XIII)$	CD_3	D	D	D	D
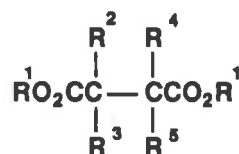
Table 3.1: *Dimethyl succinates.*
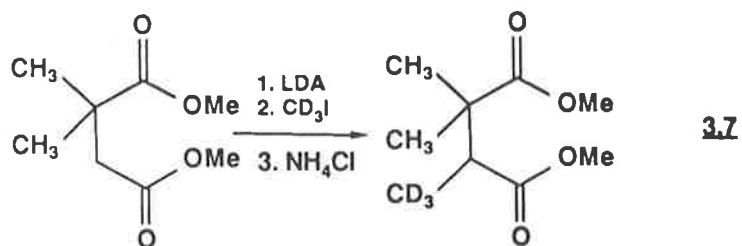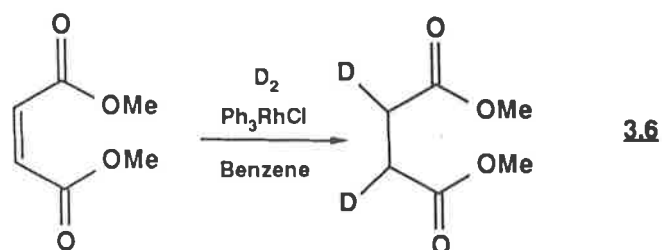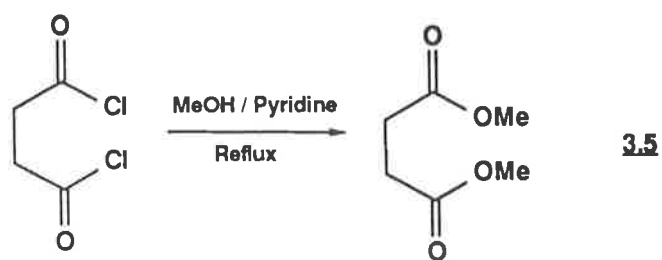
The CA mass spectra obtained for anions derived from compounds (I) to

CD₃OCOCHCH₂CO₂CD₃

The figure shows a CA mass spectrum with the following labeled peaks and transitions:

- 151
- 116, labeled - HCO₂Me
- - CD₃OH
- - CD₃·
- - CO
- (CD₃OCO) 62
- (CD₃O) 34
- (CH₂=CHCO₂) 71
- 88
- 98
- 123
- (×5)
- Volts →
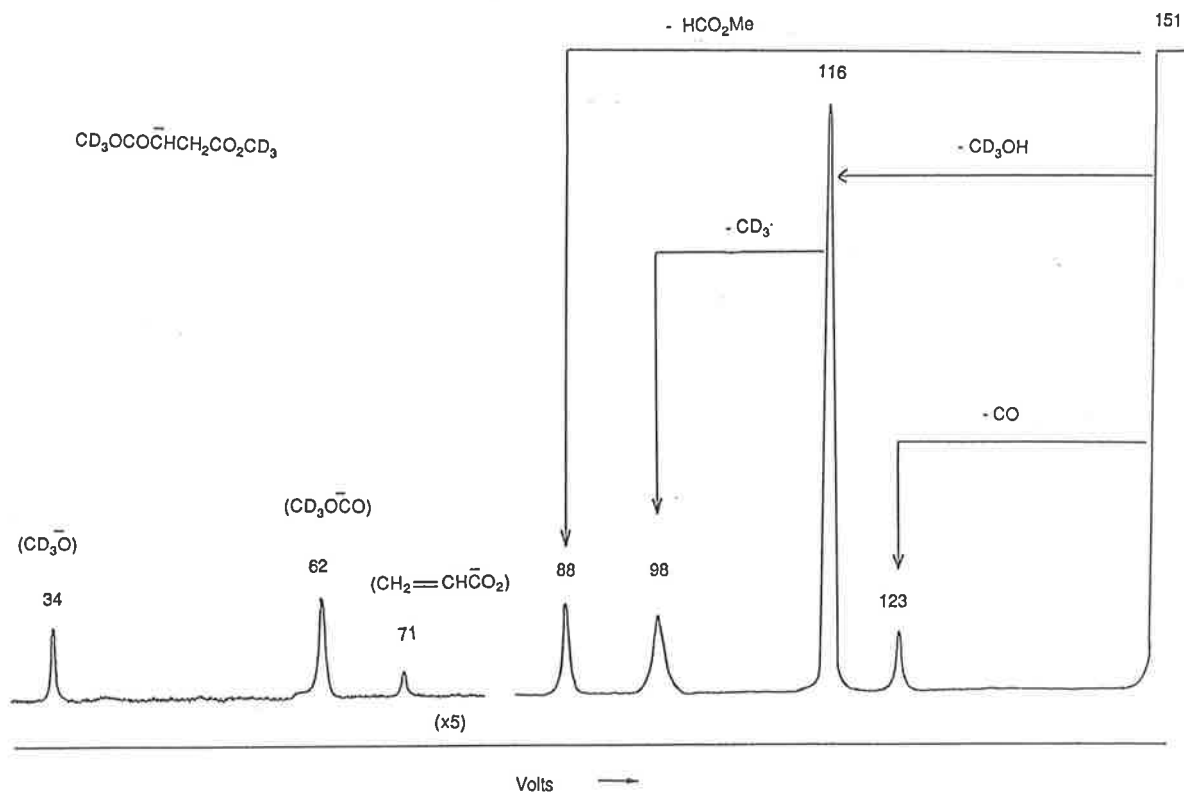
Figure 3.2: *CA Mass Spectrum of Deprotonated Dimethyl-D₆ succinate. Experimental conditions are given in the experimental section. When a voltage of 1 kV is applied to the collision cell it can be seen that m/z 123, 62 and 34 are almost unimolecular in origin (i.e. fragmentation occurs outside the collision cell). The peak at m/z 116 has both a collision induced and unimolecular component (70:30), whereas m/z 98, 88 and 71 are entirely collision induced. The voltages at half height for all peaks are [m/z (V)]: 123 (38.4), 116 (43.2), 98 (74.6), 88 (41.2), 62 (45.0) and 34 (28.5).*

($XIII$) are shown in *Table 3.2,* and in *Figure 3.2.* The basic fragmentations are rationalized as occurring through two ion/molecule complexes $\underline{a}$ and $\underline{b}$ *(Scheme 3.1).*

$$MeO-\overset{\overset{O}{\|}}{C}-\overset{-}{C}H-CH_2-\overset{\overset{O}{\|}}{C}-OMe \longrightarrow [Me\overset{\overset{O}{\|}}{O\underline{C}}(CH_2CHCO_2Me)]$$

$$\underline{b}$$

$$[Me\overset{-}{O}(MeOCOCH_2CHCO)]$$

$$\underline{a}$$

Scheme 3.1
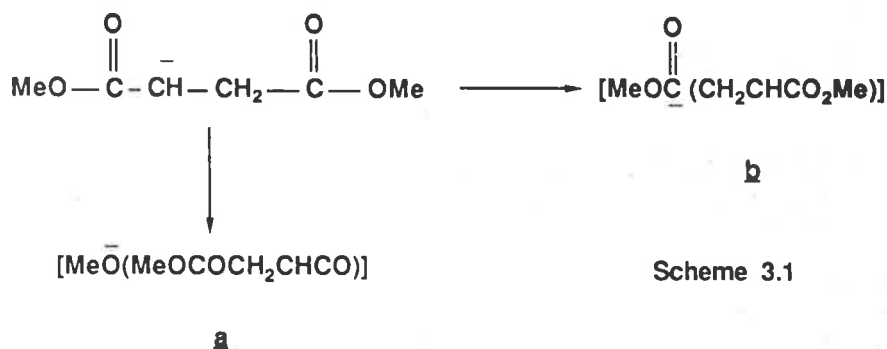
These two complexes are formed by low energy pathways because their decompositions to MeO^- and $MeO\bar{C}O$ are primarily unimolecular; this was determined by applying a voltage (1 kV) to the collision cell. The ions at m/z 123, 62 and 34 *(Figure 3.1)* are unaffected by this experiment, thus these ions are formed by unimolecular processes occurring outside the collision cell. Other decompositions of complexes **a** and **b** are primarily collisionally induced.

$$[Me\bar{O}(MeOCOCH_2CHCO)] \nearrow MeO^- + MeOCOCH_2CHCO \quad \underline{3.8}$$
$$\mathbf{a} \searrow MeOCO\bar{C}HCHCO + MeOH$$

$$\begin{array}{c} ^-O \\ \diagdown \\ C=CHCH=C=O \quad + \quad Me^- \quad \underline{3.9} \\ \diagup \\ O \end{array}$$

$$[MeO\bar{C}O(MeOCOCH=CH_2)] \longrightarrow MeO\bar{C}{\overset{O}{\diagup}} \quad + \quad MeOCOCH=CH_2 \quad \underline{3.10}$$
$$\mathbf{b}$$

$$[MeO\bar{C}O(MeOCOCH=CH_2)] \longrightarrow CH_2=C=C{\overset{\bar{O}}{\diagup}_{OMe}} \quad + \quad HCO_2Me \quad \underline{3.11}$$
$$\mathbf{b}$$

$$[MeO\bar{C}O(MeOCOCH=CH_2)] \longrightarrow CH_2=CH\bar{C}O_2 \quad + \quad MeCO_2Me \quad \underline{3.12}$$
$$\mathbf{b}$$
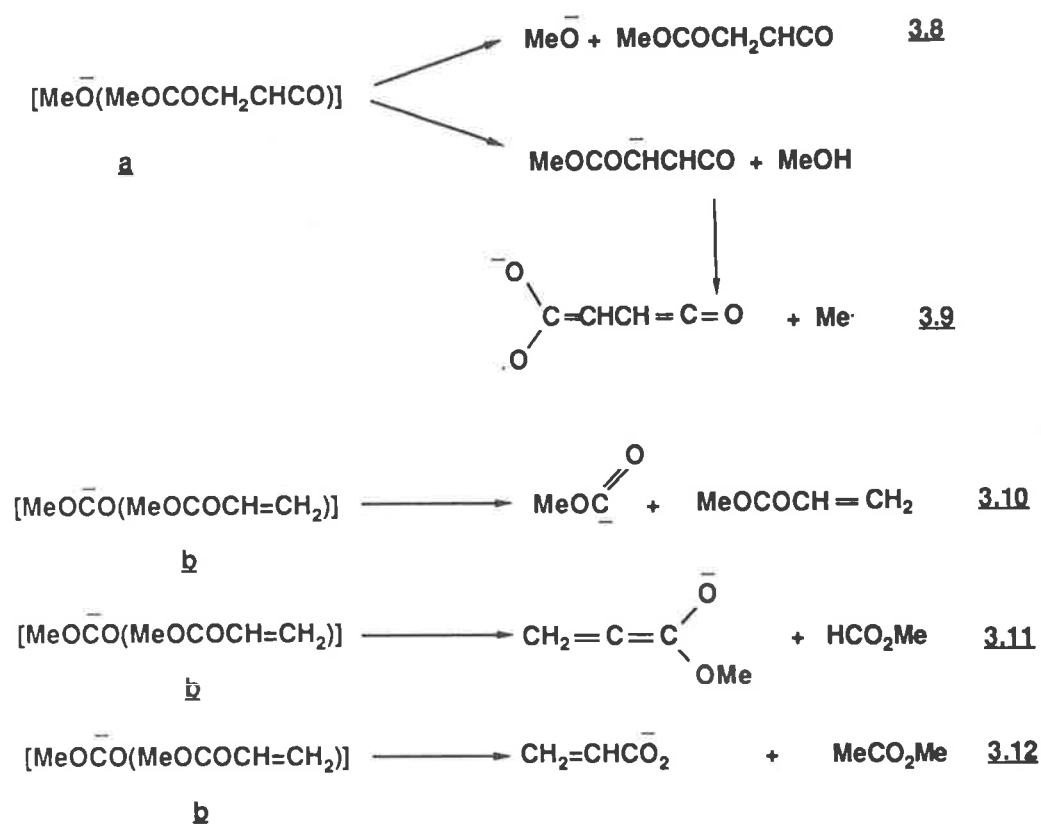
Scheme 3.2

Complex **a** undergoes two reactions; these are shown in *Scheme 3.2*. It may fragment directly to form methoxide *(equation 3.8)*, or eliminate methanol *(equation 3.9)*. Complex **b** decomposes to $MeO\bar{C}O$ *(equation 3.10)* eliminates methyl formate *(equation 3.11)*, and effects an S_Ni reaction to eliminate methyl acetate *(equation 3.12)*. Deprotonated dimethyl succinate also loses carbon monoxide by a skeletal rearrangement reaction of the type $ABC^- \longrightarrow AC^- + B$: a suggested

27

mechanism is shown in *Scheme 3.3*.

$$(MeO)_2(CH_2=CH)\overset{-}{C}O \quad + \quad CO$$

Scheme 3.3
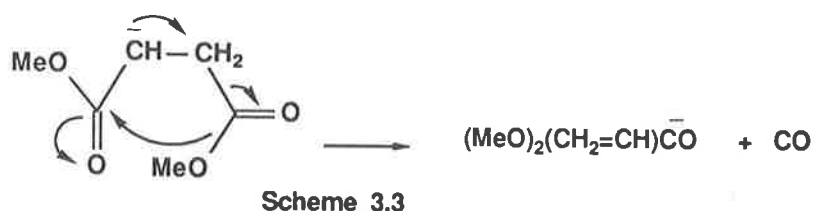
Equilibration of Central Hydrogens.

Do the central hydrogens of the anion $MeOCO\overset{-}{C}HCH_2CO_2Me$ equilibrate on collisional activation? In other words, does the equilibrium $MeOCOCH_2\overset{-}{C}HCO_2Me$ $\rightleftharpoons MeOCO\overset{-}{C}HCH_2CO_2Me$ occur? In order to answer this question, the CA mass spectra of the $[\,M - H^+\,]^-$ and the $[\,M - D^+\,]^-$ ions from $(MeOCOCHD)_2$ were measured. The spectra are recorded *Table 3.2*. The ratios for the losses of MeOH : MeOD are 68 : 100 and 100 : 35 respectively, while the losses of HCO_2Me : DCO_2Me are of 73 : 100 and 100 : 27. These results indicate at least partial equilibration of the central H/D substituents. Charge reversal spectroscopy[62,66,67] *(page 22)* has been used to determine whether a particular hydrogen equilibration occurs before or after collisional activation[68]. The charge reversal spectra are shown in *Table 3.3*. Unfortunately there are no suitable fragmentations to enable the determination of the positions of the deuteriums in the decomposing positive ions formed from $MeOCOCD_2\overset{-}{C}HCO_2Me$ and $MeOCO\overset{-}{C}DCH_2CO_2Me$.

3.2.2 The Fragmentations of the Enolate Anions from the Methyl Derivatives of Dimethyl Succinate.

Dimethyl 2,2-dimethylsuccinate.

The CA mass spectrum of the enolate ion of dimethyl 2,2-dimethylsuccinate is shown in *Table 3.2*. The fragmentation mechanisms are similar to those shown in *Scheme 3.2* in that they may be rationalized by the fragmentation of ion/molecule complexes. The two ion molecule complexes proposed in this case are c and d *(Scheme 3.4)*. All the fragmentations observed may be explained by fragmentation of these two species. Due to the lack of acidic hydrogens in c, the loss of methanol is less important than that observed for intermediate a *(cf. Scheme 3.2)*. The

28

losses of MeOD and MeOH are shown (for the labelled analogue) in *equations 3.13 and 3.14 (Scheme 3.4)*. The loss of HCO_2Me from ion complex d *(Scheme 3.4)* produces the base peak of the spectrum. The carbomethoxy anion deprotonates one of the methyl groups to form the allylic anion e *(equation 3.15, Scheme 3.4)*. This anion then loses MeOD as shown in *equation 3.16 (Scheme 3.4)*.

$$MeOCOCDC(Me)_2CO_2Me \longrightarrow [MeO(MeOCOC(Me)_2CDCO)]$$

c

$$MeOCOC(Me)_2CCO + MeOD \qquad \underline{3.13}$$

$$\begin{array}{c} \bar{C}H_2 \\ | \\ MeOCOC(Me)CD{=}C{=}O \end{array} + MeOH \qquad \underline{3.14}$$

$$MeOCOCDC(Me)_2CO_2Me \longrightarrow [MeOCO(Me_2CCDCO_2Me)]$$

d

$$\begin{array}{c} \bar{C}H_2 \qquad D \\ \diagup \diagdown \diagup \diagdown \\ Me \qquad CO_2Me \end{array} + HCO_2Me \qquad \underline{3.15}$$

e

$$\begin{array}{c} CH_2 \diagdown \\ C{-}\bar{C}{=}C{=}O \\ \diagup \\ Me \end{array} + MeOD \qquad \underline{3.16}$$
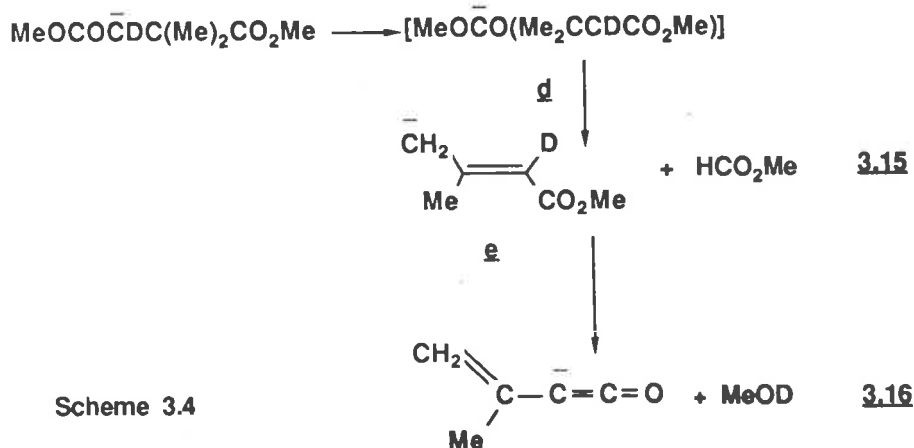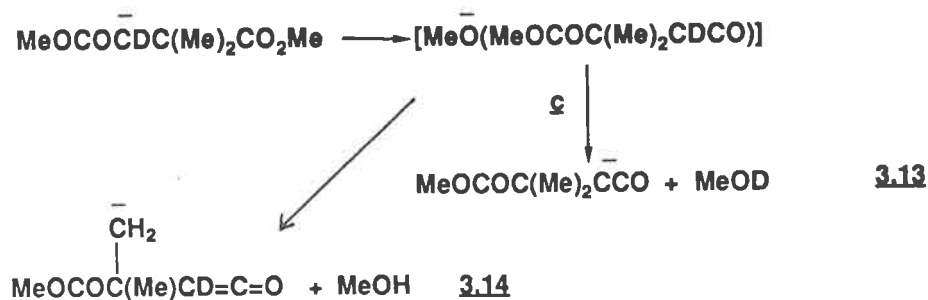
Scheme 3.4

Dimethyl 2,2,3-trimethylsuccinate.

The CA mass spectra of the enolate ion of dimethyl 2,2,3-trimethylsuccinate and of its labelled derivatives are recorded in *Table 3.2* and in *Figure 3.3*. The probable fragmentation mechanisms are summarized in *Scheme 3.5*. The ion complexes formed by deprotonated dimethyl 2,2,3-trimethylsuccinate are represented as f and g. There are small losses of methanol *(equation 3.17)* and MeOMe *(equation 3.18)*. Complex g decomposes to yield MeOCO *(equation 3.19)* and to eliminate methyl formate *(equation 3.20)*. The data in *Table 3.2* shows that the loss

29

of HCO_2Me has a measured deuterium isotope effect of 1.46, suggesting that the deprotonation step shown in *equation 3.20* is rate determining.

$$\overset{\overset{\displaystyle \bar{C}H_2}{|}}{O=C=CC(Me)_2CO_2Me} \; + \; MeOH \qquad \underline{3.17}$$

$$MeOC\bar{O}C(Me)C(Me)_2CO_2Me \longrightarrow [Me\bar{O}(O=C=C(Me)C(Me)_2CO_2Me]$$

$$f \downarrow$$

$$O=C=C(Me)C(Me)_2C\bar{O}_2 \quad + \; MeOMe \quad \underline{3.18}$$

$$\overset{O}{\underset{\|}{MeOC}}- \; + \; Me_2CMe\overset{C}{\diagup}CO_2Me \qquad \underline{3.19}$$

$$MeOC\bar{O}C(Me)C(Me)_2CO_2Me \longrightarrow [Me O\bar{C}O(Me_2CMe\overset{C}{\diagup}CO_2Me)]$$

$$g \downarrow$$

$$\overset{O}{\underset{\|}{MeOCH}} \; + \; Me_2C\bar{C}H\overset{C}{\diagup}CO_2Me \qquad \underline{3.20}$$
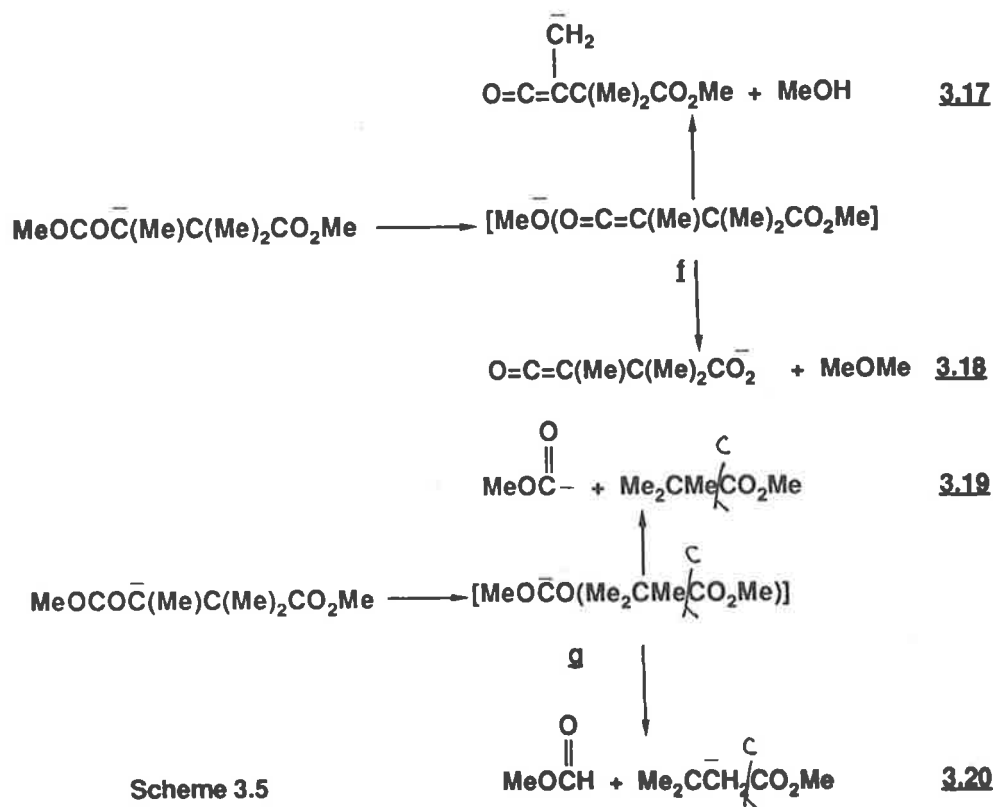
Scheme 3.5

3.2.3 The Fragmentations of Deprotonated Hexan-2,5-dione.

The CA mass spectrum of deprotonated hexan-2,5-dione was also measured (see legend to *Figure 3.4*) and the spectrum of the analogous D_9 ion is shown in *Figure 3.4*. The most important fragmentations are those corresponding to formation of the acetyl anion ($Me\bar{C}O$, $m/e=43$), and elimination of acetaldehyde. This is rationalized in terms of the formation of $\underline{h}$ *(Scheme 3.6)*, which fragments as shown in *equations 3.21* and *3.22*.
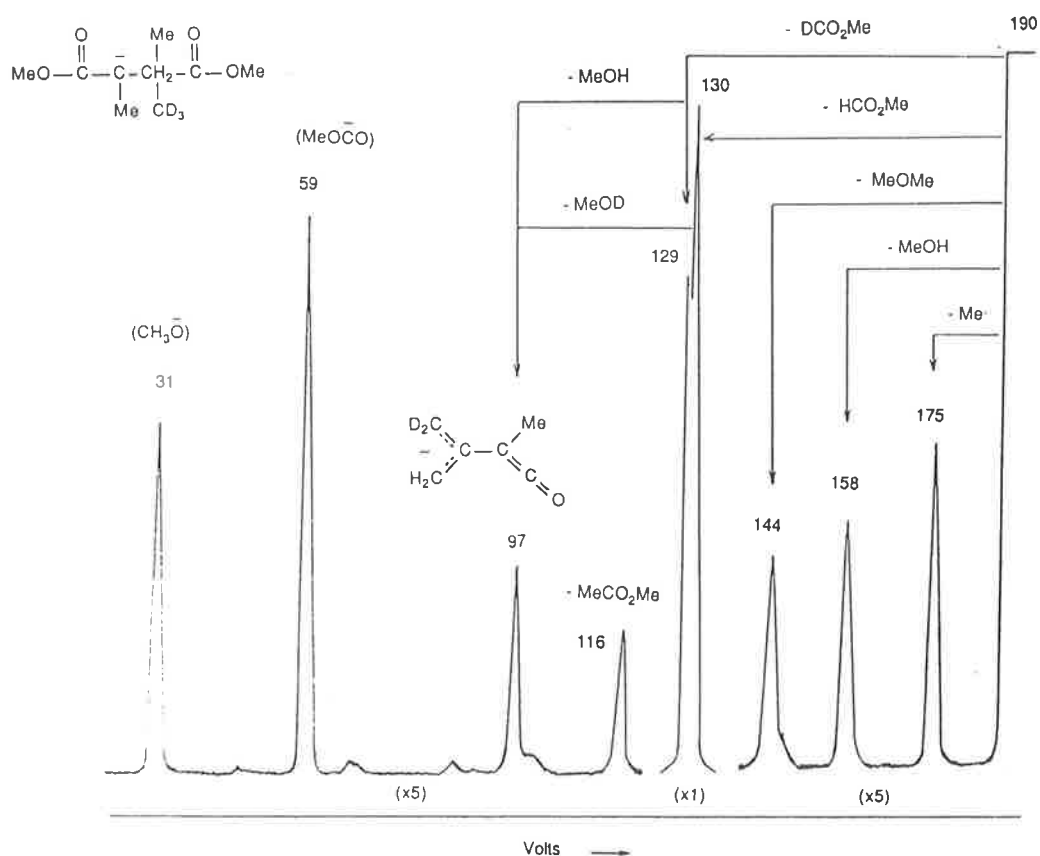
Figure 3.3: *CA MS of Deprotonated* $MeCO_2CH(Me)C(Me)(CD_3)CO_2Me$.

$$MeCO\bar{C}HCH_2COMe \longrightarrow [MeC\overset{O}{\overset{\|}{}}(CH_2=CHCOMe)] \longrightarrow MeC\overset{O}{\overset{\|}{}} + CH_2=CHCOMe \qquad \underline{\textbf{3.21}}$$

$$CH_2=C=C\overset{\bar{O}}{\underset{OMe}{\diagdown}} + MeCHO \qquad \underline{\textbf{3.22}}$$
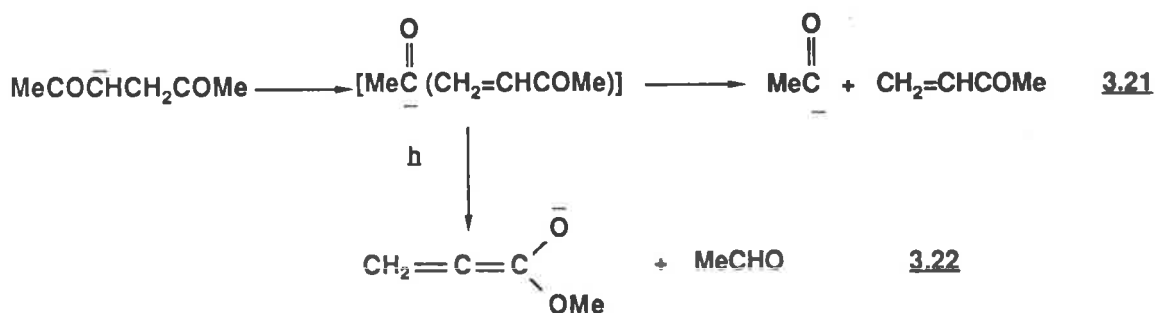
Scheme 3.6

3.2.4 The Fragmentations of Deprotonated Dimethyl glutarate.

The CA mass spectrum of the $[M-D^+]^-$ ion of dimethyl glutarate 2,2,4,4 D_4 is shown in *Figure 3.5*. A rational for the losses of HD. MeOD and the formation of $\bar{C}D_2CO_2Me$ and $DC\underset{2}{O}^-$ are outlined in *equations 3.23-3.26 (Scheme 3.7)* respectively. The fragmentation processes are analogous to those that have already been
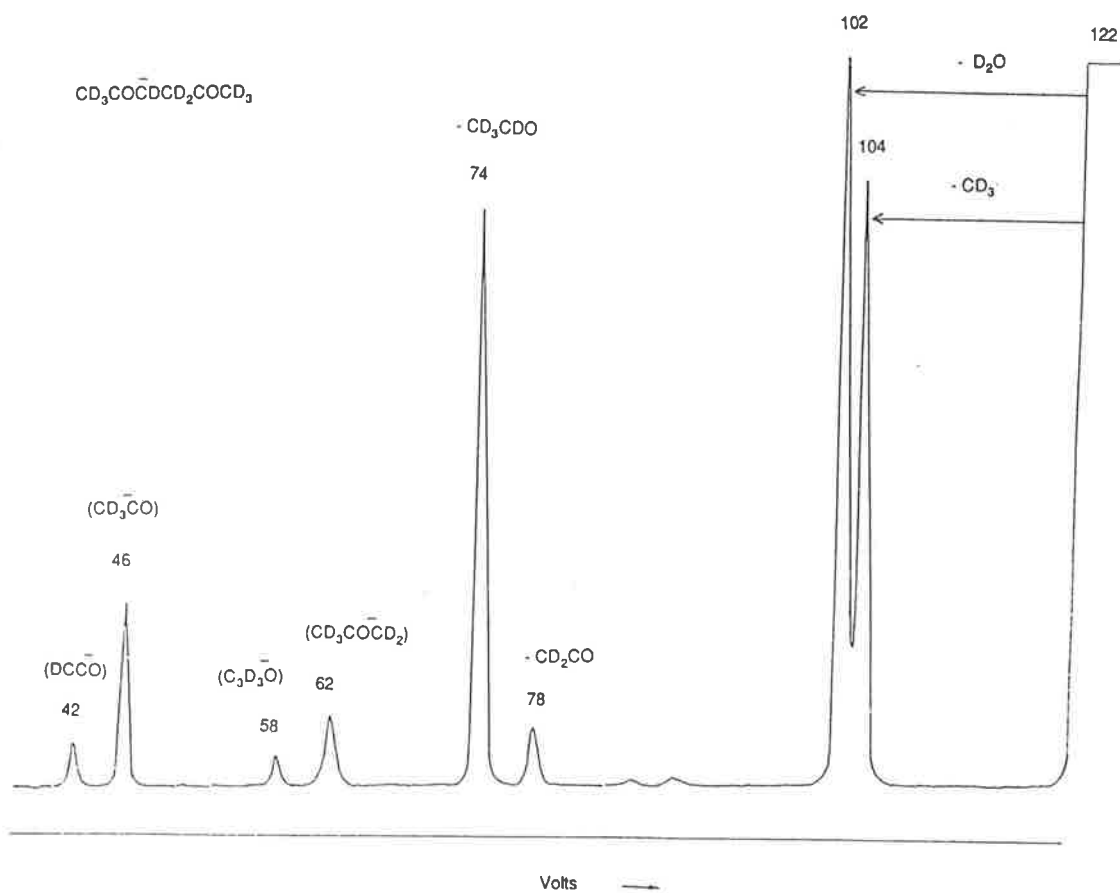
Figure 3.4: *CA Mass Spectrum of the* $(M-D^+)^-$ *ions of* $CD_3COCD_2CD_2COCD_3$. *The CA mass spectrum of deprotonated hexan-2,5-dione shows the following peaks;* m/e, *loss or formation (Abundance);* 98, $-Me$ *(15%);* 95, $-H_2O$, *(100%);* 85, *(2%);* 83, *(1.5%);* 71, $-CH_2CO$, *(2%);* 69, $-CH_3CHO$, *(4%);* 57, $CH_3CO\bar{C}H_2$, *(1.5%);* 55, $C_3H_3O^-$, *(1%);* 43, $CH_3\bar{C}O$, *(3%);* 41, HC_2O^-, *(1%)*.

32

outlined for deprotonated methyl malonates and dimethyl succinates.

$$[\text{H}(\text{MeCO}_2\overset{-}{\text{C}}\text{D}{=}\text{CHCD}_2\text{CO}_2\text{Me})] \longrightarrow \text{MeOCOCD}{=}\text{CH}\overset{-}{\text{C}}\text{DCO}_2\text{Me} \ + \ \text{HD} \quad \underline{3.23}$$

$$\text{MeO}{-}\underset{\underset{\text{O}}{\|}}{\text{C}}{-}\overset{-}{\text{C}}\text{DCH}_2\text{CD}_2\text{CO}_2\text{Me} \longrightarrow \overset{-}{\text{C}}\text{D}_2\text{CO}_2\text{Me} \ + \ \text{MeOCOCD}{=}\text{CH}_2 \quad \underline{3.24}$$

$$[\text{Me}\overset{-}{\text{O}}(\text{O}{=}\text{C}{=}\text{CDCH}_2\text{CD}_2\text{CO}_2\text{Me})] \longrightarrow \text{O}{=}\text{C}{=}\text{CDCH}_2\overset{-}{\text{C}}\text{DCO}_2\text{Me}$$

$$\underline{3.25}$$
$$+ \ \text{MeOD}$$

$$\text{DC}_2\overset{-}{\text{O}} \ + \ \text{MeOCH}_2\text{CD}_2\text{CO}_2\text{Me} \quad \underline{3.26}$$
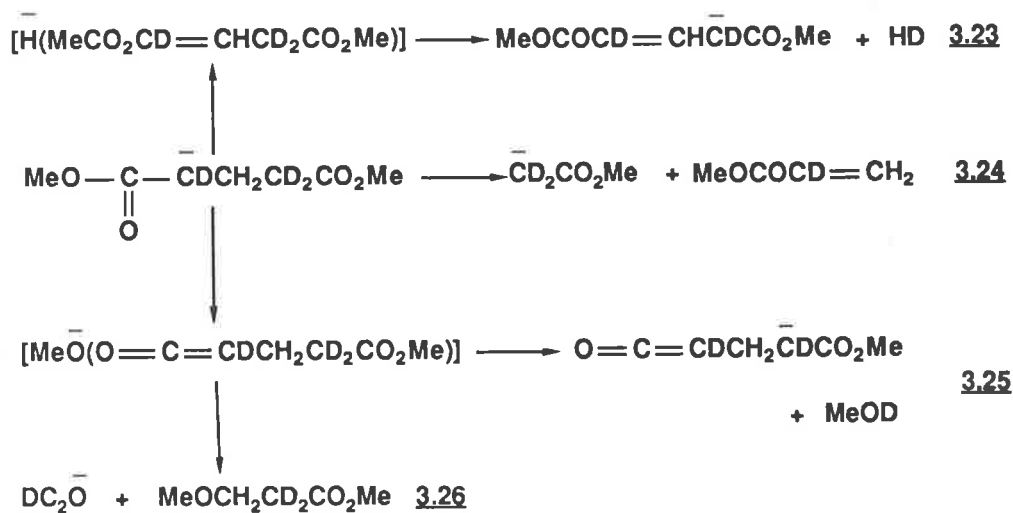
Scheme 3.7

3.2.5 The Fragmentations of the Enolate Anions of Dimethyl Adipate and Dieckmann Condensation Products.

Syntheses

All the adipates used in this study were prepared by standard procedures. The Dieckmann condensation products were prepared by the Dieckmann condensation, an example is given in *equation 3.27*. Full details can be found in the experimental section.

$$\underline{3.27}$$
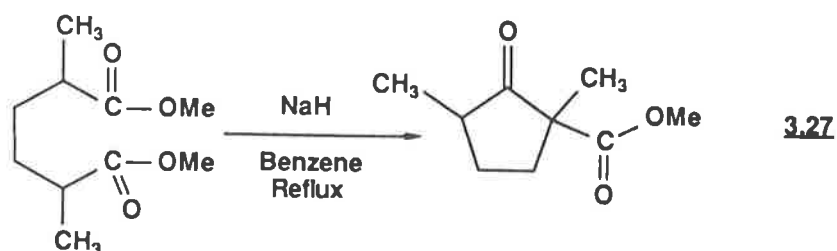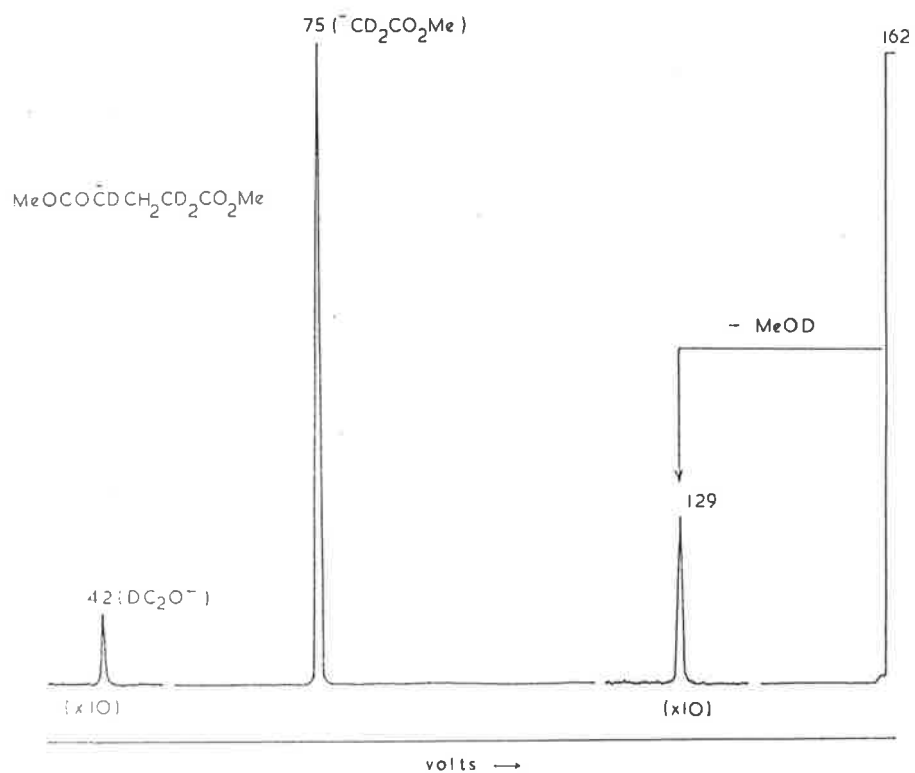
Figure 3.5: *CA Mass Spectrum of the $(M-D^+)^-$ ion derived from Dimethyl glutarate 2,2,4,4 D_4. The CA mass spectrum of deprotonated dimethyl glutarate shows the following peaks m/e, loss or formation (Abundance); 157, $-H_2$ (1%); 127, -MeOH, (1%); 73, $\bar{C}H_2CO_2Me$, (100%); 41, HC_2O^-, (0.5%).*

Dimethyl adipate and substituted analogues.

The CA mass spectra of the $[(M–H^+)–MeOH]^-$ ions derived from the reaction of OH^- with various dimethyl adipate derivatives are recorded in *Table 3.4*. The $[M–H^+]^-$ ions derived from the deprotonation of several Dieckmann condensation products are also recorded in *Table 3.4*.

There are two possible mechanisms for the loss of methanol from the enolate of dimethyl adipate, these are outlined in *Scheme 3.8*. The first (*equation 3.4*) is suggested by Cooks and Burinsky[50]. The second (*equation 3.28*) is similar to the loss of methanol observed in the enolates of alkyl malonates and dimethyl succinates, which involves the probable formation of solvated ion complex $\underline{b}$ as an intermediate. Subsequent deprotonation followed by cyclisation could yield $\underline{c}$ which should be readily convertible by proton transfer[64,65] to Dieckmann product $\underline{a}$ under collisional activation.

Scheme 3.8

35
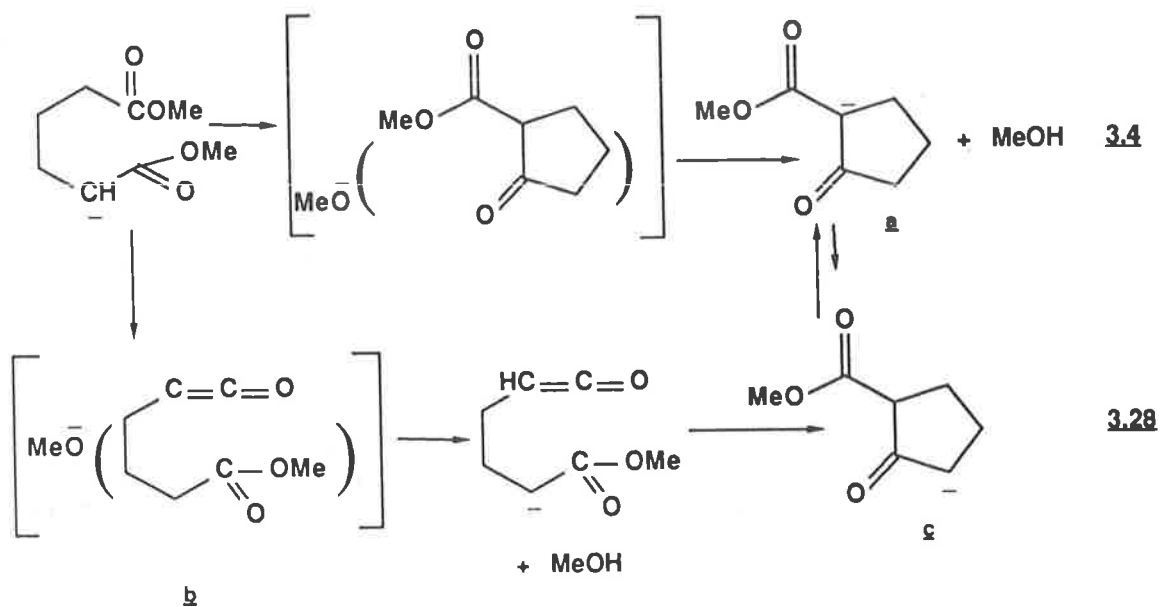
Scheme 3.9
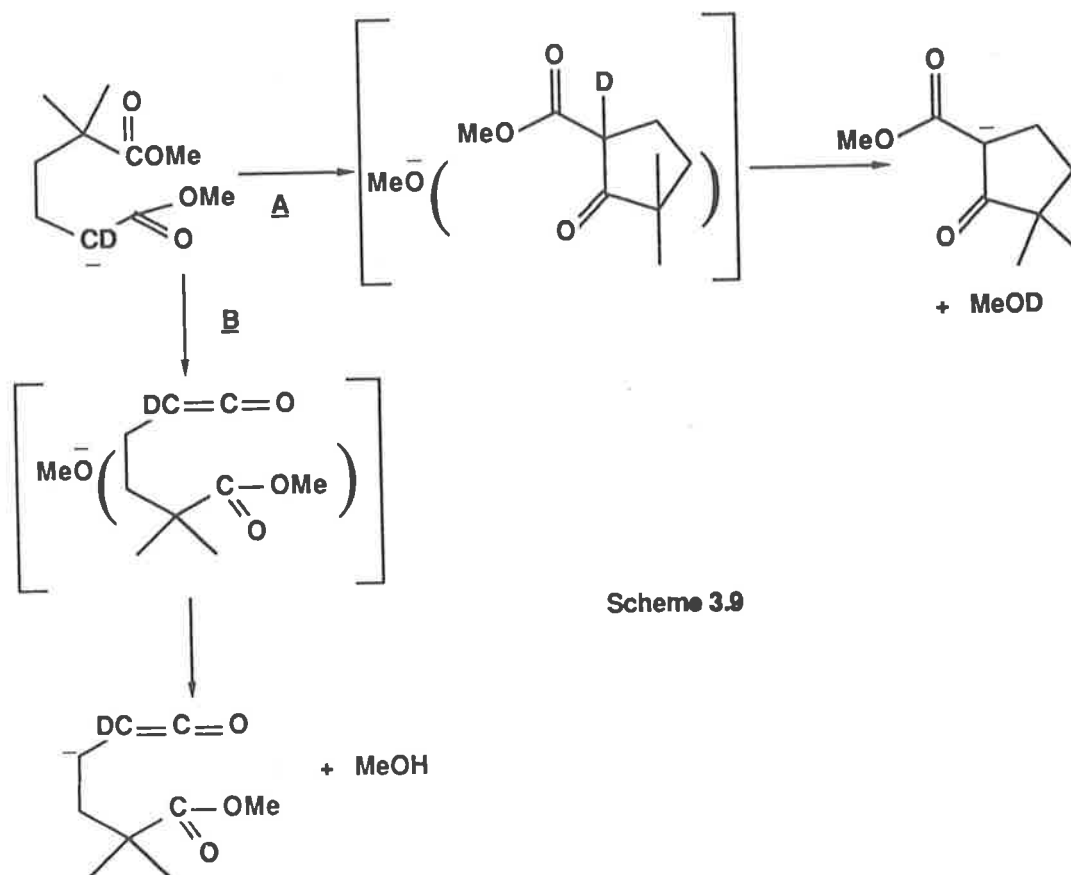
In order to investigate the mechanism of the Dieckmann condensation of adipates, the collisionally induced mass spectra of ions derived from the deprotonation of $MeOCOCD_2(CH_2)_2C(Me)_2CO_2Me$ and $MeOCOCD(Me)(CH_2)_2CD(Me)CO_2Me$ were recorded. The various arguments are summarized in *Schemes 3.9* and *3.10*. If the deuterated anion in *Scheme 3.9* decomposes *via* Dieckmann route **A**, MeOD should be eliminated specifically. If, on the other hand, route **B** is preferred, Dieckmann condensation cannot occur because of the blocked gem dimethyl position and MeOH will be eliminated. No $[M-D^+]^-$ ion is observed for this system; the only peak observed is an $[(M-D^+)-MeOD]$ ion whose CA spectrum is very similar to that of deprotonated 1-carboxy-3,3-dimethylcyclopentanone (*see Table 3.4*). Thus in this case the experimental evidence points to the exclusive operation of the Dieckmann condensation.

36
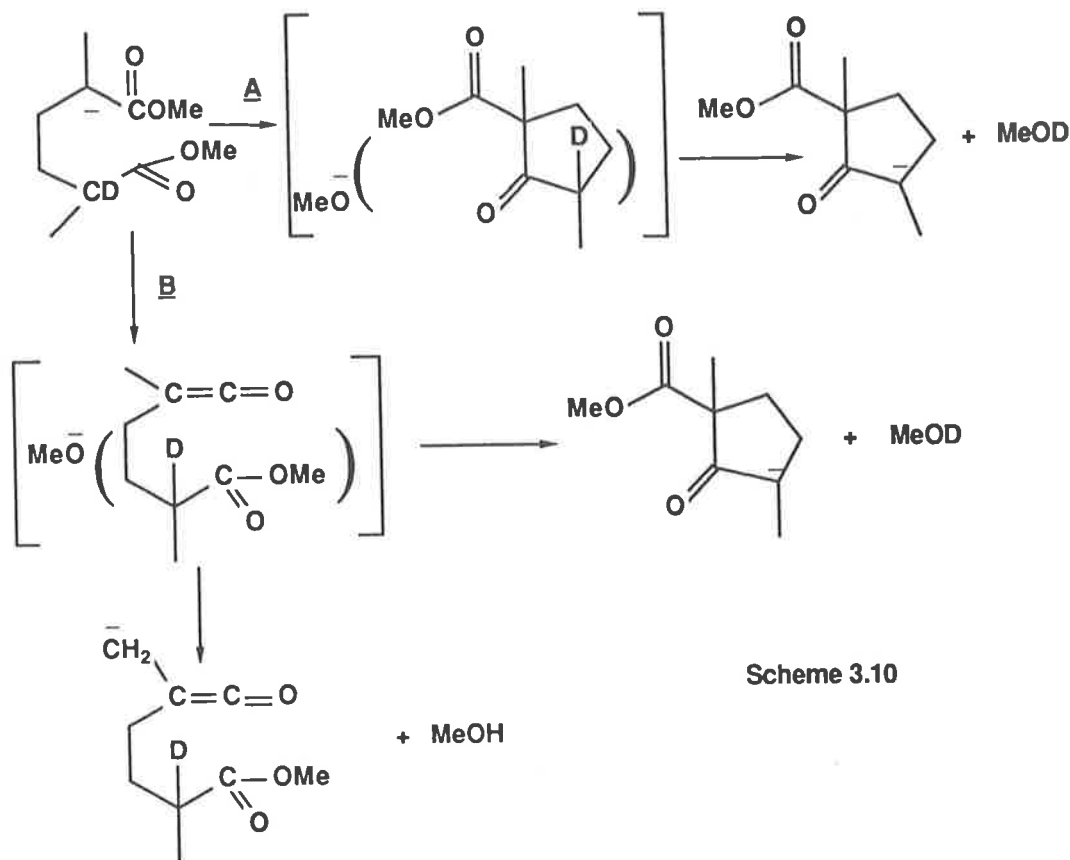
Scheme 3.10

The isomeric deuterated dimethyl dimethyladipate enolate ion that is shown in *Scheme 3.10*, could, in principle, react in one of four ways. It could either follow the Dieckmann condensation (route **A**) but in this case the intermediate ion complex must eliminate MeOD. If, in contrast route **B** is followed, then *i*) cyclisation may effect elimination of MeOD, or *ii*) elimination of a proton α to the ketene unit (two possibilities, one shown in *Scheme 3.10*) would result in specific loss of MeOH. There is no $[M-D^+]^-$ ion observed for this system; the only peak observed corresponds to $[(M-D^+)-MeOH]$. Finally, reaction of $MeOCOCD(Me)CH_2CH_2CD(Me)CO_2Me$ with DO^- yields an $[(M-D^+)-MeOD]$ ion ion whose CA spectrum is very similar to that of deprotonated 1-carbomethoxy-1,3-dimethylcyclopentanone *(see Table 3.4)*. Thus again, the experimental evidence points to the operation of a gas phase Dieckmann condensation in this case.

In conclusion, the experimental evidence presented above supports the earlier report by Burinsky and Cooks[50] that the elimination of methanol from the dimethyl adipate enolate ion occurs by a facile Dieckmann condensation.

37

Anion	Loss					
	Me·	CO	MeOH	MeOD	(MeOH+Me·)	(MeOD+Me·)
$MeOCO\bar{C}HCH_2CO_2Me$		10	100		21	
$MeOCO\bar{C}DCD_2CO_2Me$		16		100		20
"$MeOCO\bar{C}HCHDCO_2Me$"		22	100[a]	35[a]	17	7
"$MeOCO\bar{C}DCHDCO_2Me$"		25	68[a]	100[a]	12	18
$MeOCO\bar{C}(Me)CH(Me)CO_2Me$			12		16	
$MeOCO\bar{C}HC(Me)_2CO_2Me$	3[b]		45			
$MeOCO\bar{C}DC(Me)_2CO_2Me$	4[b]		23	37		
$MeOCO\bar{C}(Me)C(Me)_2CO_2Me$	8[b]		11			
$CD_3OCO\bar{C}(Me)C(Me)_2CO_2CD_3$ (c)	2[b]		3			
$MeOCO\bar{C}(CD_3)C(Me)_2CO_2Me$	6[b]		1	2		

Anion	Loss				
	MeOMe	HCO₂Me	DCO₂Me	(HCO₂Me+MeOH)	(HCO₂Me+MeOD)
$MeOCO\bar{C}HCH_2CO_2Me$		17			
$MeOCO\bar{C}DCD_2CO_2Me$			18		
"$MeOCO\bar{C}HCHDCO_2Me$"		22[a]	6[a]		
"$MeOCO\bar{C}DCHDCO_2Me$"		19[a]	25[a]		
$MeOCO\bar{C}(Me)CH(Me)CO_2Me$		100			
$MeOCO\bar{C}HC(Me)_2CO_2Me$		100		11	
$MeOCO\bar{C}DC(Me)_2CO_2Me$		100			8
$MeOCO\bar{C}(Me)C(Me)_2CO_2Me$	2	100		5	
$CD_3OCO\bar{C}(Me)C(Me)_2CO_2CD_3$ (c)	2	100		3	
$MeOCO\bar{C}(CD_3)C(Me)_2CO_2Me$	3	100		6	

a. these values are an average of ten individual scans : error ±2%

b. this is a characteristic loss of ester enolates[64,65].

c. in the case of this ion, read CD₃ for all Me column headings.

Table 3.2 cont.: CA Mass Spectra of Enolate Ions from Dimethyl succinates.

Anion	Loss	Formation					
	$MeCO_2Me$	$C_2H_3CO_2^-$	$C_2H_2DCO_2^-$	$C_2HD_2CO_2^-$	$C_2D_3CO_2^-$	$MeOCO^-$	MeO^-
$MeOCO\bar{C}HCH_2CO_2Me$		3				5	4
$MeOCO\bar{C}DCD_2CO_2Me$					3	6	4
"$MeOCO\bar{C}HCHDCO_2Me$"			4			9	6
"$MeOCO\bar{C}DCHDCO_2Me$"				6		11	7
$MeOCO\bar{C}(Me)CH(Me)CO_2Me$						8	3
$MeOCO\bar{C}HC(Me)_2CO_2Me$						8	3
$MeOCO\bar{C}DC(Me)_2CO_2Me$						6	2
$MeOCO\bar{C}(Me)C(Me)_2CO_2Me$	4					11	5
$CD_3OCO\bar{C}(Me)C(Me)_2CO_2CD_3$ (c)	2					6	3
$MeOCO\bar{C}(CD_3)C(Me)_2CO_2Me$	3					13	6

c. in the case of this ion, read CD_3 for all Me column headings.

39

Table 3.3: Charge Reversal Mass Spectra of the $[M-H^+]^-$ and $[M-D^+]^-$ ions of $(MeOCOCHD)_2$.

Initial Negative Ion	m/e, Abundance.									
	116	115	103	102	101	100	87	76	75	70
MeOCOC̄DCHDCO$_2$Me	14		0.5		1		6	1		1
MeOCOC̄HCHDCO$_2$Me		18		0.5		1	7		0.8	

Initial Negative Ion	m/e, Abundance.									
	69	59	57	56	45	43	41	29	28	15
MeOCOC̄DCHDCO$_2$Me		60	100			15		42		28
MeOCOC̄HCHDCO$_2$Me	1	64		100	4	17	5		36	29

Initial Ion	Precursor	Loss						
		H·	H$_2$	Me·	H$_2$O	MeOH	(MeOH+H$_2$)	HCO$_2$Me
$[(M-H^+)]^- - (MeOH)$	$MeCO_2(CH_2)_2CO_2Me$	20	10	0.4	0.1	100		4
$[M-H^+]^-$		20	11	0.5	0.2	100		4
$[(M-H^+)]^- - (MeOH)$	$MeCO_2(Me)_2(CH_2)_3CO_2Me$	25		21		100	34	49
$[M-H^+]^-$		28		20		100	37	53
$[(M-H^+)]^- - (MeOH)$	$MeCO_2CH(Me)(CH_2)_2CHMeCO_2Me$	16		5		96		100
$[M-H^+]^-$		16		6		96		100

Table 3.4: CA Mass Spectra of $[(M-H^+)^- -MeOH]^-$ Ions from Adipates and of the $[M-H^+]^-$ Ions of Authentic Deprotonated Dieckmann Products.

Initial Ion	Precursor	Formation			
		$CH_2C(Me)CO_2^-$	$CH_2CHCO_2^-$	HC_2O^-	CH_3^-
$[(M-H^+)]^- - (MeOH)$	$MeCO_2(CH_2)_2CO_2Me$		0.5	0.15	0.2
$[M-H^+]^-$			0.5	0.1	0.2
$[(M-H^+)]^- - (MeOH)$	$MeCO_2(Me)_2(CH_2)_3CO_2Me$				6
$[M-H^+]^-$					5
$[(M-H^+)]^- - (MeOH)$	$MeCO_2CH(Me)(CH_2)_2CHMeCO_2Me$	16			
$[M-H^+]^-$		16			

Chapter 4

CA Mass Spectra of the Enolate Anions of Cyclohexanone Derivatives.

4.1   Introduction.

Previous work on the CA fragmentations of enolate ions[44,45] derived from carbonyl compounds, has uncovered a number of rearrangement reactions. For example, the enolate ions of 1-substituted heptan-4-ones eliminate ethylene *(equation 4.1)* and substituted ethylene[44] *(equation 4.2)* on collisional activation.

$$\text{4.1}$$

$$\text{4.2}$$
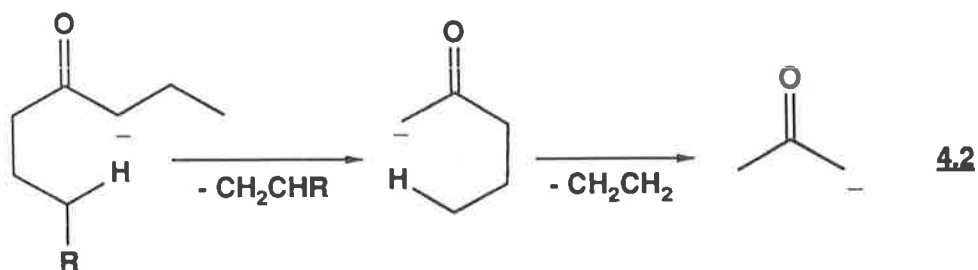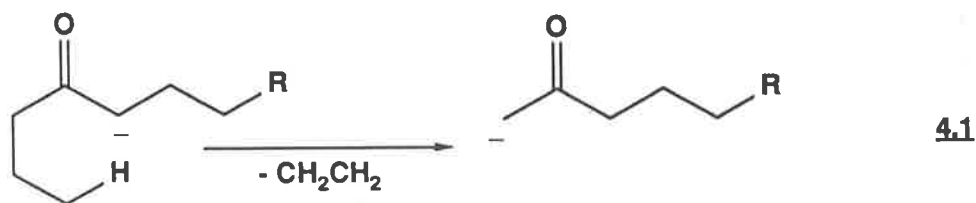
It has recently been shown[70] that the loss of ethylene from the heptan-4-one enolate is stepwise *(equation 4.3)* with the rate determining step being the deprotonation (step 1 *equation 4.3*). The heptan-4-one enolate also loses methane *(equation 4.4)* in this case both steps were shown to be rate determining by application of the double isotopic labelling technique[70,71].

43

Step 1 → **Step 2** → $+ C_2H_4$ **4.3**

Step 1 → **Step 2** → $+ CH_4$ **4.4**
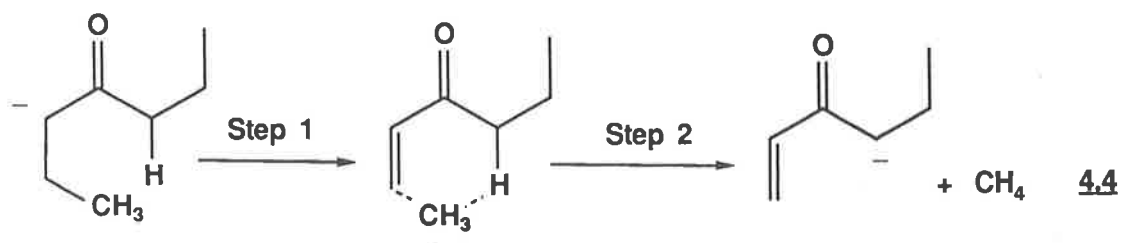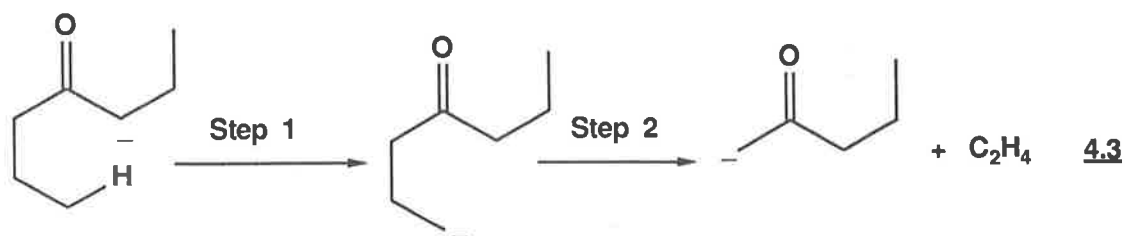
Hunt [45,69] has also reported that the cyclohexanone enolate undergoes a specific retro reaction on collision activation *(equation 4.5)*.

$+ CH_2CH_2$ **4.5**
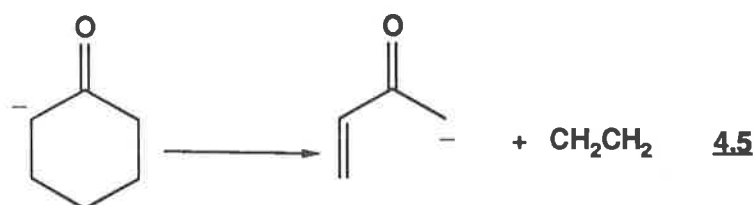
In this chapter the basic fragmentations of cyclohexanone and alkylcyclohexanone enolate ions are described. The study was aided by the examination of the spectra of a variety of deuterium labelled derivatives. The aims were: *i)* to confirm that the characteristic retro process of deprotonated cyclohexanones occurs by a simple mechanism *(equation 4.5)*; *ii)* to determine the fragmentations of differently substituted alkylcyclohexanone enolate ions; and *iii)* to investigate whether fragmentations analogous to those shown in *equations 4.3* and *4.4* occur for 2-substituted cyclohexanone enolates where the substituent is ≥ ethyl.

4.1.1 Synthesis of the Unlabelled Derivatives.

Compounds used *(see Tables 4.1 to 4.4)* were either commercially available or synthesised by standard procedures; *viz i)* the 2-substituted cyclohexanones were prepared by simple alkylation of the imine prepared from the ketone and cyclohexylamine *(equation 4.6, Scheme 4.1)*; the imine was then cooled to $-78°$ C in tetrahydrofuran and lithium diisopropylamine added to form the enolate anion.

The alkyl iodide was then added and the solution stirred for 1 – 2 hours. Standard workup with acid or base gave the required cyclohexanone. *ii*) The 3-substituted derivatives of cyclohexanone were all synthesised using a 1–4 Grignard reaction with 2-cyclohexenone and a 10% copper cyanide/alkyl magnesium iodide reagent at 0° C. The reactions proceeded in approximately 80 to 90% yield (*equation 4.7, Scheme 4.1*). *iii*) The alkylation of 4-iodocyclohexanones provided the route to the 4 substituted cyclohexanones. The alkylation involved the preparation of a lithium dialkyl cuprate using the alkyl lithium and copper (I) cyanide (*equation 4.8, Scheme 4.1*). Standard workup followed by removal of the protecting group gave the 4 substituted cyclohexanone.
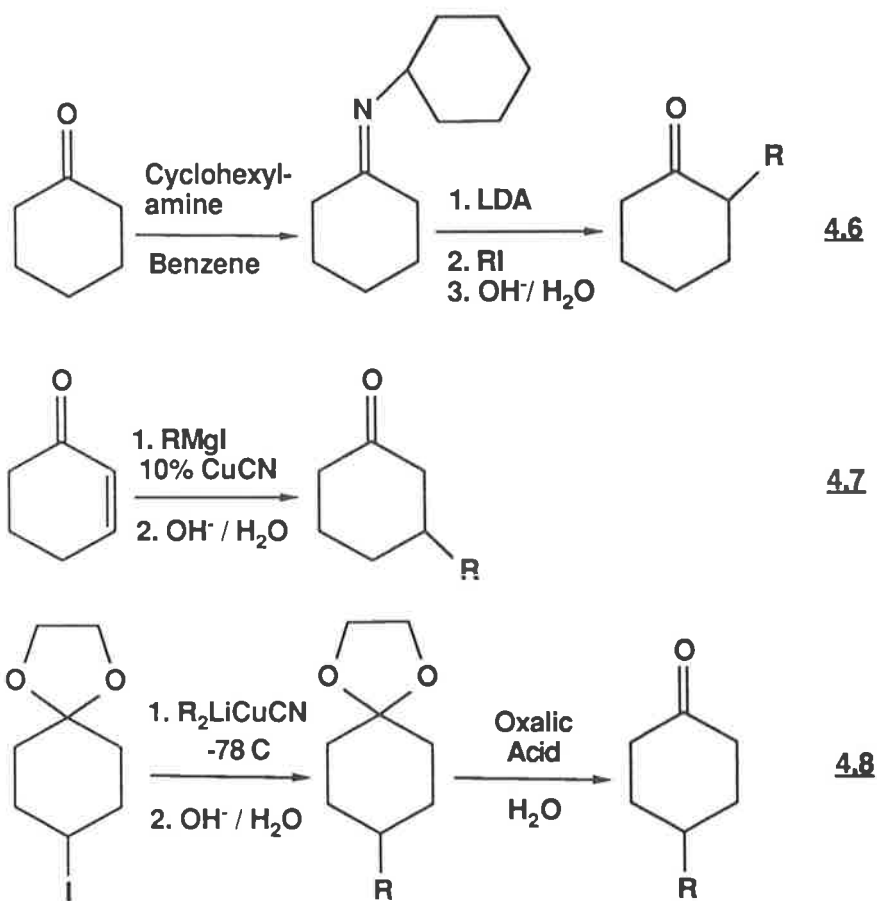
Scheme 4.1

4.1.2 Syntheses of the Labelled Derivatives.

Most of the labelled derivatives were prepared from either cyclohexanone 2,2,6,6-D_4 (from cyclohexanone by the exchange of the hydrogens α to the carbonyl), or

from cyclohexanone 3,3,5,5-D_4 (*Scheme 4.2*) and cyclohexanone 4,4-D_2. The reactions described above for the unlabelled derivatives were then used to alkylate the cyclohexanone ring in the desired position. A particular example is shown in *Scheme 4.3*.
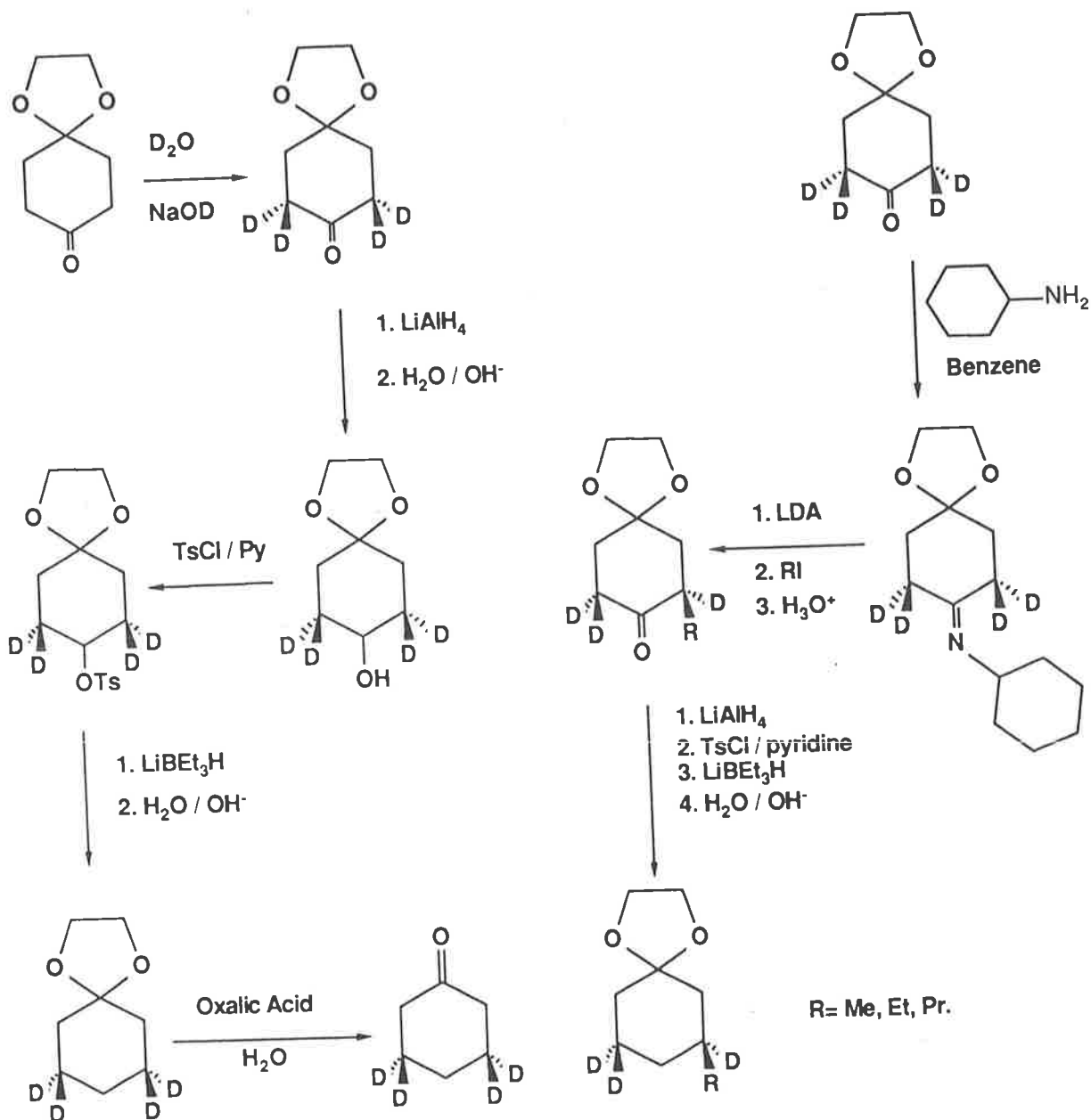
Scheme 4.2

Scheme 4.3

46

4.2 Results and Discussion.

4.2.1 Fragmentations of the Cyclohexanone Enolate Anion.

The CA mass spectra of the cyclohexanone enolate and the labelled derivatives are shown in *Table 4.1*. There are four major fragmentation pathways; *viz* losses of H· (*equation 4.9*), H_2 (*equations 4.10* and *4.11, Scheme 4.4*), C_2H_4 (*equation 4.5*) and C_4H_8 (*equation 4.12, Scheme 4.4*). The peaks all show major collision induced components, the ratios of collisionally induced to unimolecular fragmentations varying from 60:40 for the loss of H_2 to 70:30 for the loss of C_2H_4 (see footnote *Table 4.1*). Ethylene is believed to be lost by a retro Diels Alder reaction as suggested previously by Hunt[45,69] (*equation 4.5*).

Scheme 4.4
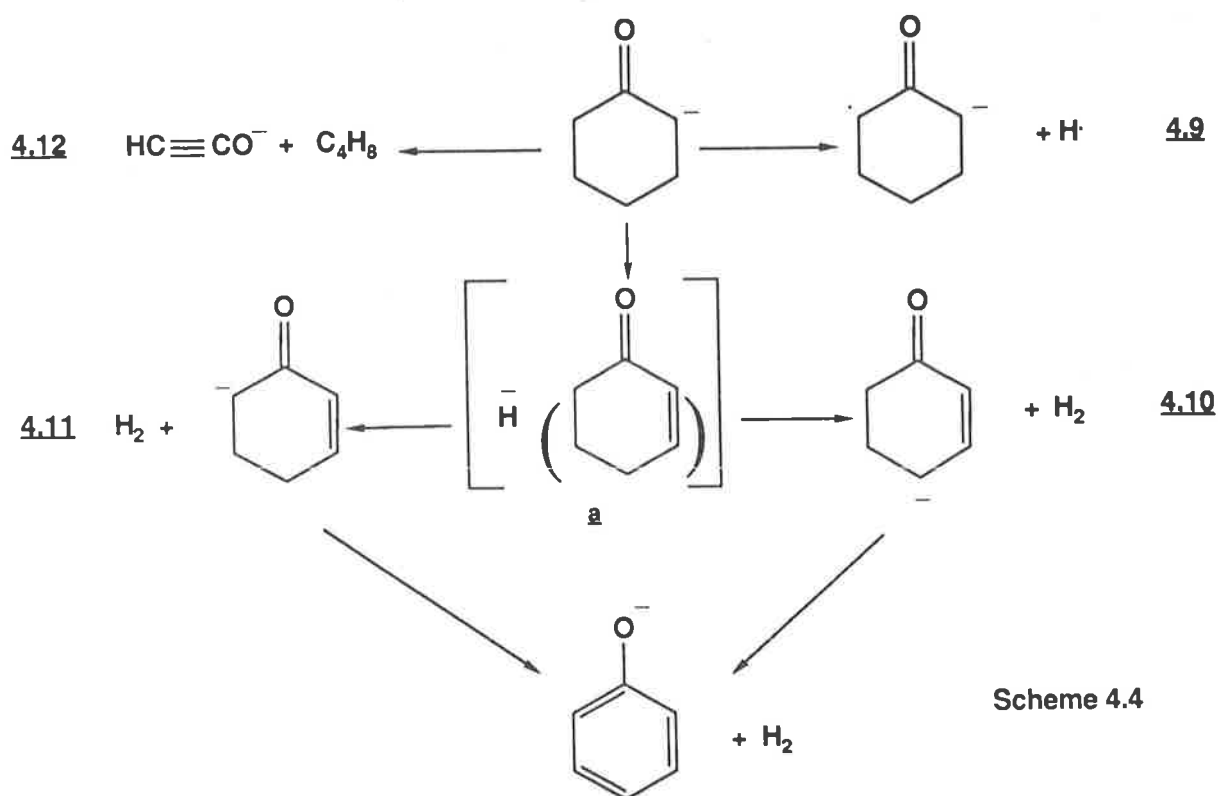
The peak at $m/e=69$ which corresponds to the loss of ethylene has no fine structure, is step sided and is wide, with a half height of 99 V, suggestive of a reaction with a reverse activation barrier. All retro reactions observed in this study show this feature. The elimination of H· and the formation HC_2O^- are characteristic

reactions of ketone enolates[44,69,70], see *equations 4.9* and *4.12 (Scheme 4.4)*. The loss of hydrogen is somewhat more complicated since this loss occurs by two specific mechanisms as evidenced by the deuterium labelling studies *(Table 4.1)*. It is suggested that the first step in each process involves the formation of solvated ion complex a, this complex can then decompose by the processes shown in *equations 4.10* and *4.11 (Scheme 4.4)*. The major process is that which involves the elimination of dihydrogen from the 3 and 4 positions *(equation 4.10)*.

4.2.2   Fragmentations of variously substituted Methylcyclohexanone Enolate Ions.

The CA mass spectra of the 2-, 3- and 4-methylcyclohexanone enolate anions are shown in *Figures 4.1* to *4.3*; those of the deuterium labelled derivatives are listed in *Table 4.2*. As can be seen from these three figures the spectra are different and allow ready identification of each isomer.

2-Methylcyclohexanone

2-Methylcyclohexanone on deprotonation can form two different enolate anions a and b *(Scheme 4.5)*; these are likely to interconvert on collisional activation[70]. The major losses from the 2 substituted derivative are H· *(equation 4.13)*, H_2, C_2H_4, C_3H_6 *(equation 4.15)*, C_4H_8 *(equation 4.16)*, and C_5H_{10} *(equation 4.17)*; these fragmentations are outlined in *Scheme 4.5*. The loss of hydrogen and ethylene occur by the same mechanism as shown in *Scheme 4.4* for deprotonated cyclohexanone and can occur from either anion. There is an unusual loss of C_3H_6 which only occurs for the 2 substituted methyl derivative; deuterium labelling studies *(Table 4.2)* indicate losses from positions 3,4 and 5; the process is summarized in *equation 4.15 (Scheme 4.5)*.

48

4.16 C_4H_8 + $MeC{\equiv}CO^-$ $HC{\equiv}CO^-$ + C_5H_{10} **4.17**

4.13   H· +

b   a

Scheme 4.5

+ C_3H_6 **4.15**
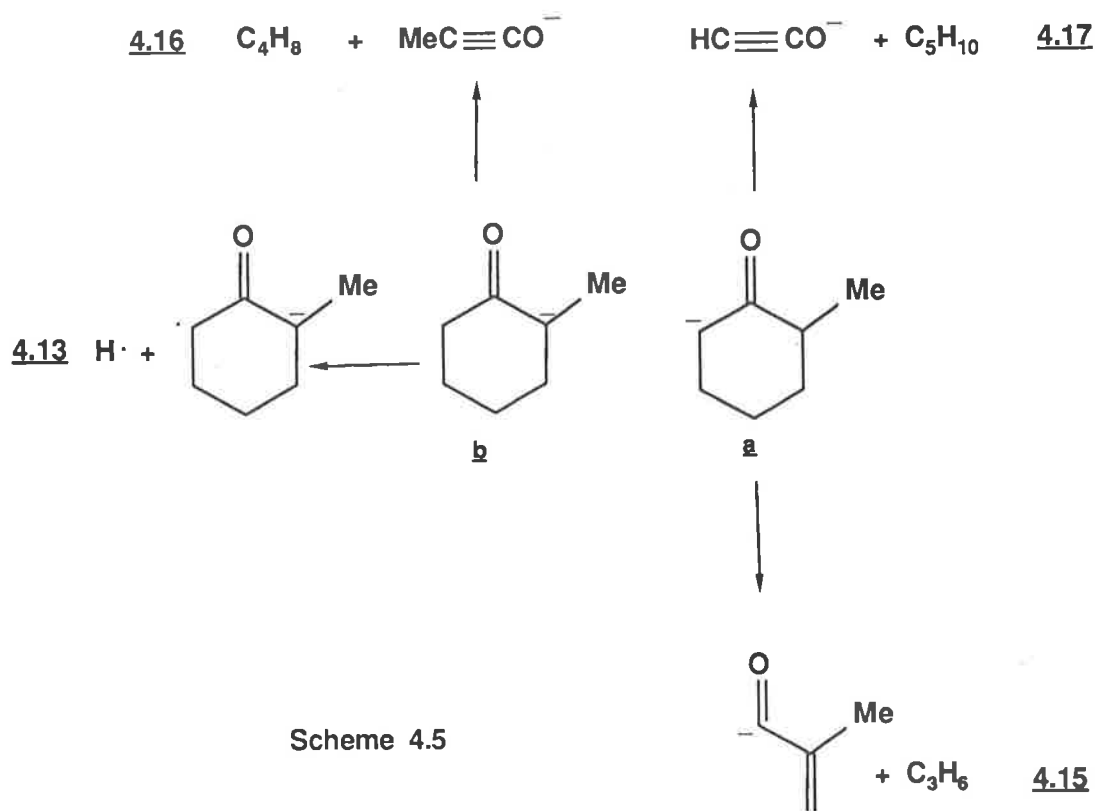
3-Methylcyclohexanone

The 3 substituted derivative of methylcyclohexanone can again form 2 anions on deprotonation; these are represented by a and b (*Scheme 4.6*). For this example there are two possible retro reactions that can occur from the two anions. The first is the loss of ethylene (*equation 4.18*), and the other is the loss of propene (*equation 4.19. Scheme 4.6*). The more favoured process is loss of the larger alkene. i.e. propene. Methane represents a large loss in the spectrum of the 3-methylcyclohexanone enolate (see *Figure 4.2*); it is analogous to the losses of dihydrogen from the cyclohexanone enolate (*equations 4.10* and *4.11, Scheme 4.4*). The data in *Table 4.2* indicate that the ions of 3-methylcyclohexanone 2,2,6,6-D_4 lose CH_4 and CH_3D in the ratio 64:12, whereas the $[M - H^+]^-$ ion of 3-methylcyclohexanone 4,4-D_4 loses CH_4 and CH_3D in the ratio 40:60. This indicates that there are two losses of methane (*equations 4.20* and *4.21*). Deuterium isotope effects occur for these processes; nevertheless it is clear that *equation 4.20* is the predominate process. Dihydrogen is again the major loss; labelling data (*Table 4.2*) indicate two processes analogous to those in *equations 4.10* and *4.11* (*Scheme 4.4*).

49
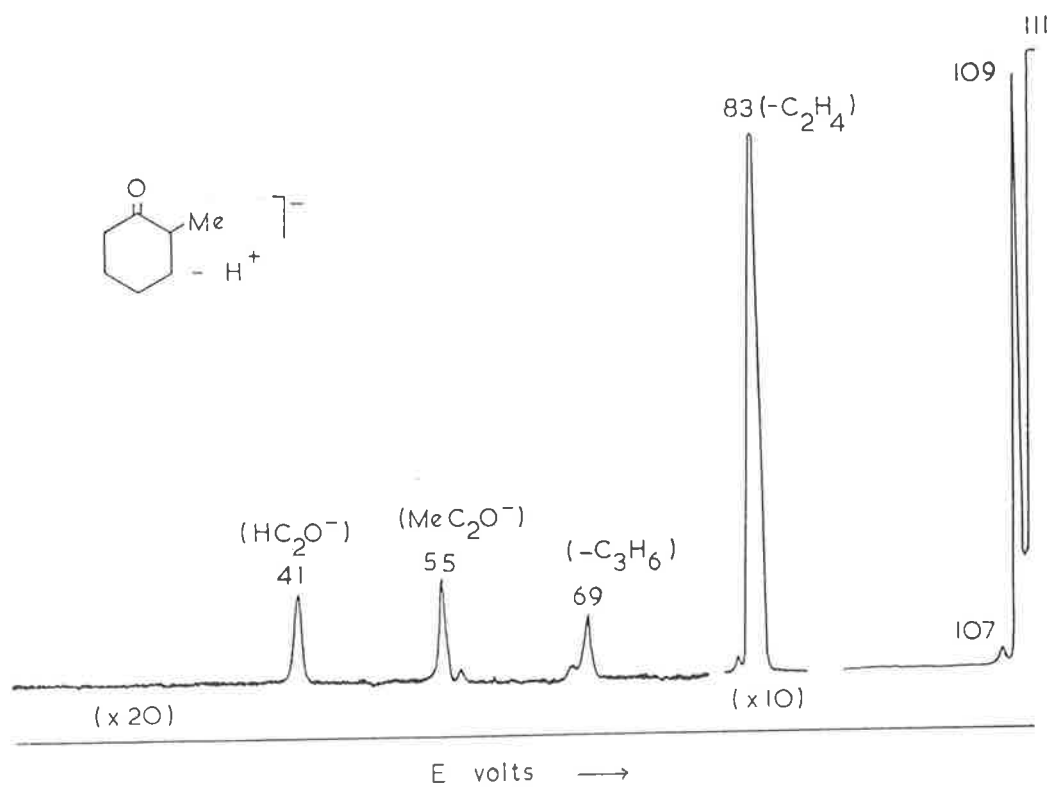
Figure 4.1: *CA Mass Spectrum of Enolate Ions from 2-Methylcyclohexanone. Width of major peaks at half height, m/z (volts ± 0.3) loss; 109 (44.1) H_2, 83 (93.8) C_2H_4, 55 (40.6) C_4H_8 and 41 (41.8) C_5H_{10}. When a voltage of +2000 V is applied to the collision cell, the following collisional induced:unimolecular peak ratios are observed, m/z (CI:u); 109 (50:50), 83 (70:30), 69 (90:10), 55 (40:60) and 41 (60:40).*
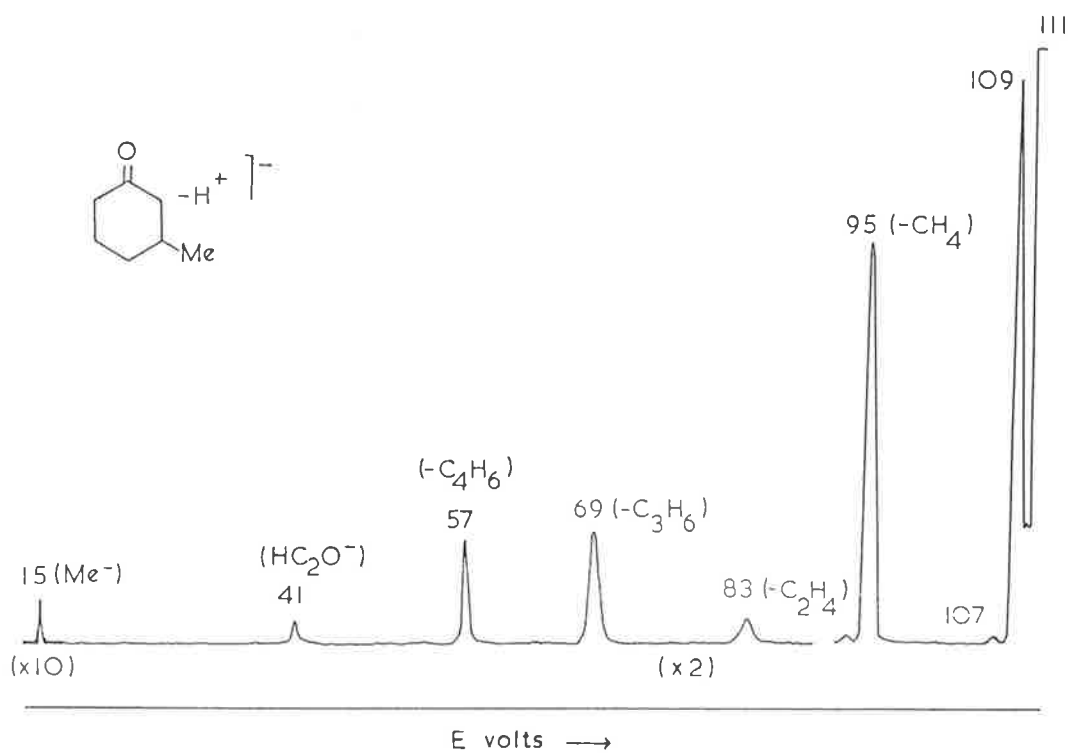
Figure 4.2: *CA Mass Spectrum of Enolate Ions from 3-Methylcyclohexanone. Width of major peaks at half height. m/z (volts ± 0.3) loss; 109 (47.2) H_2, 95 (53.3) CH_4, 83 (95.5) C_2H_4, 69 (87.3) C_3H_6, 57 (42.7) C_4H_6 and 41 (45.5) C_5H_{10}. When a voltage of +2000 V is applied to the collision cell. the following collisional induced:unimolecular peak ratios are observed, m/z (CI:u); 109 (40:60), 95 (60:40), 83 (80:20), 69 (80:20), 57 (45:55) and 41 (60:40).*
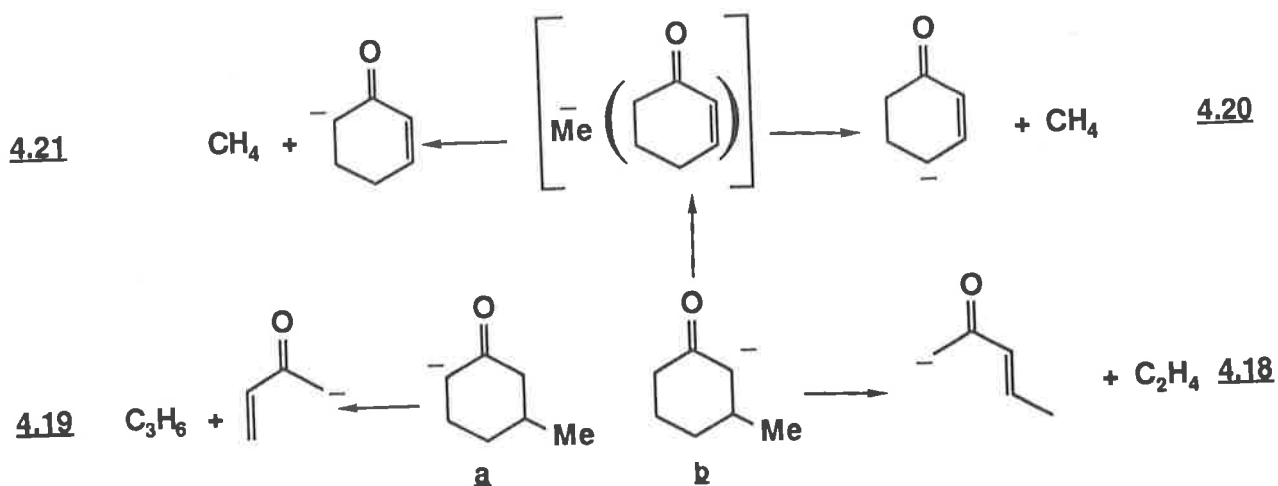
Scheme 4.6

The loss of C_4H_6 shown in *Scheme 4.7* is the first example of a specific double hydrogen transfer reaction reported for negative ions. The spectra of the three deuterated derivatives (*Table 4.2*) show that a methyl hydrogen and a hydrogen from position 4 are involved. It is proposed that the first step is a proton transfer reaction from the methyl group to the carbanion centre. The resulting ion then rearranges to form a (*Scheme 4.7*). The second proton transfer (from position 4) followed by cleavage yields the acetone enolate ion and butadiene. The reaction is characteristic of all 3-alkyl substituted cyclohexanone enolates studied; the ethyl, propyl, butyl and pentyl derivatives eliminate respectively, C_5H_8, C_6H_{10}, C_7H_{12} and C_8H_{14}.
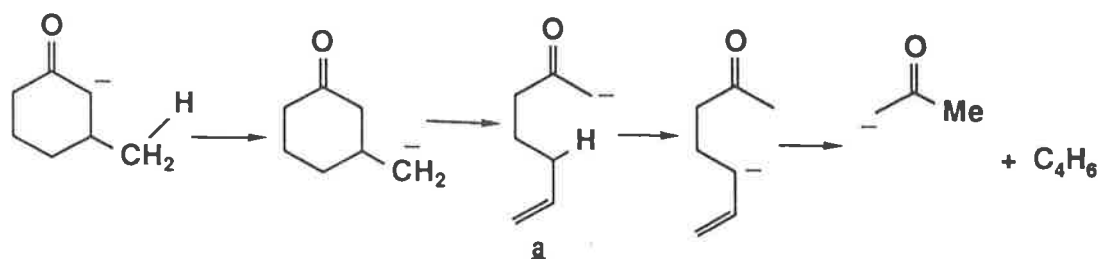
Scheme 4.7
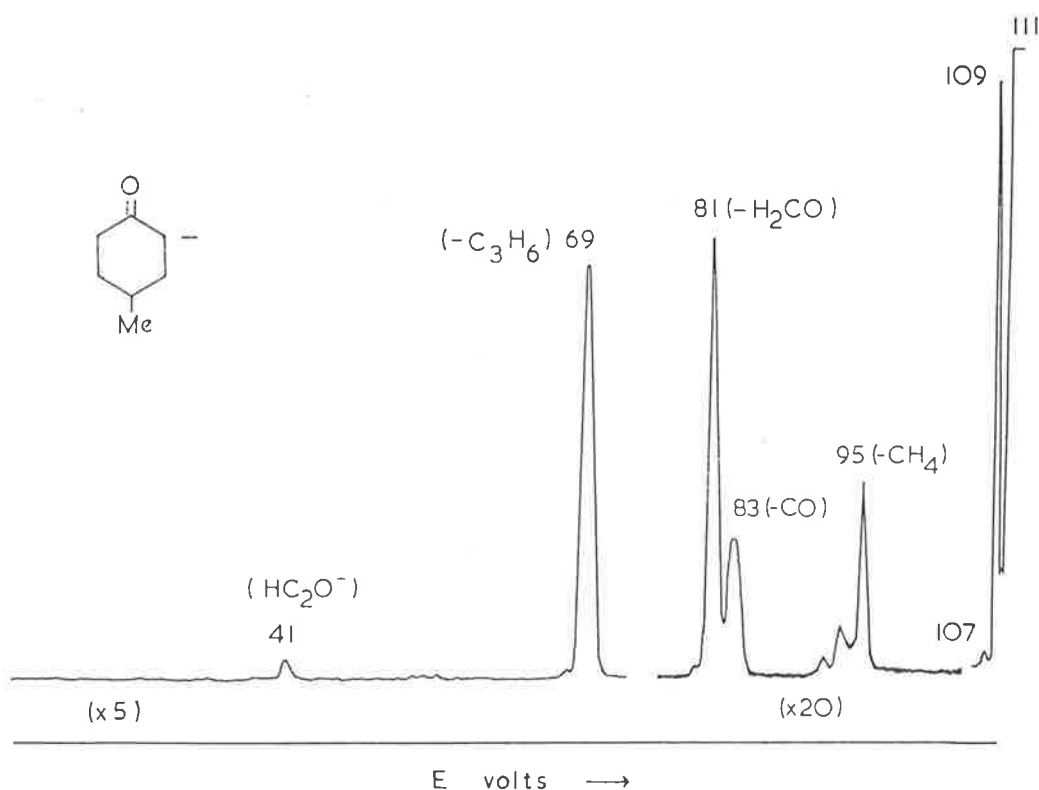
Figure 4.3: *CA Mass Spectrum of the Enolate Ion from 4-Methylcyclohexanone. Width of major peaks at half height, m/z (volts ± 0.3) loss; 109 (45.4) H_2, 95 (57.1) CH_4, 83 (104.3) CO, 81 (56.2) H_2CO, 69 (96.4) C_4H_6 and 41 (41.8) C_5H_{10}. When a voltage of +2000 V is applied to the collision cell, the following collisional induced:unimolecular peak ratios are observed, m/z (CI:u); 109 (40:60), 95 (80:20), 83 (70:30), 81 (70:30), 69 (70:30) and 41 (50:50).*

4-Methylcyclohexanone

The 4 substituted methylcyclohexanone enolate shows basically the same fragmentations as seen earlier for the 2 and 3 substituted cyclohexanones (*see Schemes 4.5* and *4.6*). Again the major loss is of dihydrogen originating from both the 3,4 and 3,6 positions (the major loss is from the 3,4 positions).

There are minor losses of methane, carbon monoxide and formaldehyde which are unique in this series of compounds. These processes are outlined in *Scheme 4.8*. The loss of methane may proceed through a: the products formed are methane and deprotonated cyclohexenone (*equation 4.22*). The loss of carbon monoxide (*equation 4.23*) and is predominately a collisionally induced process: a possible product ion is b (*Scheme 4.8*). This ion can then lose dihydrogen *via* a number of different pathways (*see Scheme 4.8*). Labelling studies (*Table 4.2*) suggest that

53

the major loss of hydrogen occurs to form $\underline{c}$ and $\underline{d}$ with minor contributions from other processes, which may form the ions $\underline{e}$ and $\underline{f}$. A minor reaction must involve a 1,2 hydride shift to form $\underline{g}$ *(Scheme 4.8)*. A 1,2 hydride shift is considered to be a "forbidden reaction"[72], and it has been calculated that the energy required for the 1,2 hydride shift in the ethyl anion[72] is 202 kJmol^{-1}. However a number of other examples of 1,2 hydride shift reactions have been observed on collisional activation of suitable carbanions[73].
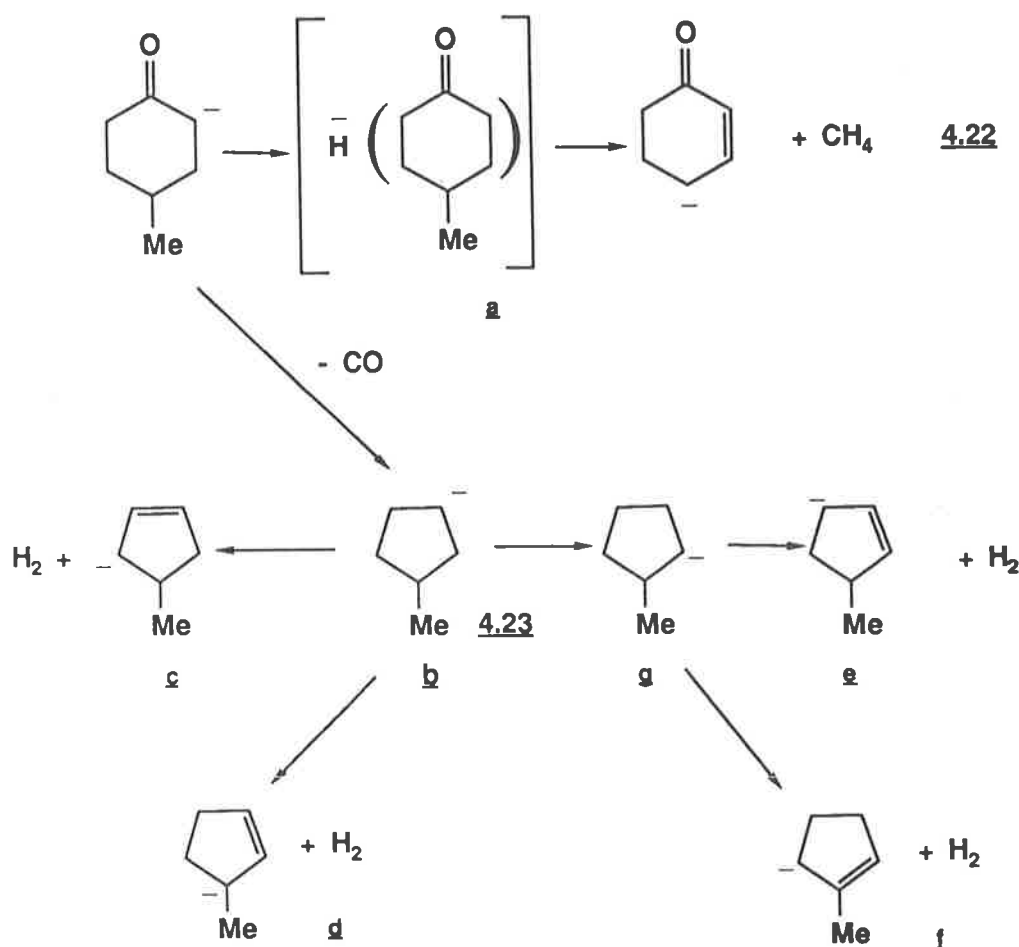
Scheme 4.8

4.2.3 The Fragmentations of the Enolates of Ethyl, Propyl and higher Alkyl Homologues of Cyclohexanone.

The CA mass spectra of deprotonated ethyl, propyl, butyl and pentyl substituted cyclohexanones are shown in *Table 4.3* and *4.4*. Again the major loss is of dihydrogen as shown in *equations 4.10* and *4.11 (Scheme 4.4)*; other fragmentations are similar to those already discussed in *Schemes 4.5* to *4.8*. One

fragmentation of the 2-ethylcyclohexanone enolate anion is the extrusion of ethylene from the side chain. This is the direct analogue of the loss of olefins from acyclic ketone enolates (*equations 4.1* and *4.2*) and in this case may be represented by *equation 4.24 (Scheme 4.9)*. Higher homologues show a corresponding loss (e.g. deprotonated 2-propylcyclohexanone shows loss of propene from the side chain). Another characteristic reaction involves the loss of methane from the side chain. Labelling studies *(Table 4.3)* indicate that the reaction involves the methyl of the side chain together with a hydrogen from the 6 (or 2) positions. This process is directly analogous to the loss of CH_4 from the heptan-4-one enolate *(equation 4.4)* and is represented in *equation 4.25 (Scheme 4.9)*.
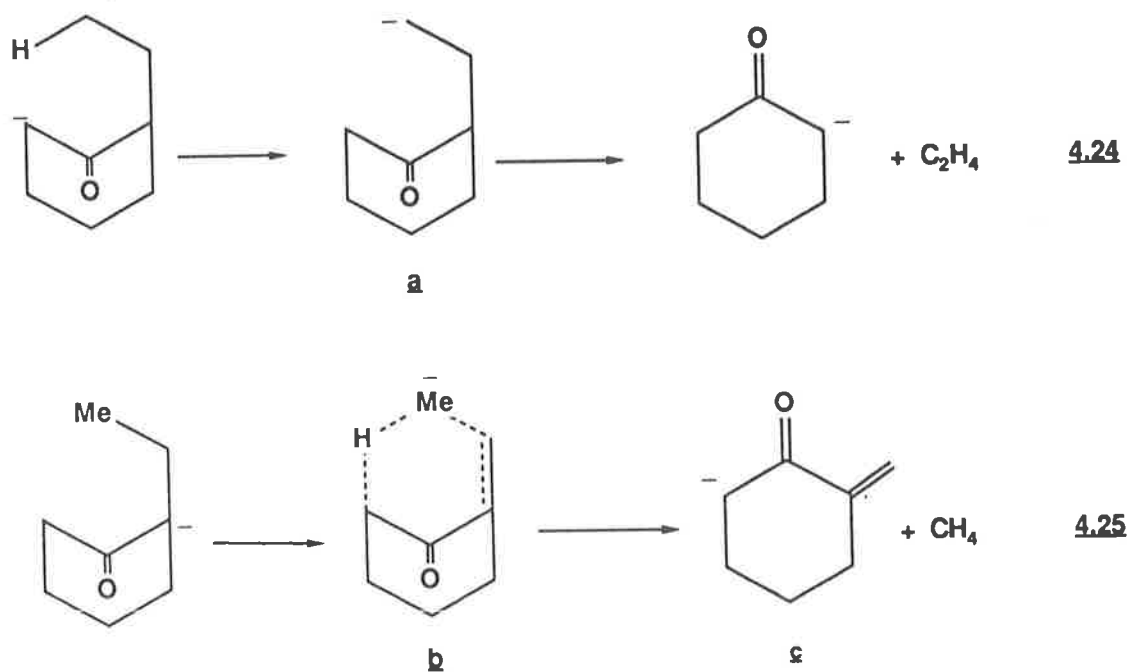
Scheme 4.9

The loss of ethene from the side chain of deprotonated 2-ethylcyclohexanone involves an anion on the opposite side of the molecule to the alkyl chain. The ethyl group can effect a conformation which allows proton transfer from the terminal position of the ethyl group to form a *(equation 4.24)*. Anion a then cleaves to form ethene and the cyclohexanone enolate anion as shown in *equation 4.24 (Scheme 4.9)*. In the alternative reaction *(equation 4.25)* the incipient methyl an-
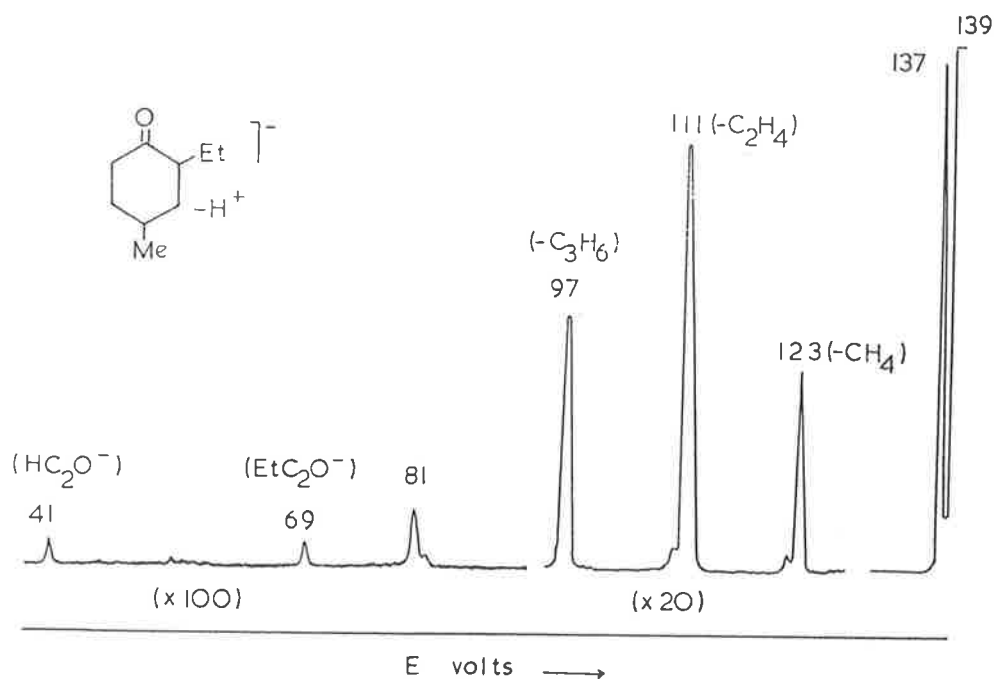
Figure 4.4: *CA MS of Enolate Ions from 2-Ethyl-4-Methylcyclohexanone. Width of major peaks at half height, m/z (volts ± 0.3) loss; 137 (44.6) H_2, 123 (50.8) CH_4, 111 (105.0) C_2H_4, 97 (91.6) C_3H_6. When a voltage of +2000 V is applied to the collision cell, the following collisional induced:unimolecular peak ratios are observed, m/z (CI:u); 137 (35:65), 123 (60:40), 97 (55:45), 81 (35:65) 69 (70:30) and 41 (90:10).*

ion of <u>b</u> removes an α proton to form <u>c</u> and methane. These two side-chain fragmentations together with the characteristic ring retro reaction are illustrated in the spectrum *(Figure 4.4)* of deprotonated 2-ethyl-4-methylcyclohexanone. *Figure 4.4* shows pronounced loss of CH_4 *(cf. equations 4.25)*, C_2H_4 *(cf. equations 4.24)* and C_3H_6 (the retro process; *cf. equations 4.25* and *Figure 4.3*)

In conclusion, *i*) the retro mechanism first described by Hunt[44,69], and shown in *equation 4.5* is specific, occurring without migration of hydrogens on the cyclohexanone ring. In the case of a 3-substituted cyclohexanone (which may form two enolate ions), the retro process involving the loss of the larger olefin is the major process; *ii*) differently substituted alkylcyclohexanones have characteristic fragmentation patterns, thus the technique is a viable one for analytical purposes, and *iii*) 2-substituted (≥Et) cyclohexanone enolates undergo the same characteristic fragmentations *(equations 4.3* and *4.4)* as acyclic ketone enolates.

Neutral Precursor	Anion	Loss						
		H·	D·ᵃ	H₂ᵃ	HD	(H₂+H₂)	(H₂+HD)	(HD+HD)
Cyclohexanone[ℵ]	$[M-H^+]^-$	18		100		3		
Cyclohexanone 2,2,6,6-D₄	$[M-D^+]^-$		100	100	12		2	
Cyclohexanone 3,3,5,5-D₄	$[M-H^+]^-$	21			100			2
Cyclohexanone 4,4-D₂	$[M-H^+]^-$	20			100		2	

Neutral Precursor	Anion	Loss					
		C_2H_4	$C_2H_2D_2$	C_4H_8	$C_4H_6D_2$	$C_4H_5D_3$	$C_4H_4D_4$
Cyclohexanone	$[M-H^+]^-$	15		3			
Cyclohexanone 2,2,6,6-D₄	$[M-D^+]^-$	13			3	0.5	
Cyclohexanone 3,3,5,5-D₄	$[M-H^+]^-$		10			0.5	2.5
Cyclohexanone 4,4-D₂	$[M-H^+]^-$		11		3		

[ℵ] Width of peaks at half height, m/z (volts ± 0.3) loss; 95 (46.5) H_2, 69 (99) C_2H_4, and 41 (45.2) C_4H_8. When a voltage of +2000 V is applied to the collision cell, the following collision induced : unimolecular ratio is indicated, m/z (CI:u); 95 (60:40), 69 (70:30) and 41 (60:40).

a. D· and H_2 = 2 a. m. u.

Neutral Precursor	Anion	Loss										
		H·	D·a	H2a	HD	(H2+H2)	(H2+HD)	(HD+HD)	CH3	CD3b	CH4	CH3D
2-Methyl D3 cyclohexanone	[M–H+]−	¶	100	100		3				1.5		
2-Methylcyclohexanone 2,6,6-D3	[M–D+]−		100	100	28		2			2		
2-Methylcyclohexanone 3,3,5,5-D4	[M–H+]−	15			100			2		2		
3-Methylcyclohexanone 2,2,6-D3	[M–D+]−		100	100	9		2				64	12
3-Methylcyclohexanone 3,5,5-D3	[M–H+]−	18			100			2			92	
3-Methylcyclohexanone 4,4-D2	[M–H+]−	¶	78	78	100		3	2			40	76
4-Methylcyclohexanone 2,2,6,6-D3	[M–D+]−		100	100	18	3					1	
4-Methylcyclohexanone 3,3,5,5-D3	[M–H+]−	18			100		2					1
4-Methylcyclohexanone 4-D	[M–H+]−	16		41	100	3					1	

Neutral Precursor	Anion	Loss									
		H2Ob	HOD	C2H4	C2H2D2	CO	C3H6	C3H5D	C3H4D2	C4H6	C4H5D
2-Methyl D3 cyclohexanone	[M–H+]−	1.5	1	10			1				
2-Methylcyclohexanone 2,6,6-D3	[M–D+]−		2	13					1		
2-Methylcyclohexanone 3,3,5,5-D4	[M–H+]−	2			11						
3-Methylcyclohexanone 2,2,6,6-D3	[M–D+]−		2	2			6			4	
3-Methylcyclohexanone 3,5,5-D3	[M–H+]−		2		2			6			
3-Methylcyclohexanone 4,4-D2	[M–H+]−	2			3				9		7
4-Methylcyclohexanone 2,2,6,6-D3c	[M–D+]−					2	15				
4-Methylcyclohexanone 3,3,5,5-D3d	[M–H+]−					2			15		
4-Methylcyclohexanone 4-De	[M–H+]−					2		13			

¶= not resolved but < 10%

a. D· and H2 = 2 a. m. u.

b. CD3 and H2O = 18 a. m. u.

Neutral Precursor	Anion	Loss									
		$C_4H_3D_3$	C_4H_8	$C_4H_5D_3$	$C_4H_4D_4$	C_5H_9D	$C_5H_8D_2$	$C_5H_7D_3$	$C_5H_6D_4$	$C_6H_6D_2O$	$C_6H_5D_3O$
2-Methyl D_3 cyclohexanone	$[M-H^+]^-$		2					2			
2-Methylcyclohexanone 2,6,6-D_3	$[M-D^+]^-$			2			2				
2-Methylcyclohexanone 3,3,5,5-D_4	$[M-H^+]^-$				2				2		
3-Methylcyclohexanone 2,2,6,6-D_3	$[M-D^+]^-$						2				1
3-Methylcyclohexanone 3,5,5-D_3	$[M-H^+]^-$	5						2			1
3-Methylcyclohexanone 4,4-D_2	$[M-H^+]^-$						2			1	
4-Methylcyclohexanone 2,2,6,6-D_3[c]	$[M-D^+]^-$						1				
4-Methylcyclohexanone 3,3,5,5-D_3[d]	$[M-H^+]^-$								1		
4-Methylcyclohexanone 4-D[e]	$[M-H^+]^-$					1					

c. The following losses are also observed; H_2CO (2%), $HDCO$ (4%), D_2CO (5%);

d. The following losses are also observed; $HDCO$ (6%);

e. The following losses are also observed; H_2CO (6%), $HDCO$ (2%).

Neutral Precursor	Anion	Loss											
		$H\cdot$	$D\cdot^a$	H_2^a	HD	(H_2+H_2)	(H_2+HD)	$(HD+HD)$	CH_4	CH_3D	C_2H_4	$C_2H_2D_2^b$	$C_2H_6^b$
2-Ethylcyclohexanone	$[M-H^+]^-$	¶		100		2			5		20		
2-(Ethyl-1,1-D$_2$cyclohexanone	$[M-H^+]^-$	¶		100		2			6		8	9	
2-Ethylcyclohexanone 2,6,6-D$_3$	$[M-D^+]^-$		100	100	17		2			6	22		
3-Ethylcyclohexanone	$[M-H^+]^-$	18		100		3					5		22
3-Ethylcyclohexanone 2,2,6,6-D$_3$	$[M-D^+]^-$		100	100	15		2				6		25
3-Ethylcyclohexanone 3,5,5-D$_3$	$[M-H^+]^-$	17			100			2				37	37
4-Ethylcyclohexanone	$[M-H^+]^-$	28		100		2							2
4-Ethylcyclohexanone 2,2,6,6-D$_3$	$[M-D^+]^-$		100	100	21		2						2
4-Ethylcyclohexanone 3,3,5,5-D$_3$	$[M-H^+]^-$	23			100			1					2
4-Ethylcyclohexanone 4-D	$[M-H^+]^-$	20			100		2						2

Neutral Precursor	Anion	Loss									
		C_2H_5D	C_4H_8	C_4H_7D	$C_4H_6D_6$	C_5H_8	$C_5H_5D_3$	C_6H_{12}	$C_6H_{11}D$	$C_6H_{10}D_2$	$C_6H_8D_8$
2-Ethylcyclohexanone	$[M-H^+]^-$		1					1			
2-(Ethyl-1,1-D$_2$cyclohexanone	$[M-H^+]^-$		1							1	
2-Ethylcyclohexanone 2,6,6-D$_3$	$[M-D^+]^-$				1				1		
3-Ethylcyclohexanone	$[M-H^+]^-$		8			3		2			
3-Ethylcyclohexanone 2,2,6,6-D$_3$	$[M-D^+]^-$		7			3				1	
3-Ethylcyclohexanone 3,5,5-D$_3$	$[M-H^+]^-$			8			3	1.5			
4-Ethylcyclohexanone	$[M-H^+]^-$		9					0.5			
4-Ethylcyclohexanone 2,2,6,6-D$_3$	$[M-D^+]^-$		12							1	
4-Ethylcyclohexanone 3,3,5,5-D$_3$	$[M-H^+]^-$	1.5			9						0.5
4-Ethylcyclohexanone 4-D	$[M-H^+]^-$			10					0.5		

¶not resolved but < 15%

a. $D\cdot$ and H_2 = 2 a. m. u.

b. $C_2H_2D_2$ and C_2H_6 = 30 a. m. u.

Table 4.3: CA Mass Spectra of Ethylcyclohexanone Enolates and Labelled derivatives.

Neutral Precursor	Anion	Loss									
		$H^{\cdot}$	$D^{\cdot a}$	H_2^a	HD	(H_2+H_2)	(H_2+HD)	$(HD+HD)$	C_2H_4	$C_2H_2D_2$	C_2H_6
2-n Propylcyclohexanone	$[M-H^+]^-$	¶		100		3			13		
2-n Propylcyclohexanone 2,6,6-D$_3$	$[M-D^+]^-$		100	100			2		15		
2-n Propylcyclohexanone 3,3,5,5-D$_3$	$[M-H^+]^-$	16			100			2	5	16	2
3-n Propylcyclohexanone	$[M-H^+]^-$	¶		100		3			6		
3-n Prpylcyclohexanone 2,2,6,6-D$_3$	$[M-D^+]^-$		100	100			2			6	
3-n Propylcyclohexanone 3,5,5-D$_3$	$[M-H^+]^-$	22			100			3	15		
2-n Butylcyclohexanone	$[M-H^+]^-$	¶		100		4			3		
3-n Butylcyclohexanone	$[M-H^+]^-$	¶		100		2			10		
2-iso Butylcyclohexanone	$[M-H^+]^-$	¶		100		2			1		
3-iso Butylcyclohexanone	$[M-H^+]^-$	¶		100		5			12		
2-n Pentylcyclohexanone	$[M-H^+]^-$	¶		100		2			5		
3-n Pentylcyclohexanone	$[M-H^+]^-$	¶		100		2			5		

Neutral Precursor	Anion	Loss								
		C_2H_5D	C_3H_6	C_3H_8	C_4H_6	$C_4H_4D_2$	$C_4H_3D_3$	C_4H_8	$C_4H_6D_2$	$C_4H_4D_4$
2-n Propylcyclohexanone	$[M-H^+]^-$		18					1		
2-n Propylcyclohexanone 2,6,6-D$_3$	$[M-D^+]^-$		18						1	
2-n Propylcyclohexanone 3,5,5-D$_3$	$[M-H^+]^-$		15							1
3-n Propylcyclohexanone	$[M-H^+]^-$			50	2					
3-n Prpylcyclohexanone 2,2,6,6-D$_3$	$[M-D^+]^-$	1.5		53		2				
3-n Propylcyclohexanone 3,5,5-D$_3$	$[M-H^+]^-$			55			2			
2-n Butylcyclohexanone	$[M-H^+]^-$			6				15		
3-n Butylcyclohexanone	$[M-H^+]^-$			1						
2-iso Butylcyclohexanone	$[M-H^+]^-$			4				6		
3-iso Butylcyclohexanone	$[M-H^+]^-$			0.5						
2-n Pentylcyclohexanone	$[M-H^+]^-$								1	
3-n Pentylcyclohexanone	$[M-H^+]^-$									

¶ = not resolvable; a. $D^{\cdot}$ and H_2 = 2 a. m. u.

Table 4.4: CA Mass Spectra of 2- and 3-Propylcyclohexanone Enolates and Higher Homologues.

Table 4.4 cont.: CA Mass Spectra of 2- and 3-Propylcyclohexanone Enolates and Higher Homologues.

Neutral Precursor	Anion	Loss								
		C_4H_{10}	C_5H_{10}	C_5H_9D	C_5H_{12}	C_6H_{10}	$C_6H_7D_3$	C_6H_{14}	C_7H_{12}	C_7H_{14}
2-n Propylcyclohexanone	$[M-H^+]^-$									2
2-n Propylcyclohexanone 2,6,6-D₃	$[M-D^+]^-$									
2-n Propylcyclohexanone 3,5,5-D₃	$[M-H^+]^-$									
3-n Propylcyclohexanone	$[M-H^+]^-$		5			6				1
3-n Prpylcyclohexanone 2,2,6,6-D₃	$[M-D^+]^-$		6			6				
3-n Propylcyclohexanone 3,5,5-D₃	$[M-H^+]^-$			7			6			
2-n Butylcyclohexanone	$[M-H^+]^-$									
3-n Butylcyclohexanone	$[M-H^+]^-$	29						5	4	
2-iso Butylcyclohexanone	$[M-H^+]^-$									
3-iso Butylcyclohexanone	$[M-H^+]^-$	8						0.5	0.5	
2-n Pentylcyclohexanone	$[M-H^+]^-$	5	8							
3-n Pentylcyclohexanone	$[M-H^+]^-$				31					

Neutral Precursor	Anion	Loss							
		$C_7H_{14}D$	$C_7H_{12}D_2$	$C_7H_{11}D_3$	$C_7H_{10}D_4$	C_7H_{16}	C_8H_{14}	C_8H_{16}	C_9H_{18}
2-n Propylcyclohexanone	$[M-H^+]^-$								
2-n Propylcyclohexanone 2,6,6-D₃	$[M-D^+]^-$	2							
2-n Propylcyclohexanone 3,5,5-D₃	$[M-H^+]^-$				2				
3-n Propylcyclohexanone	$[M-H^+]^-$								
3-n Prpylcyclohexanone 2,2,6,6-D₃	$[M-D^+]^-$		1						
3-n Propylcyclohexanone 3,5,5-D₃	$[M-H^+]^-$			1					
2-n Butylcyclohexanone	$[M-H^+]^-$							1	
3-n Butylcyclohexanone	$[M-H^+]^-$							1	
2-iso Butylcyclohexanone	$[M-H^+]^-$							0.5	
3-iso Butylcyclohexanone	$[M-H^+]^-$							0.1	
2-n Pentylcyclohexanone	$[M-H^+]^-$								1
3-n Pentylcyclohexanone	$[M-H^+]^-$					2	2		0.2

Chapter 5

CA Mass Spectra of Aromatic Alkoxide Ions.

5.1 Introduction.

Fragmentation studies have been carried out for a number of alkoxide ions. These include ethoxide[74,75] and methoxide[76,77] negative ions. The loss of dihydrogen from ethoxide is reported to be a two step process, the first step of the reaction involving the formation of a solvated hydride/acetaldehyde anion, the second, the removal of a proton from the methyl group of acetaldehyde by the hydride ion. This reaction is shown in *equation 5.1*. The loss of dihydrogen from methoxide is however a 1,1 loss. An experimental/*ab initio* study indicates the reaction to be a two step process involving the intermediacy of the solvated hydride/formaldehyde anion as shown in *equation 5.2*.

$$CH_3CH_2O^- \longrightarrow [H^-(CH_3CHO)] \longrightarrow \bar{C}H_2CHO + H_2 \qquad (5.1)$$

$$CH_3O^- \longrightarrow [H^-(H_2CO)] \longrightarrow [HCO]^- + H_2 \qquad (5.2)$$
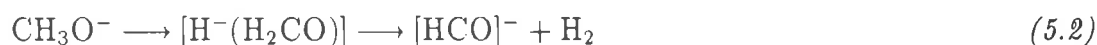
In this chapter the CA fragmentations of a number of alkoxides derived from aryl alcohols are discussed *(cf. also refs 78 and 96)*. The main aims of this study were to determine whether *i*) $PhCH_2O^-$ undergoes 1,1 elimination of H_2 like MeO^- and *ii*) whether ions $Ph(CH_2)_nCH_2CH_2O^-$ (n=0-2) undergo 1,2 elimination of H_2 like EtO^-, or whether they fragment by alternative pathways.

5.2 Results and Discussion.

Compounds used in this study are listed in *Tables 5.1* to *5.4*. Several syntheses used to produce deuterium labelled compounds are summarized in *equations 5.3* to *5.6*; full details are given in the experimental section.
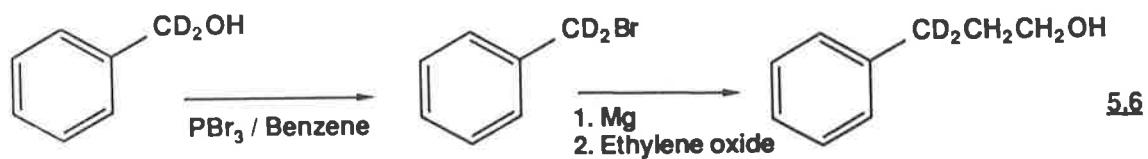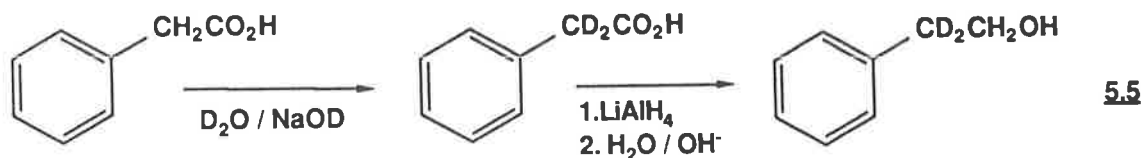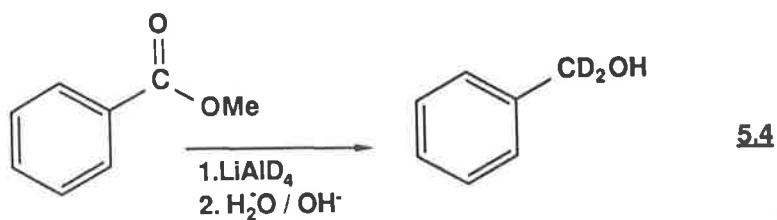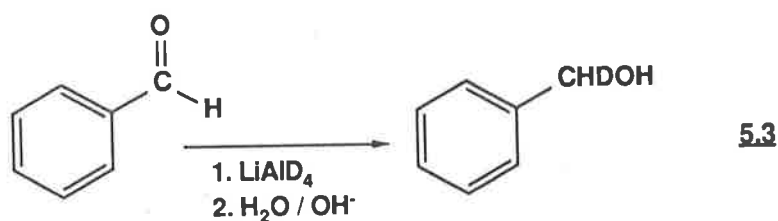
5.2.1 Fragmentations of the Benzyloxy Negative Ion.

The CA mass spectra of $PhCH_2O^-$ and of its deuterium labelled derivatives are listed in *Table 5.1*. The major fragmentations observed for the benzyloxy ion are losses of $H\cdot$, H_2, CH_2O and C_6H_6.

The competitive losses of formaldehyde and benzene are summarized in *equations 5.7* and *5.8 (Scheme 5.1)* respectively. They are likely to proceed through solvated ion complex $\underline{a}$. This ion complex can either fragment directly to form the phenyl anion and formaldehyde or the phenyl anion can deprotonate formaldehyde to give benzene and deprotonated formaldehyde. These losses are also preceded and/or accompanied by partial hydrogen/deuterium scrambling of the benzylic and phenyl hydrogens. For example, $C_6D_5CH_2O^-$ loses CH_2O and $CHDO$ and C_6HD_5 and $C_6H_2D_4$ in the respective ratios 3.5:1 and 6:1. Benzylic/phenyl scrambling has been observed previously for negative ions[79,80,81]; in this case it is suggested that the randomization either occurs as shown in *equation 5.9*, or by hydrogen interchange in complex $\underline{a}$.

$$C_6H_5CH_2O^- \longrightarrow [\,C_6H_5^-(CH_2O)\,] \underset{\underline{a}}{\Big\langle} \begin{array}{l} C_6H_5^- + CH_2O \qquad \underline{5.7} \\[2em] H\bar{C}{=}O + C_6H_6 \qquad \underline{5.8} \end{array}$$

$$\text{Ph—}CH_2\bar{O} \rightleftharpoons \text{Ph—}CH_2OH \rightleftharpoons \text{Ph—}\bar{C}HOH \qquad \underline{5.9}$$

$$\underline{5.11} \quad (C_6H_4)\,CH_2\bar{O} + H\cdot \longleftarrow PhCH_2O^- \longrightarrow [PhCHO]^- + H\cdot \qquad \underline{5.10}$$
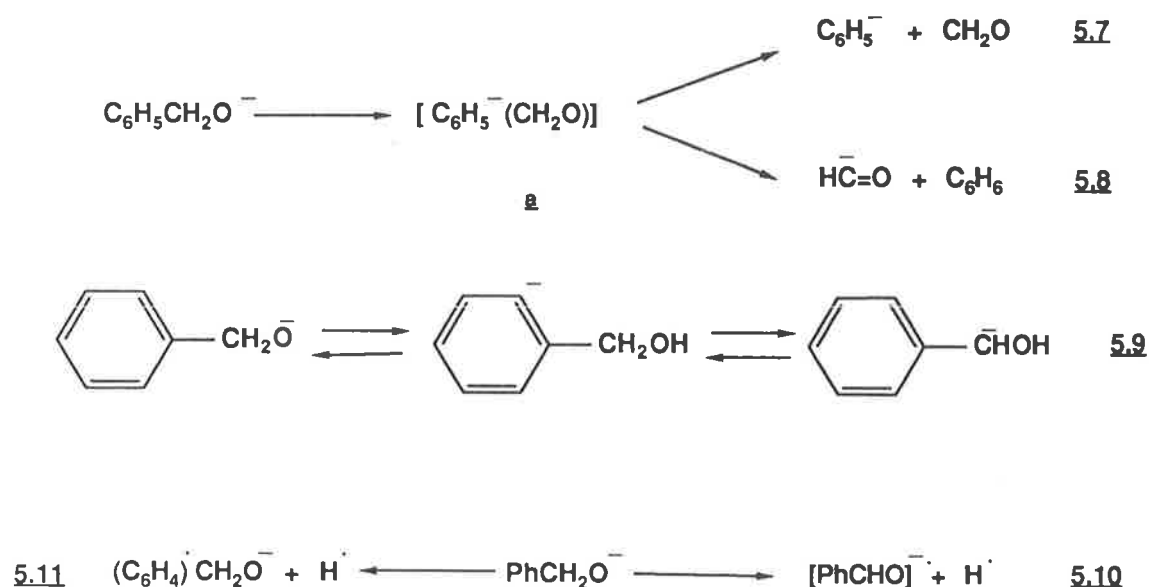
Scheme 5.1

It is not possible to make anything more than qualitative statements concerning the losses of $H\cdot$ and H_2 from $PhCH_2O^-$ because the deuterium labelled ions can, in principle, lose 1, 2, 3 and 4 a. m. u. [i.e. $H\cdot$, ($D\cdot$ or H_2), HD and D_2]. In

addition, deuterium isotope effects may operate for the various losses. However since $PhCD_2O^-$ and $C_6D_5CH_2O^-$ both lose $H\cdot$ to a large extent, the processes shown in *equations 5.10* and *5.11* must both occur.

Loss of Dihydrogen from the Benzyloxy Anion.

There have been a number of studies concerning the losses of H_2 from simple anions in the gas phase such as $EtO^{-74,75}$ and MeO^{-76}. In the first example, the loss of hydrogen was shown to be specific 1,2 elimination reaction, while for methoxide the loss is a 1,1 elimination *(equations 5.1* and *5.2)*.

In the case of $PhCH_2O^-$, it is possible for dihydrogen to be eliminated by the pathways outlined in *equations 5.12* and *5.13 (Scheme 5.2)*.

$$PhCH_2O^- \longrightarrow [\bar{H}\,(PhCHO)] \begin{array}{c} \nearrow Ph\bar{C}{=}O + H_2 \qquad \underline{5.12} \\ \\ \searrow (C_6H_4)^-CHO + H_2 \qquad \underline{5.13} \end{array}$$

$$\mathbf{a}$$
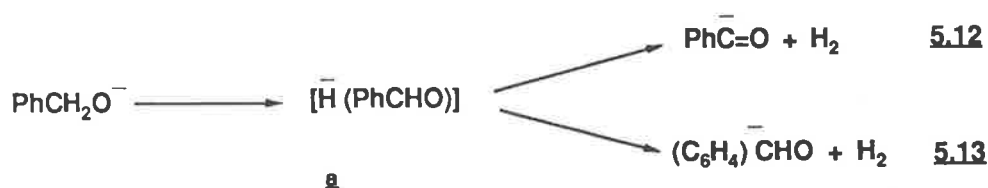
Scheme 5.2

Both reactions are likely to proceed though solvated intermediate $\underline{a}$. If the loss of hydrogen is specifically 1,1, the products will be H_2 and $Ph\bar{C}O$. If the hydride ion deprotonates the phenyl ring, the products will be H_2 and $(C_6H_4)^-CHO$. The data in *Table 5.1*, shows that $PhCD_2O^-$ loses HD but not D_2, while $C_6D_5CH_2O^-$ loses mainly HD together with a small amount of D_2. In the latter case there is also a peak corresponding to loss of 2 a. m. u; the magnitude of the loss of H_2 could not be determined because H_2 has the same mass as $D\cdot$. Ion $C_6H_2D_3CD_2O^-$ loses $(H_2, D\cdot)$, HD and D_2; the relative loss of H_2 could not be determined. Nevertheless it is clear that the major loss of dihydrogen from $PhCH_2O^-$ occurs as shown in *equation 5.13*; a lesser amount may be lost by the route indicated in *equation 5.12 (Scheme 5.2)*. Some hydrogen scrambling also occurs, it is not possible to determine whether the scrambling occurs before the solvated intermediate is formed or whether there
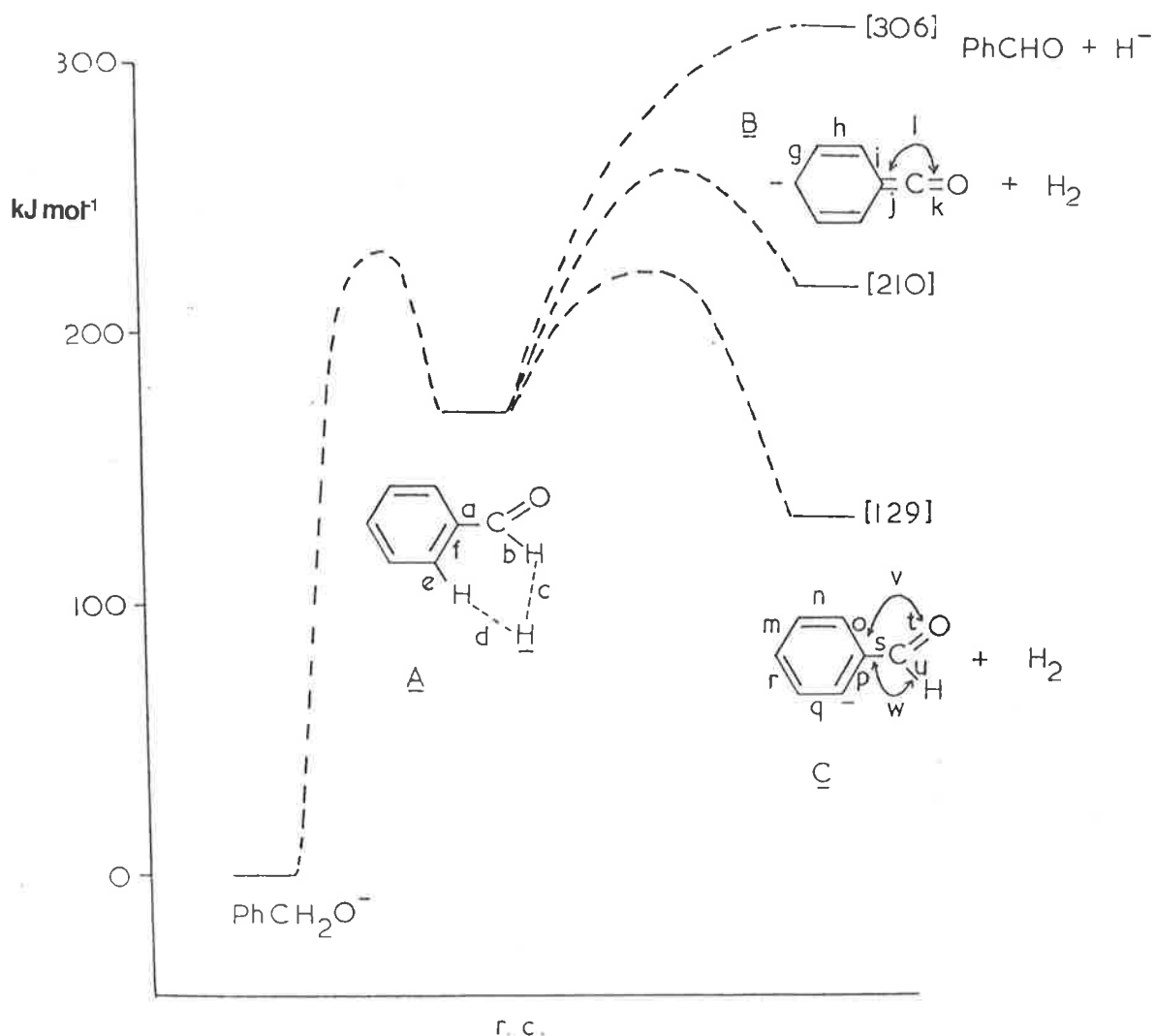
Figure 5.1: Ab initio *calculations (3-21G) for the loss of* H_2 *from Deprotonated Benzyl alcohol. Geometries* (Å, °) *as follows:* $PhCH_2O^-$, $C—C = 1.56$, $C—H = 1.12$, $C—O = 1.35$; *A*, $a = 1.46$, $b = 1.09$, $c = 2.10$, $d = 2.02$, $e = 1.08$, $f = 1.39$; *B*, $g = 1.41$, $h = 1.36$, $i = 1.48$, $j = 1.30$, $k = 1.21$, $l = 180$; *C*, $m = 1.40$, $n = 1.37$, $o = 1.40$, $p = 1.42$, $q = 1.43$, $r = 1.38$, $s = 1.46$, $t = 1.23$, $u = 1.09$, $v = 128$, $x = 112$. *Energies (a.u.):* $PhCH_2O^- = -342.02814$, *B* $= -340.32535$, *C* $= -340.85606$, $H_2 = -1.12296$ *hartrees.*

is some hydrogen equilibration occurring in the solvated hydride **a** *(Scheme 5.2)* before fragmentation.

Ab Initio Calculations of the Benzyloxy Anion

Ab initio calculations[82] using GAUSSIAN 82[83] at the 3-21G[84] level have been used to determine possible products and intermediates of the reactions shown in *equations 5.12* and *5.13 (Scheme 5.2)*. The medium level calculation was done because of the large size of the system and the data obtained should only be used in a qualitative fashion. It can be seen *(Figure 5.1)* that the first step in the reaction involves lengthening of a benzylic C—H bond with the formation of

intermediate $\underline{A}$ *(cf. Scheme 5.2)* in which the hydride ion is closer to an ortho ring hydrogen (a=2.02 Å) than to the formyl hydrogen (c=2.10 Å). Intermediate $\underline{A}$ can fragment in three ways: *i*) to form H^- and benzaldehyde, a reaction endothermic by 306 kJmol^{-1}, *ii*) the formyl proton may be removed to yield $\underline{B}$ (calculations have shown that the charged species is symmetrical), a reaction calculated to be 210 kJmol^{-1} endothermic and *iii*) deprotonation of an ortho proton of the aromatic ring forms $\underline{C}$; this reaction is calculated to be 129 kJmol^{-1} endothermic. Thus the *ab initio* calculations indicate that $\underline{C}$ is the thermodynamically favoured product, in agreement with the experimental observations outlined above.

5.2.2 Fragmentations of the 2-Phenylethanoxide Anion.

The fragmentations of the alkoxide ions derived from 2-phenylethanol and its labelled derivatives are shown in *Table 5.2*.

$$[\bar{H}\,(PhCH_2CHO)] \longrightarrow Ph\bar{C}HCHO + H_2 \qquad \underline{5.14}$$

$$PhCH_2CH_2O^-$$

$$[Ph\bar{C}H_2\,(CH_2O)] \longrightarrow Ph\bar{C}H_2 + CH_2O \qquad \underline{5.15}$$

$$(C_6H_4)CH{=}CH_2 + H_2O \qquad \underline{5.16}$$

$$PhCH_2CH_2O^- \longrightarrow Ph\bar{C}HCH_2OH \longrightarrow [HO^-(PhCH{=}CH_2)]$$

$$\underline{a} \qquad\qquad \underline{b}$$

Scheme 5.3

$$PhCH{=}\bar{C}H + H_2O \qquad \underline{5.17}$$
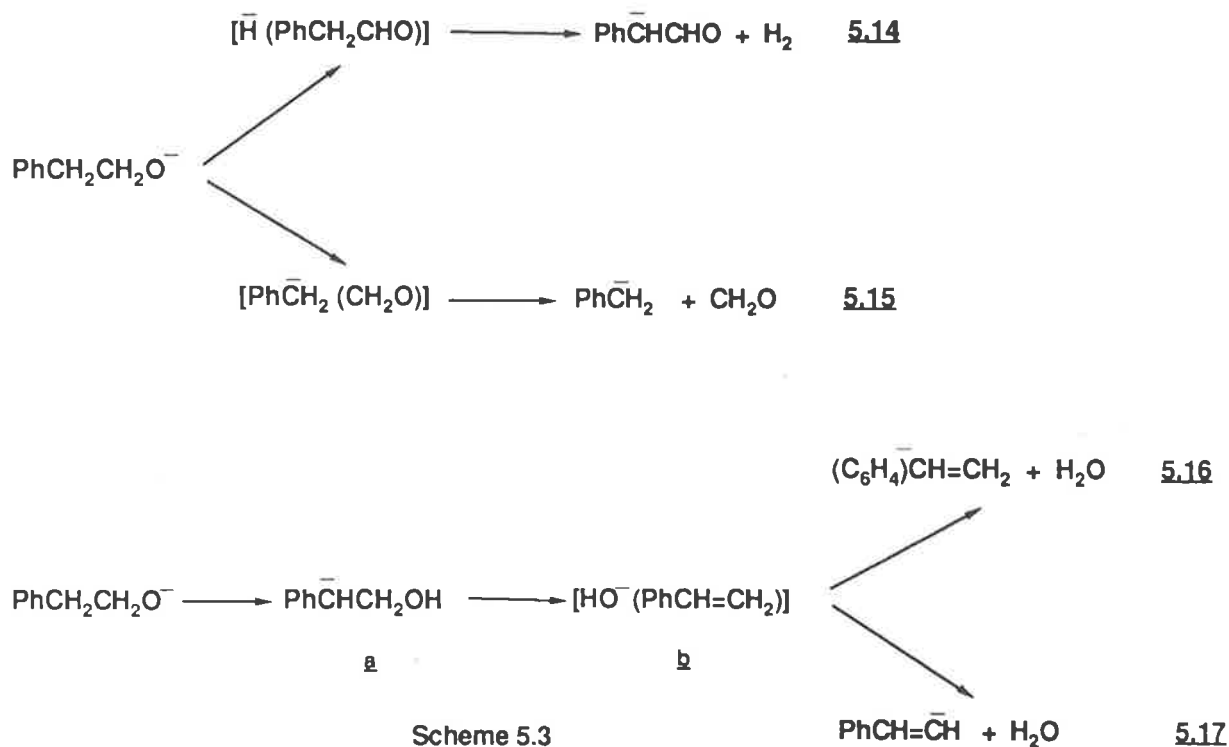
The fragmentations observed for these compounds are quite simple. There are three basic fragmentations observed for $PhCH_2CH_2O^-$; *viz i*) loss of dihydrogen as shown in *equation 5.14 (Scheme 5.3)* to form $Ph\bar{C}HCHO$, *ii*) loss of formaldehyde to form the benzyl anion either by a concerted process, or by the stepwise reaction

68

$PhCH_2CH_2O^-$

91 $(-CH_2O)$

121

119

$(-H_2O)$

103

E   volts $\longrightarrow$
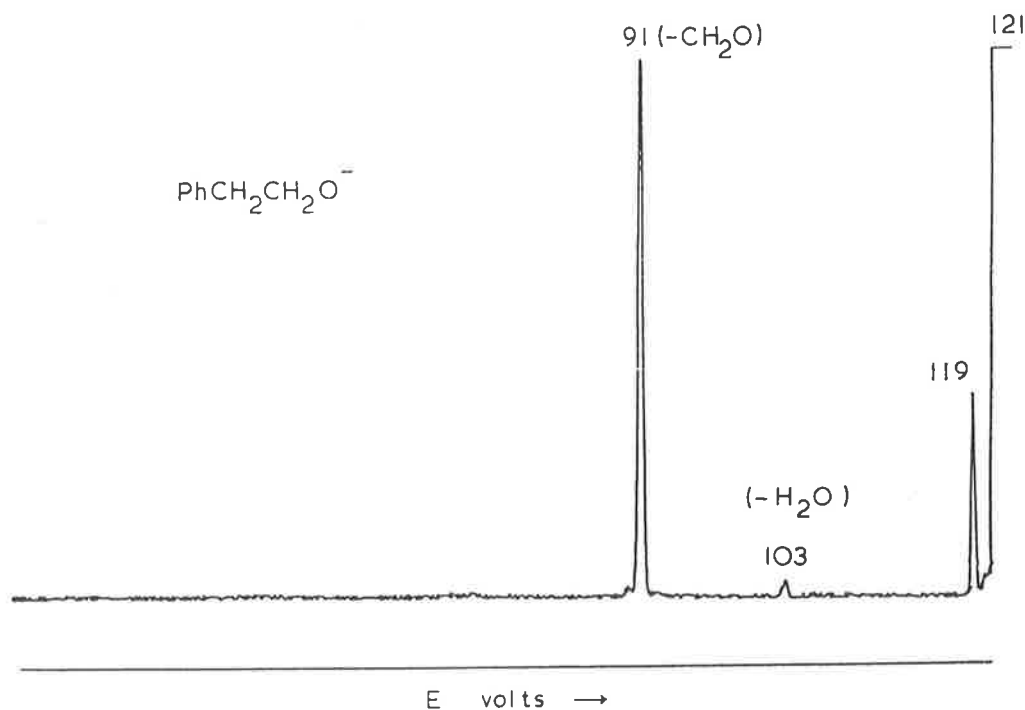
Figure 5.2: *CA Mass spectrum of PhCH$_2$CH$_2$O$^-$.*

shown in *equation 5.15 (Scheme 5.3)* and *iii*) the loss of water which although only a minor process is also the most complicated. The ion $PhCD_2CH_2O^-$ specifically loses HOD, whereas $PhCH_2CD_2O^-$ loses H_2O and HOD (3:1). Thus the loss of water from $PhCH_2CH_2O^-$ occurs *via* two mechanisms; it is suggested that the initial step in both is a proton transfer reaction in which a benzylic hydrogen specifically migrates to oxygen to form a. This anion may then form solvated intermediate b *(Scheme 5.3)*. The OH$^-$ ion of b can then either deprotonate the ring as shown in *equation 5.16*, or the side chain *(equation 5.17)*.

77   91   105

$Ph|CH_2|CH_2|CH_2O^-$

$(-C_7H_8)$
43

$(-C_6H_6)$
57

$(-C_3H_4O)$

$(HC=O)$
29

77

79

91

103

115

105 $(-CH_2O)$

117 $(-H_2O)$

133

135

$(\times 50)$

E   volts $\longrightarrow$
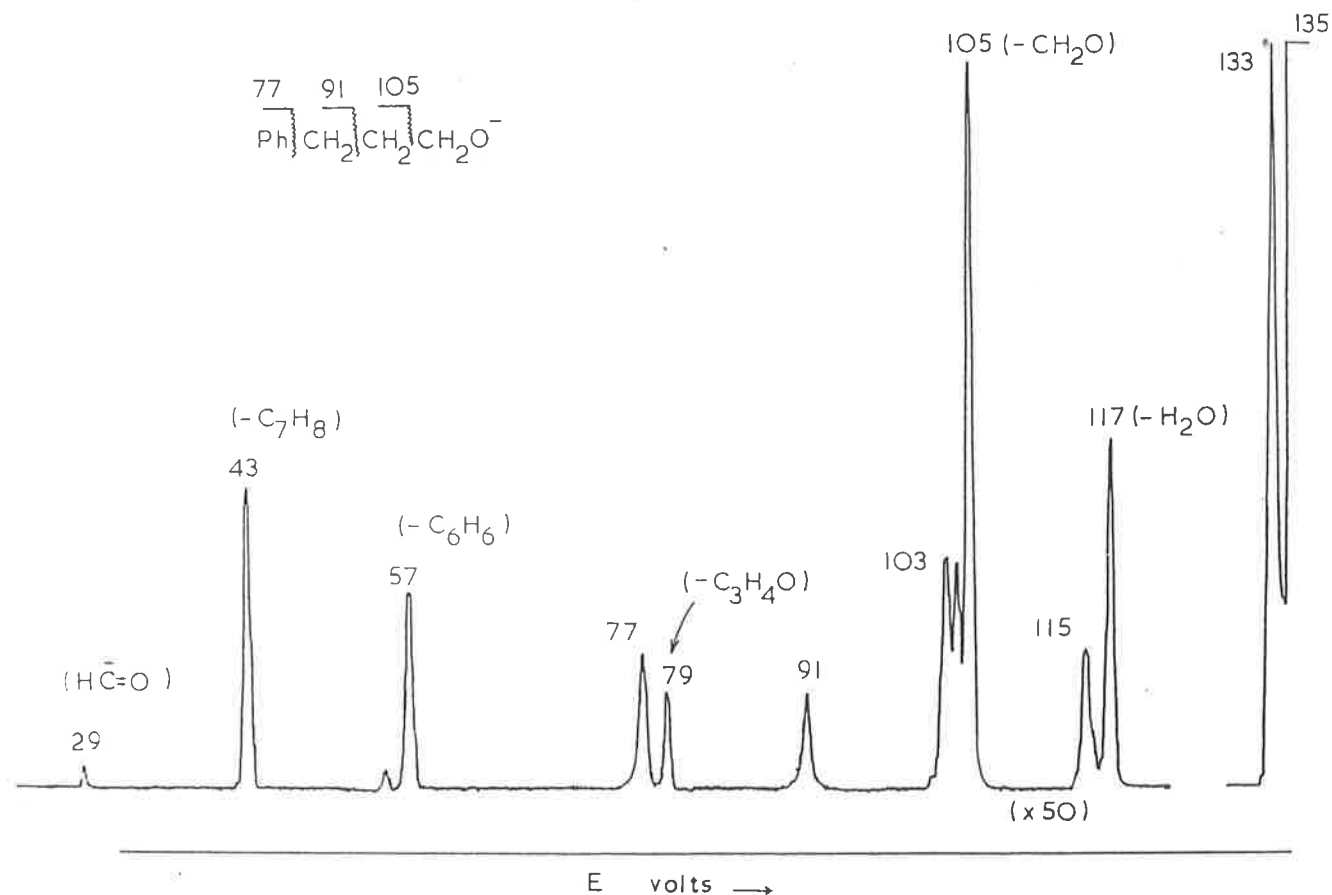
Figure 5.3: *CA Mass spectrum of* $PhCH_2CH_2CH_2O^-$.

5.2.3   Fragmentations of the 3-Phenylpropanoxide Anion.

The fragmentations of the alkoxide ions derived from 3-phenylpropan-1-ol and its deuterium labelled derivatives are shown in either *Table 5.3* or *Figure 5.3*.

The fragmentations of these compounds are the most complicated of all the aromatic alkoxides studied. Fragmentations are summarized in *Schemes 5.4* and *5.5*.

Loss of dihydrogen is again the major process. The spectra of the deuterium labelled analogues show there are two specific losses of dihydrogen. Both can be rationalized by the initial formation of complex a *(Scheme 5.4)*. The major loss is the 1,2 elimination shown in *equation 5.18 (Scheme 5.4)*; the minor loss occurs by removal of a benzylic hydrogen *(equation 5.19, Scheme 5.4)* The loss of C_3H_4O shown in *Figure 5.3* must involve two proton transfers. Labelling data *(Table 5.3)* indicate that protons from carbons 1 and 2 transfer to the aromatic ring. This can be rationalized in terms of an initial intermediate a undergoing nucleophilic substitution to form b which then further rearranges by intramolecular proton transfer to yield $C_6H_7^-$ as shown in *equation 5.20 (Scheme 5.4)*. This reaction

70

represents only the second reported example of a specific double hydrogen transfer reaction in negative ion gas phase chemistry *(see chapter 4)*.

$$Ph(CH_2)_3O^- \longrightarrow [H^-(PhCH_2CH_2CHO)]$$

a

$$\longrightarrow PhCH_2\overset{-}{C}HCHO + H_2 \qquad \underline{5.18}$$

$$\longrightarrow Ph\overset{-}{C}HCH_2CHO + H_2 \qquad \underline{5.19}$$

$$\longrightarrow CHO \longrightarrow C_6H_7^- + CH_2=CHCHO \qquad \underline{5.20}$$

b   **Scheme 5.4**
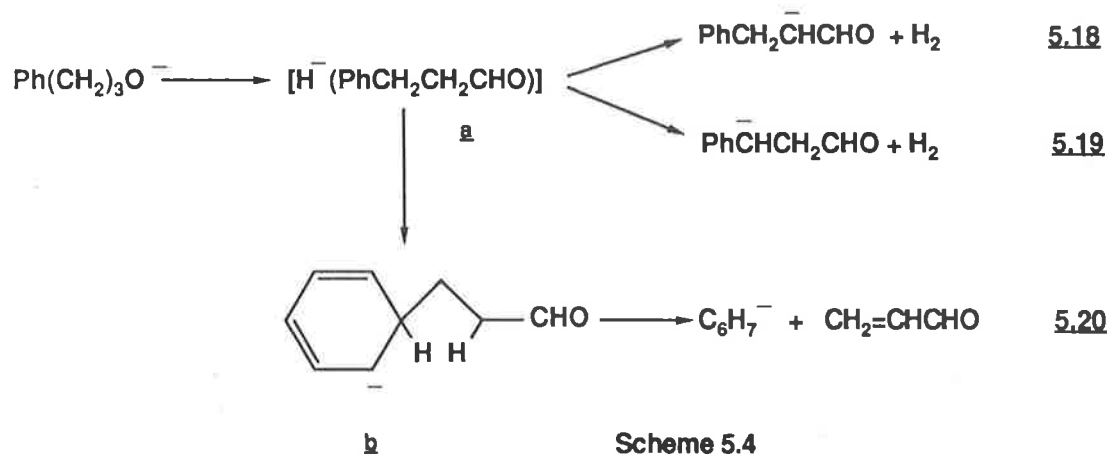
The loss of water from $PhCH_2CH_2CH_2O^-$ requires an initial hydrogen transfer reaction to oxygen. Labelling data *(Table 5.3)* indicate that the transferred hydrogen comes from either the central carbon to form **a** *(equation 5.21)* or from the benzylic position to form **b** *(equation 5.22)*. It is likely that the first process then proceeds through a OH^-/3-phenylpropene complex; deprotonation then occurs from the most acidic position [i.e. the benzylic position *(equation 5.23)*]. In the second reaction, an OH^-/phenylcyclopropane complex may be formed which then deprotonates at the benzylic position as shown in *equation 5.24*.

$$\underline{5.21} \quad PhCH_2\overset{-}{C}HCH_2OH \longleftarrow PhCH_2CH_2CH_2O^- \longrightarrow Ph\overset{-}{C}HCH_2CH_2OH \quad \underline{5.22}$$

a   b

$$[HO^-(PhCH_2CH=CH_2)] \qquad\qquad [HO^-(Ph\text{—}\triangleleft)]$$

$$\underline{5.23} \quad Ph\overset{-}{C}HCH=CH_2 + H_2O \qquad \textbf{Scheme 5.5} \qquad Ph\triangleleft + H_2O \quad \underline{5.24}$$
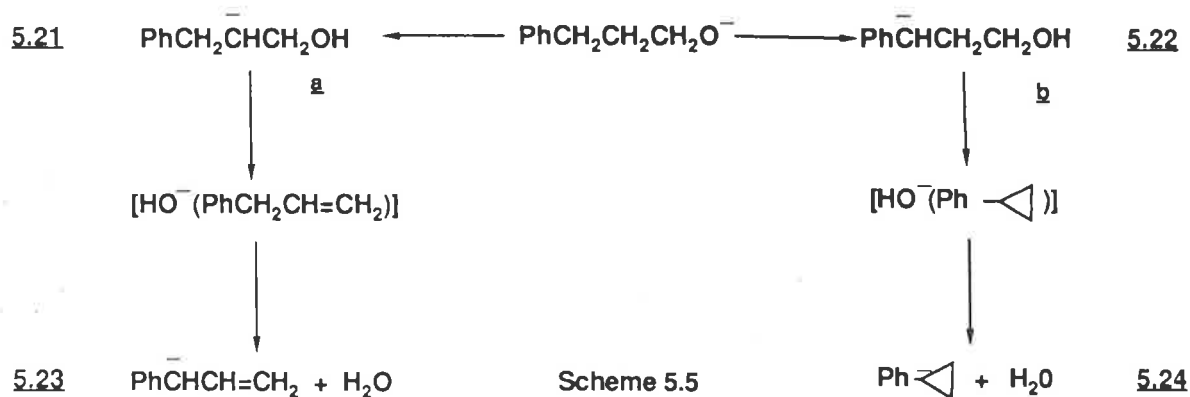
Two other reactions involve the probable formation of solvated intermediate **a**

71

(Scheme 5.6). This complex can; *i*) form deprotonated formaldehyde and C_8H_{10} as shown in *equation 5.26* and *ii*) fragment directly to form $C_8H_9^-$ and formaldehyde *(equation 5.27)*. The ion $C_8H_9^-$ *(m/z=105)* formed by this process could have two possible structures; these are shown as $\underline{A}$ and $\underline{B}$ in *Scheme 5.6*. Anion $\underline{A}$ can be stabilized by negative hyperconjugation[85], but it seems the less likely of the two possible structures. The alternative structure is the spiro intermediate $\underline{B}$. We have not been able to differentiate experimentally between the two structures.

$$Ph(CH_2)_3O^- \longrightarrow [C_8H_9^-(CH_2O)] \nearrow H\bar{C}{=}O + C_8H_{10} \qquad \underline{5.26}$$
$$\underline{a} \searrow C_8H_9^- + CH_2O \qquad \underline{5.27}$$

$$PhCH_2CH_2^-$$

$$\underline{A} \qquad\qquad\qquad \underline{B}$$
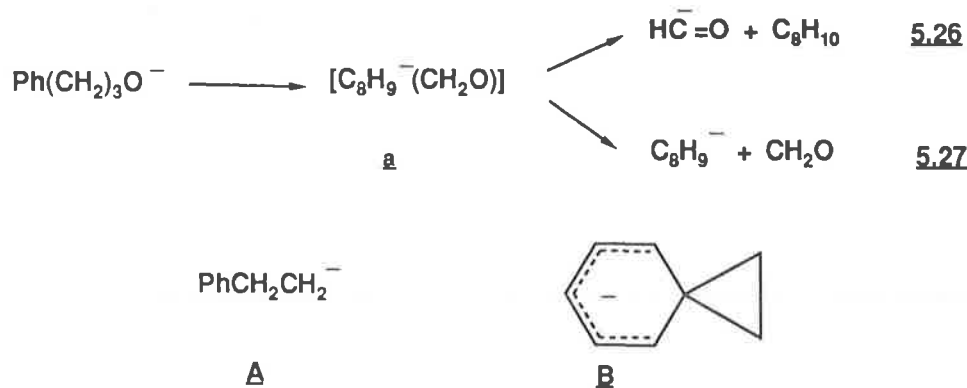
Scheme 5.6

There are several other fragmentations that can be seen in *Figure 5.3*, they can be rationalized as follows: *i*) formation of deprotonated benzene and deprotonated oxetane *(equations 5.27 and 5.28)*, *ii*) formation of deprotonated ethylene oxide[1] and the benzyl anion *(equations 5.31 and 5.32)*. The precise mechanism for the formation of these product ions is not known, and some hydrogen/deuterium scrambling occurs for each process. For example, $C_6D_5(CH_2)_3O^-$ yields $C_6D_5^-$, $C_6HD_4^-$ and $C_6H_2D_3^-$ (5:4:1); $PhCD_2(CH_2)_2O^-$ and $Ph(CH_2)_2CD_2O^-$ give only $C_6H_5^-$, while $PhCH_2CD_2CH_2O^-$ gives $C_6H_5^-$ and $C_6H_4D^-$ (4:1) (see *Table 5.3* for other examples). A rationale for the scrambling is shown in *equations 5.29* and *5.30 (Scheme 5.7)*. The structures of the intermediates involved in the losses of ethylene oxide *(equation 5.31)* and oxetane *(equation 5.27)* are not known; they may be simple ion complexes of the standard type. Alternatively, $\underline{B}$ and $\underline{C}$ *(Scheme 5.7)* could have spiro structures; for example $\underline{C}$ could correspond to the Smiles intermediate $\underline{D}$[86] *(see Chapter 8 for further details)*.

---

[1]The possibility that the deprotonated ethylene oxide rearranges to the acetaldehyde ion cannot be discounted.

Scheme 5.7
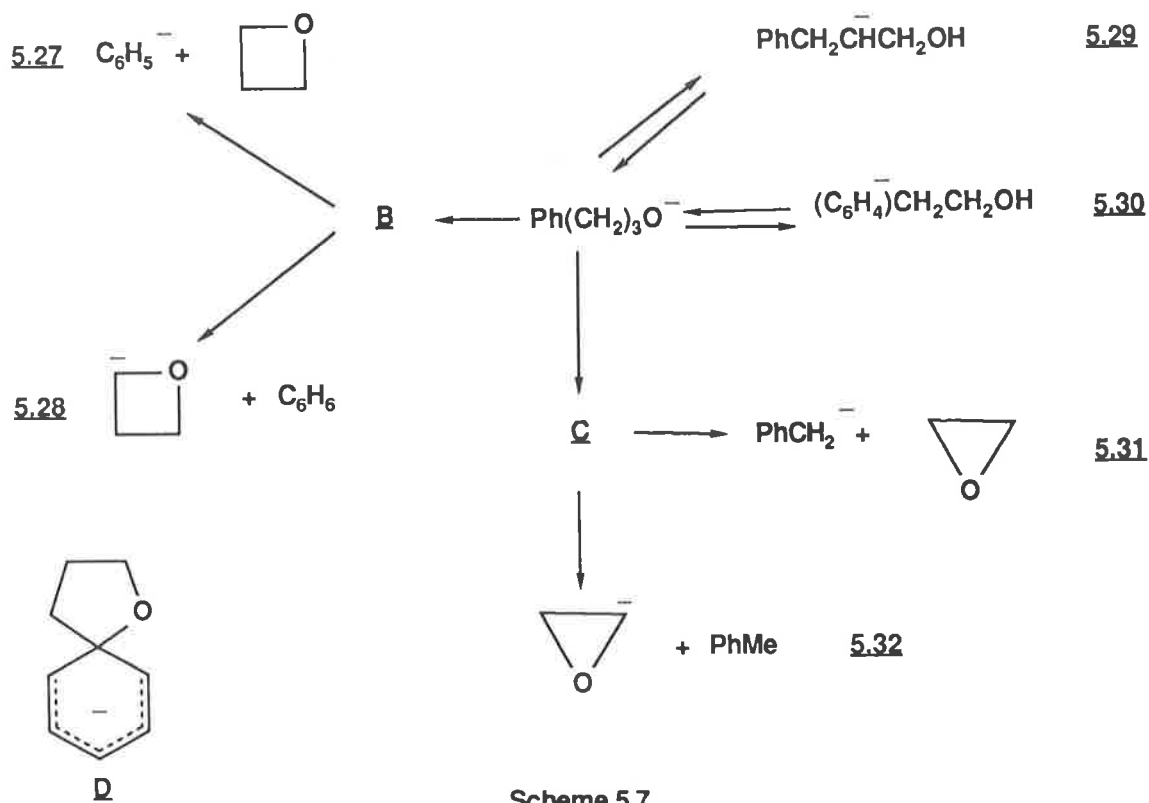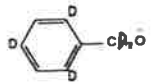
5.2.4 Fragmentations of the 4-Phenylbutanoxide and 5-Phenylpentanoxide Anion.

The CA mass spectra of the alkoxide ions derived from 4-phenylbutan-1-ol and 5-phenylpentan-1-ol and their labelled derivatives are shown in *Table 5.4*.

The base peak of the spectra of both unlabelled alkoxides is formed by the loss of dihydrogen; as in previous cases this loss occurs mainly *via* a 1,2 elimination. Loss of formaldehyde is likely to occur *via* a spiro intermediate analogous to that described in *Scheme 5.6*. Another interesting reaction is the hydrogen transfer reaction which occurs from the benzylic position to the oxygen. This is illustrated for example by the formation of DO^- from $PhCD_2(CH_2)_3O^-$. The benzyl anion is also formed, this ion is formed from all alcohols reported in this chapter. In the case of $PhCH_2CH_2O^-$ the formation of $PhCH_2^-$ is due to direct cleavage of the $[M - H^+]^-$ anion, but in all the other cases the exact mechanism is not known. Two possibilities are: *i*) S_Ni attack of the oxygen at the carbon *3* to the aromatic ring. or *ii*) nucleophilic attack of the oxygen onto the aromatic ring *via* a Smiles rearrangement *(cf.* D. *Scheme 5.7).*

In conclusion, the answers to the questions posed initially are; i) the major loss of H_2 from $PhCH_2O^-$ is not a 1,1 elimination; the major product of the reaction is $(C_6H_4)^-CHO$, ii) ions $Ph(CH_2)_nCH_2CH_2O^-$ (n=0-2) undergo 1,2 elimination of H_2 (like EtO^-).

Table 5.1: CA Mass Spectra of the Alkoxide ions derived from Benzyl Alcohol and Labelled Analogues.

Initial Ion	Loss												
	H·	D·a	H₂a	HD	D₂	CH₂O	CHDO	CD₂O	C₆H₆	C₆H₅D	C₆H₄D₂	C₆H₂D₄	C₆HD₅
PhCH₂O⁻	81		44			100			2				
PhCHDO⁻	40	23	23	7		15	100		1.0	0.8			
PhCD₂O⁻	55	5.5	5.5	8			26	100		0.4	0.04		
C₆D₅CH₂O⁻	100	58	58	17	0.02	88	25					0.1	0.6
	18	6	6	5	2		13	100				0.3	0.02

a. D· and H₂ = 2 a. m. u.

Table 5.2: CA Mass Spectra of Labelled Phenylethanol Alkoxide ions.

Initial Ion	Loss				
	HD	H_2O	HOD	CH_2O	CD_2O
$PhCD_2CH_2O^-$	18		0.5	100	
$PhCH_2CD_2O^-$	24	2.2	0.7		100

Initial Ion	Loss										
	H_2	HD	H_2O	HOD	(H_2O+H_2)	(H_2O+HD)	CH_2O	CD_2O	$(CH_2O+H\cdot)$	$(CH_2O+D\cdot)^{a\cdot}$	$(CD_2+H\cdot)$
$PhCH_2CH_2CH_2O^{-\aleph}$	100		1.0		0.5		2.2		0.6		
$C_6D_5CH_2CH_2CH_2O^-$	100		1.2		0.2	0.4	2.9			1.6	
$PhCD_2CH_2CH_2O^-$	100	8		0.5			2.7		0.2		
$PhCH_2CD_2CH_2O^-$	52	100	0.9	0.8		$0.5^{b\cdot}$	4.2		1.2	1.0	
$PhCH_2CH_2CD_2O^-$		100	1.2			0.4		2.5			0.9

Initial Ion	Loss			Formation				
	$(CH_2O+H_2)^{a\cdot}$	(CH_2+HD)	(CD_2+H_2)	$C_7H_7^-$	$C_7H_6D^-$	$C_7H_5D_2^-$	$C_7H_3D_4^-$	$C_7H_2D_5^-$
$PhCH_2CH_2CH_2O^{-\aleph}$	0.7			0.2				
$C_6D_5CH_2CH_2CH_2O^-$	1.6						0.05	0.2
$PhCD_2CH_2CH_2O^-$		0.2				0.1		
$PhCH_2CD_2CH_2O^-$	1.0	0.5		0.1	0.02			
$PhCH_2CH_2CD_2O^-$			0.6	0.2				

$\aleph$ Ion formed from $PhCH_2CH_2CH_2OD$.

a. $(CH_2O+D\cdot)$ and (CH_2O+H_2) both = 32 a. m. u.

b. This peak is a combination of $-(H_2O+HD)$ and $-(HOD+H_2)$

Initial Ion	Formation							
	$C_6H_7^-$	$C_6H_6D^-$	$C_6H_2D_5^-$	$C_6H_5^-$	$C_5H_4D^-$	$C_6H_2D_3^-$	$C_6HD_4^-$	$C_6D_5^-$
$PhCH_2CH_2CH_2O^-$	1.0			1.6				
$C_6D_5CH_2CH_2CH_2O^-$			0.5			0.1	0.4	0.5
$PhCD_2CH_2CH_2O^-$	0.6			0.7				
$PhCH_2CD_2CH_2O^-$		0.6		1.5	0.4			
$PhCH_2CH_2CD_2O^-$		0.6		0.7				

Initial Ion	Formation							
	$C_3H_5O^-$	$C_3H_4DO^-$	$C_3H_3D_2O^-$	$C_2H_3O^-$	$C_2H_2DO^-$	$C_2HD_2O^-$	CHO^-	CDO^-
$PhCH_2CH_2CH_2O^-$	1.9			2.5			0.1	
$C_6D_5CH_2CH_2CH_2O^-$	1.2	0.2		2.2			0.2	
$PhCD_2CH_2CH_2O^-$			0.8	2.0			0.1	
$PhCH_2CD_2CH_2O^-$		0.3	2.6		0.6	3.5	0.3	
$PhCH_2CH_2CD_2O^-$		2.2			2.7			0.1

Initial Ion	H_2	HD	H_2O	HOD	CH_2O	CD_2O	(CH_2O+H_2)	(CH_2O+HD)
$Ph(CH_2)_3CH_2O^-$	100		0.8		0.4		0.6	
$PhCD_2(CH_2)_2CH_2O^-$	100		0.3	0.5	0.6			0.4
$Ph(CH_2)_2CD_2O^-$	12	100	0.6			0.2		
$Ph(CH_2)_4CH_2O^-$	100		0.5		0.3		0.2	
$PhCD_2(CH_2)_3CH_2O^-$	100							

Initial Ion	(CD_2+H_2)	C_2H_6O	CH_5DO	$CH_2H_4D_2)$	C_3H_8O
$Ph(CH_2)_3CH_2O^-$		1.2			
$PhCD_2(CH_2)_2CH_2O^-$			0.8		
$Ph(CH_2)_2CD_2O^-$	0.7			0.5	
$Ph(CH_2)_4CH_2O^-$					0.3
$PhCD_2(CH_2)_3CH_2O^-$					

Initial Ion	Formation					
	$C_7H_9^-$	$C_7H_8D^-$	$C_7H_7D_2^-$	$C_7H_7^-$	$C_7H_7D_5^-$	$C_3H_3O_2^-$
$Ph(CH_2)_3CH_2O^-$	1.9			8.2		
$PhCD_2(CH_2)_2CH_2O^-$			1.1		9.0	
$Ph(CH_2)_2CD_2O^-$		0.4		8.0		
$Ph(CH_2)_4CH_2O^-$				5.2		1.3
$PhCD_2(CH_2)_3CH_2O^-$					5.5	1.0

Initial Ion	Formation					
	$C_3H_5O^-$	$C_3H_4DO^-$	$C_2H_3O^-$	$C_2H_2DO^-$	OH^-	OD^-
$Ph(CH_2)_3CH_2O^-$			0.6		0.1	
$PhCD_2(CH_2)_2CH_2O^-$			0.7			0.1
$Ph(CH_2)_2CD_2O^-$				0.3	0.1	
$Ph(CH_2)_4CH_2O^-$	0.4					
$PhCD_2(CH_2)_3CH_2O^-$		0.5				

Chapter 6

CA Mass spectra of Deprotonated Amides.

6.1   Introduction.

6.1.1   General.

There has been no investigation of the CA fragmentations of the anions derived from the deprotonation of amides in the gas phase. The basic collisionally induced fragmentations of the radical anions derived from secondary electron capture[29] have been described, and are outlined below. The major fragmentations are generally α to the carbonyl or amino functions.

$$R^2NH-\overset{\cdot}{C}=O \longleftarrow R^1-\overset{\overset{\displaystyle \overset{-}{O}}{|}}{\underset{\cdot}{C}}-NH-R^2 \longrightarrow R^1NH-C\overset{NH}{\underset{O}{\diagup}}^{-}$$

$$+ \quad \overset{-}{R^1} \qquad\qquad\qquad \qquad\qquad\qquad + \quad R^2\cdot$$

$$R^2\overset{-}{NH} + \quad R^1-\overset{\cdot}{C}=O$$
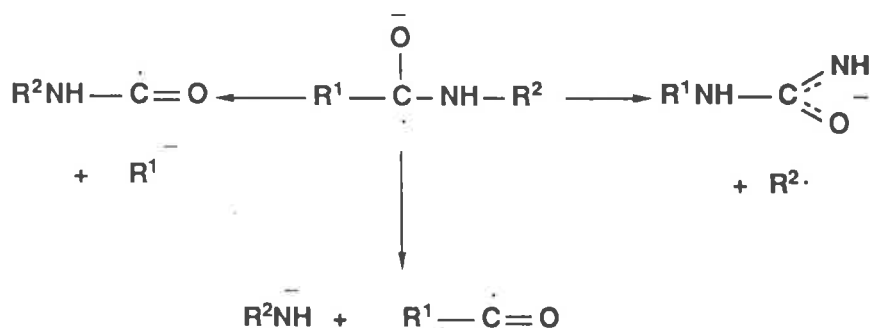
6.1.2   Syntheses of Labelled Derivatives.

The most important reaction used in this study for the preparation of both the labelled and unlabelled amides is the reaction between an acid chloride and an amine *(equation 6.1* see experimental section for full details). This reaction can be used to produce a variety of labelled amides from readily obtainable labelled starting materials, e.g. the acetyl group was readily labelled by the use of acetyl chloride D_3 and the appropriate amine (see experimental section for further de-

tails). The labelled amines were prepared from the corresponding labelled alkyl iodides by the Gabriel synthesis (see experimental for details of the synthesis of labelled amines).

$$CD_3-\overset{\overset{\displaystyle O}{\|}}{C}-Cl \ + \ 2HNMe_2 \ \longrightarrow \ CD_3-\overset{\overset{\displaystyle O}{\|}}{C}-NMe_2 \ + \ H_2\overset{+}{N}MeCl^- \qquad \underline{6.1}$$
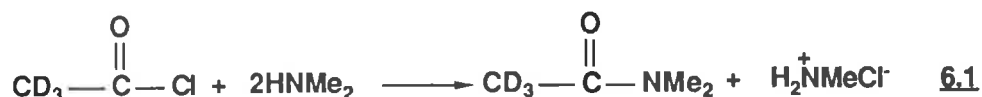
6.2 Results and Discussion.

6.2.1 The CA Fragmentations of Deprotonated Formamide, N-Methylformamide and N,N-Dimethylformamide .

The CA mass spectra of the anions derived from the deprotonation (NH_2^-) of formamide, N-methylformamide, N,N-dimethylformamide and their labelled derivatives are shown in *Table 6.1*.

Formamide.

Deprotonation of formamide (and its labelled derivatives) by amide ion occurs by removal of a proton on nitrogen, the product ion is represented as $\underline{a}$ in *Scheme 6.1*. This species fragments by competitive losses of H·, H_2 and H_2O. Loss of H· *(equation 6.2, Scheme 6.1)* forms the radical anion $\underline{b}$. The major fragmentation involves loss of dihydrogen. This is rationalized in terms of formation of solvated ion complex $\underline{c}$ which decomposes to form dihydrogen and NCO^- *(equation 6.3, Scheme 6.1)*. Loss of water is best explained by a 1-3 proton transfer in $\underline{a}$ to form anion $\underline{d}$ which then fragments through solvated ion complex $\underline{e}$ to form CN^- and H_2O *(equation 6.4, Scheme 6.1)*.

82

O
‖
H—C—NH$_2$

↓ $\bar{N}H_2$

6.2　H· + H—C—N$^{\cdot -}$ ⟵ H—C—$\bar{N}$H ⟶ $\left[\bar{H}\ (O{=}C{=}N{-}H) \right]$
　　　‖　　　　　　　　‖
　　　O　　　　　　　　O
　　　b　　　　　　　　a　　　　　　　　c

O$^-$
‖... H—C=NH

↓

OH
|
H—C=N$^-$ ⟶ $\left[\bar{O}H\ (H{-}C{\equiv}N) \right]$
d　　　　　　　　　　　　　e

H$_2$ + N$\bar{C}$O　　6.3

$\bar{C}$N + H$_2$O　　6.4
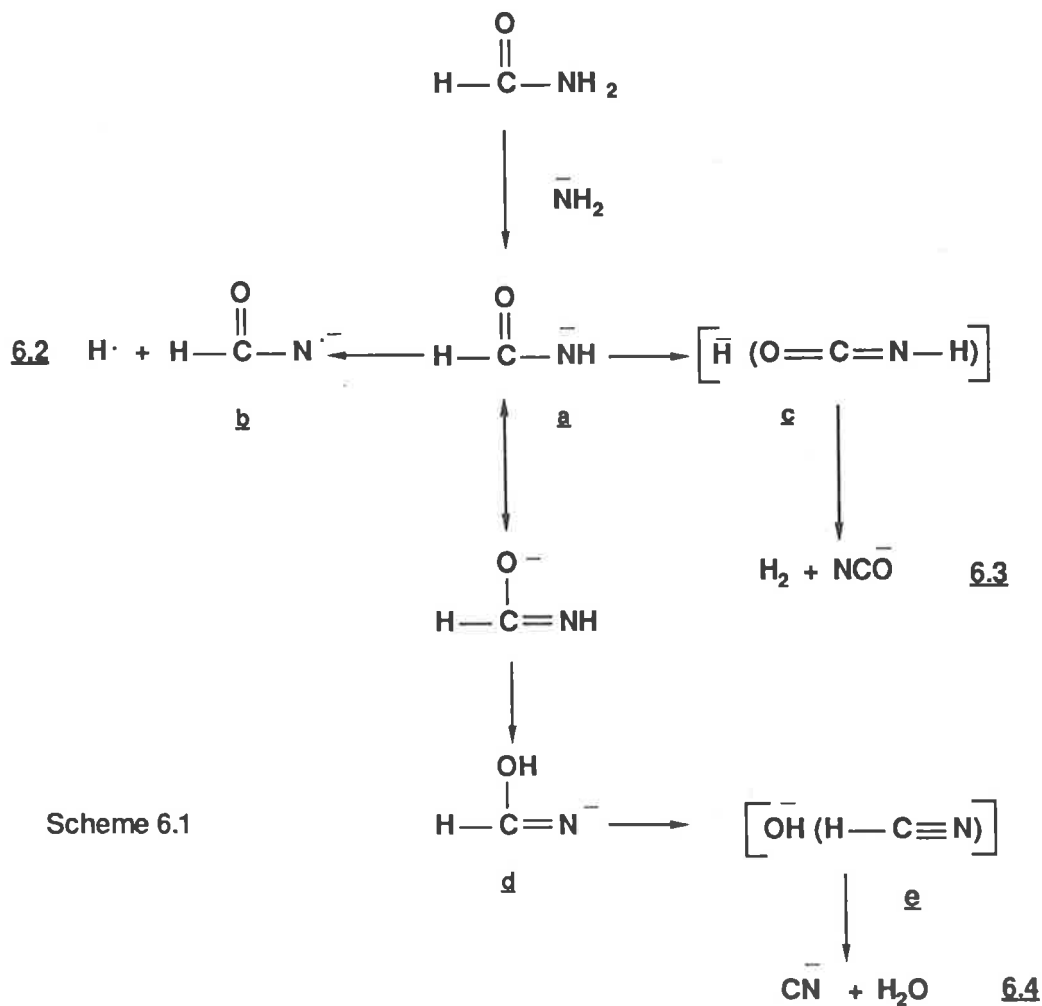
Scheme 6.1

N-Methylformamide.

N-Methylformamide is also deprotonated by removal of the hydrogen on the nitrogen to form **a** (*Scheme 6.2*). The competitive losses of **a** are outlined in *Scheme 6.2*. There are two simple cleavage reactions, *viz*; *i*) loss of H· to give radical anion **b** (*equation 6.5, Scheme 6.2*) and *ii*) methyl loss to give **c** (*equation 6.6, Scheme 6.2*).

A number of fragmentations can be rationalized as proceeding through ion complexes. The first hydride ion complex **d** can fragment either by; *i*) deprotonation of the formyl proton to form H$_2$ and $^-$CH$_2$NCO *(equation 6.7, Scheme 6.2)*, or *ii*) the hydride ion attacking the carbonyl to form formaldehyde and CH$_2$N$^-$ *(equation 6.8, Scheme 6.2)*. Deuterium labelling studies indicate that a second solvated

83

hydride ion complex $\underline{e}$ is also formed, this complex decomposes *via* S_N2 attack of the hydride ion on the methyl group to form methane and NCO^- *(equation 6.9, Scheme 6.2).*
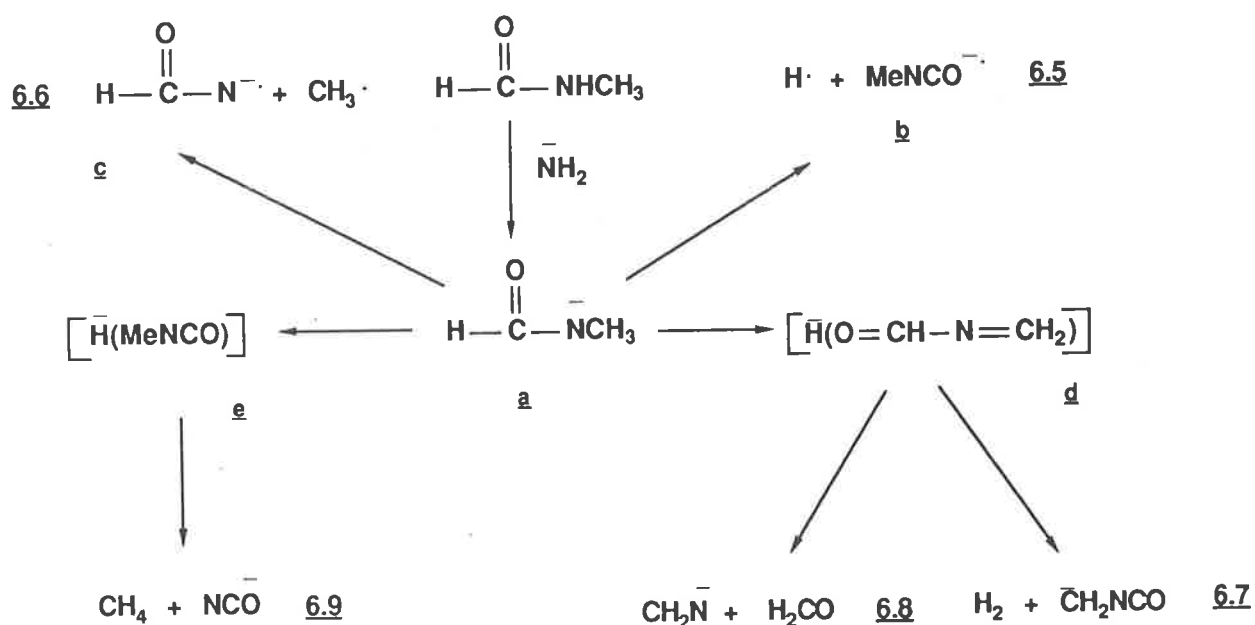
Scheme 6.2

N,N-Dimethylformamide.

Disubstituted amides are of particular interest since they cannot be deprotonated on nitrogen. Deprotonation of this system is more difficult than previous examples since ΔH°_{acid} of the methyl protons has been bracketed at 1671 kJ mol^{-1}[89]. Reaction of Me_2NCDO with NH_2^- results in $[M-H^+]^-$ and $[M-D^+]^-$ peaks in the ratio of 2:1. Thus two ions are formed by deprotonation of dimethylformamide, i.e. $\underline{a}$ and $\underline{b}$ *(Scheme 6.3)*. The CA mass spectra of $\underline{a}$ and $\underline{b}$ are recorded in *Table 6.1*. The ion Me_2NCO^- $\underline{a}$ *(Scheme 6.3)* gives a pronounced CA mass spectrum showing

minor loss of H_2O and major loss of CO: the loss of CO is shown in *equation 6.10 (Scheme 6.3)*. In contrast, $^-CH_2MeNCDO$ shows a weak CA mass spectrum with the loss of H_2O, HOD and CO. The losses of H_2O and CO in the two spectra give peaks with the same widths (within experimental error) at half height [H_2O (23.8 ± 0.3V) and CO (25.0 ± 0.3V)]. Thus, at least in the case of CO loss, it is likely that 1,3 H^+ transfer ($\underline{b} \longrightarrow \underline{a}$, *Scheme 6.3*) precedes fragmentation. The mechanism for the loss of water is not known.

Scheme 6.3
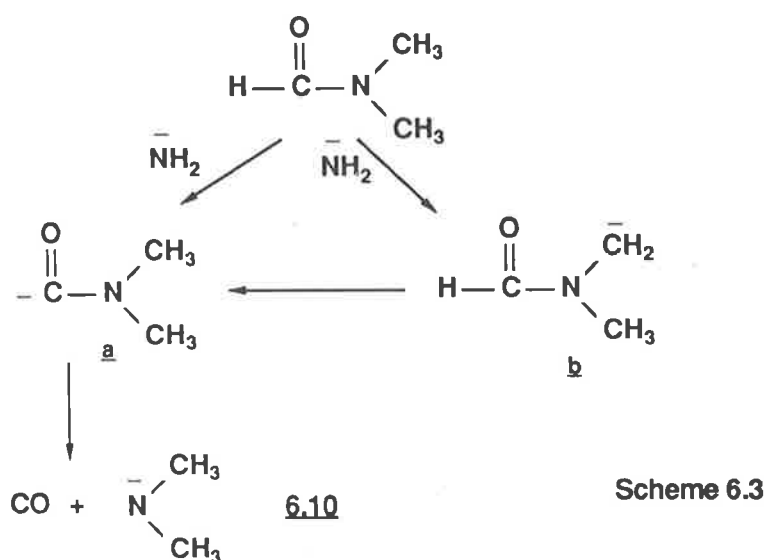
6.2.2 The CA Fragmentations of Deprotonated Acetamide and Substituted Acetamides, $MeCONR^1R^2$ (R^1 = H, Me and Et, R^2 = H, Me or Et).

The CA mass spectra of the anions derived from the reaction of acetamide, N-methylacetamide, N, N-dimethylacetamide, N-ethylacetamide, N,N-diethylacetamide and their labelled derivatives with OH^- (or DO^- where appropriate) are listed in *Tables 6.2* and *6.3*.

Acetamide.

The deprotonation of acetamide occurs by specific removal of the proton on the nitrogen ($\triangle H^°_{Acid}$ $MeCON\underline{H}_2$ = 1430 kJ mol^{-1}, *cf.* 1569.5 kJ mol^{-1}[88] for CH_3CONMe_2) to form $\underline{a}$ *(Scheme 6.4)*. The mass spectrum of deprotonated acetamide and its labelled derivatives show two major losses: i.e. i) loss of H· by

two reactions to form radical anion b *(equation 6.11, Scheme 6.4)* and c *(equation 6.12, Scheme 6.4)* of which the former is formed in the higher yield, and *ii)* loss of methane which plausibly proceeds through ion complex d to products *(equation 6.13, Scheme 6.4)*.

$$CH_3-\overset{\overset{\displaystyle O}{\|}}{C}-NH_2$$

$$\downarrow \ \ \overline{N}H_2$$

$$\underline{6.11} \quad H\cdot \ + \ \overset{.}{C}H_2-\overset{\overset{\displaystyle O}{\|}}{C}-\overset{-}{N}H \longleftarrow CH_3-\overset{\overset{\displaystyle O}{\|}}{C}-\overset{-}{N}H \longrightarrow CH_3-\overset{\overset{\displaystyle O}{\|}}{C}-\overset{-\cdot}{N} \ + \ H \quad \underline{6.12}$$

$$\underline{b} \qquad\qquad\qquad \underline{a} \qquad\qquad\qquad \underline{c}$$

$$\downarrow$$

$$\left[\overline{C}H_3 \ (O=C=N\overline{H}) \right]$$

$$\underline{d}$$

Scheme 6.4

$$\downarrow$$

$$CH_4 \ + \ \overline{N}CO \quad \underline{6.13}$$
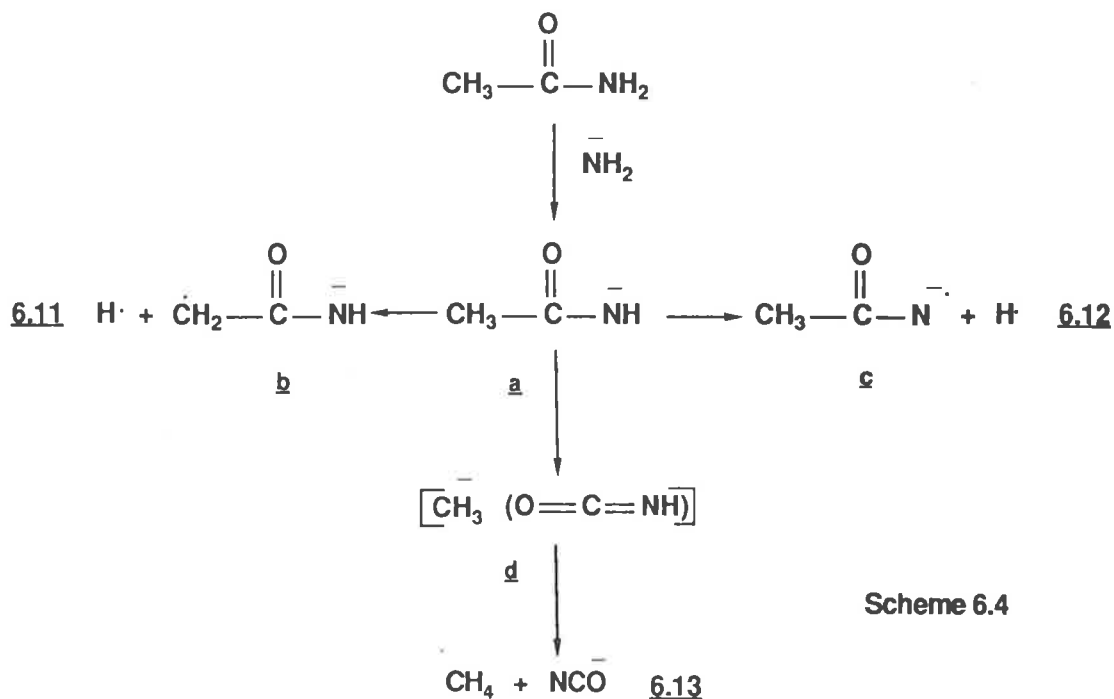
N-Methylacetamide.

The deprotonation of N-methylacetamide by NH_2^- occurs by the removal of the hydrogen on the nitrogen. The losses observed $\overset{\sim}{\text{in}}$ the CA mass spectrum of deprotonated N-methylacetamide are: $H\cdot$, $CH_3\cdot$, CH_4, H_2O and also the formation of NCO^-, HC_2O^-, H_2CN^-, CN^- and CH_3^-. These fragmentations are analogous to those of deprotonated N-ethylacetamide, which will be outlined in full in the next section.

N-Ethylacetamide.

The CA mass spectra of the anions derived from the deprotonation of N-ethylacetamide and its labelled derivatives are recorded in *Table 6.3* and *Figure 6.1.*

The initial deprotonation by NH_2^- (as before) occurs by the removal of the proton on the nitrogen to form anion a *(Scheme 6.5)*. The losses from depro-
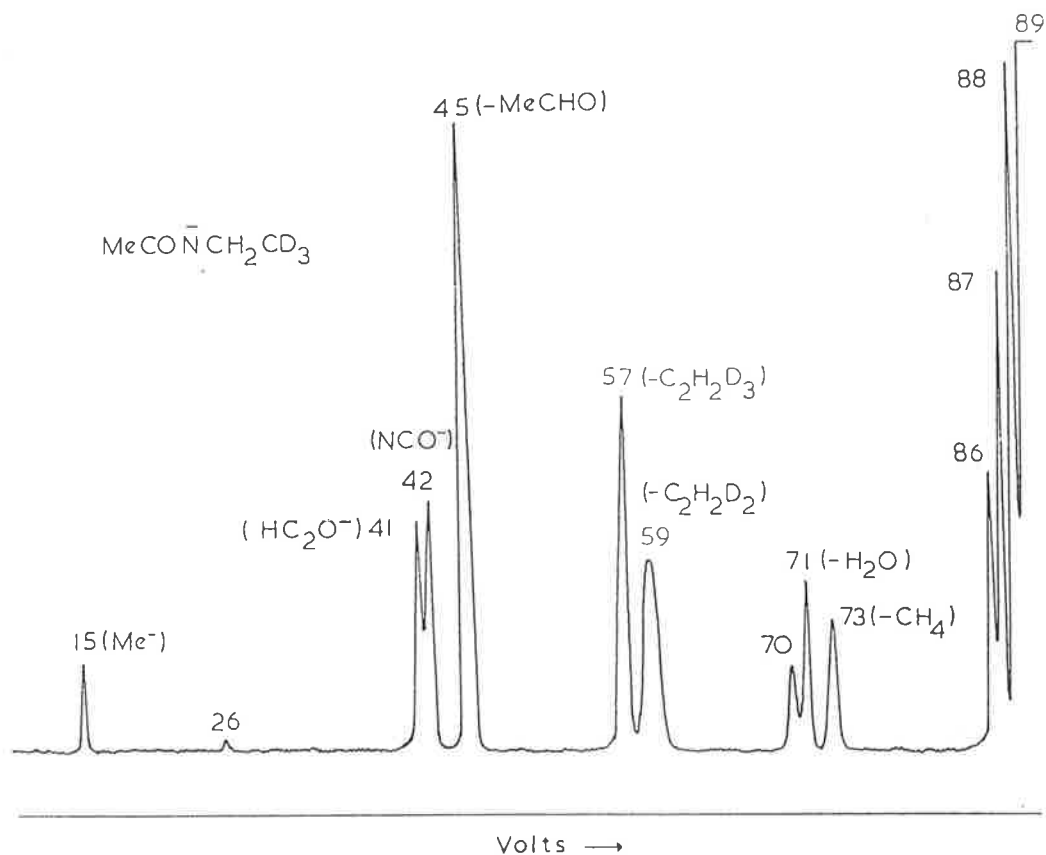
Figure 6.1: *CA Mass spectrum of Deprotonated* MeCONHCH$_2$CD$_3$. *Full experimental details are listed in the Experimental Section. Width of m/z 59 at half height = 98 ± 0.5 V.*

tonated N-ethylacetamide are: H·, H$_2$, CH$_4$, H$_2$O, C$_2$H$_4$, Et· and the formation of CH$_3$CHN$^-$, NCO$^-$, HC$_2$O$^-$, CN$^-$ and CH$_3^-$. All fragmentations are explained through the fragmentation of anions derived from a.

There are two losses of a hydrogen radical; *i)* the major process involves elimination of a hydrogen radical from the acetyl methyl to form radical anion b *(equation 6.14, Scheme 6.5). ii)* in the minor process a hydrogen atom is eliminated from the ethyl group to form radical anion c *(equation 6.15, Scheme 6.5)*. There are two distinct losses of dihydrogen; both can be rationalized by fragmentation of solvated hydride ion complex d, i.e. *i)* the hydride ion can deprotonate the methyl of the side chain *(equation 6.16b, Scheme 6.5)* and *ii)* the hydride ion can remove a proton from the acetyl group *(equation 6.16a, Scheme 6.5)*. In addition, the hydride ion of d can attack the carbonyl group as shown in *equation 6.17 (Scheme 6.5)*.

87

$\underline{6.15}$ $MeCONCH_2CH_2^-$ + $H\cdot$ ⟵———— $MeCONEt$ ————➤ $\overset{-}{C}H_2CONEt$ + $H\cdot$ $\underline{6.14}$

  $\underline{c}$ $\underline{a}$ $\underline{b}$

$\underline{6.16a}$ $\overset{-}{C}H_2CON=CHMe$ + H_2 ⟵ $\left[\overset{-}{H}\,(CH_3CON=CHMe) \right]$ ———➤ $CH_3CON=CH\overset{-}{C}H_2$ + H_2 $\underline{6.16b}$

                                              $\underline{d}$

                                                                                                    Scheme 6.5

                          $MeCHO$ + $CH_3CH=\overset{-}{N}$ $\underline{6.17}$

There are two specific losses of methane from anion $\underline{a}$; *i*) in one case the methyl is lost from the acetyl group perhaps through solvated ion complex $\underline{b}$ (*Scheme 6.6*), the methyl anion then deprotonates the ethyl side chain (*equation 6.18, Scheme 6.6*), *ii*) the methyl anion can also come from the ethyl side chain to form solvated ion complex $\underline{c}$ which then deprotonates as shown in *equation 6.19* (*Scheme 6.5*). Labelling studies suggest that loss of water occurs through intermediate $\underline{d}$ (*Scheme 6.6*) and occurs by two separate mechanisms (*equations 6.20 and 6.21*) of which *equation 6.20* is the main contributor.

$\overset{-}{C}H_2CON=CH_2$ + CH_4 $\underline{6.19}$ $Me\overset{-}{C}HNCO$ + CH_4 $\underline{6.18}$

        ↑   ↑

$\left[M\overset{-}{e}\,(MeCON=CH_2) \right]$ ⟵——— $MeCONEt$ ——➤ $\left[M\overset{-}{e}\,(EtNCO) \right]$

        $\underline{c}$ $\underline{a}$ $\underline{b}$

                                      $\overset{OH}{\underset{|}{}}$
$MeCONEt$ ——➤ $\overset{-}{C}H_2-C=NEt$ ——➤ $\left[H\overset{-}{O}\,(CH_2=C=NEt) \right]$

                                                              $\underline{d}$
     Scheme 6.6

        $\underline{6.21}$ $CH=C=NEt$ + H_2O $CH_2=C=\overset{-}{N}CHCH_3$ + H_2O $\underline{6.20}$

There are two possible mechanisms for the loss of ethylene; i) the first involves a four centre proton transfer from the terminal methyl to the nitrogen *(equation 6.22, Scheme 6.7)*, or ii) the initial proton transfer may be a six centre process to oxygen *(equation 6.23)*. It is not known which mechanism is the correct one. Loss of the C_2H_5 radical occurs overall as shown in *equation 6.24 (Scheme 6.7)*. The formation of HC_2O^- occurs after a 1-3 proton transfer from the acetyl methyl perhaps to form ion complex $\underline{a}$ *(Scheme 6.7)*, which then fragments as shown in *equation 6.25*. Finally, the formation of NCO^- occurs as shown in *equation 6.26 (Scheme 6.7)*.

MeCON⟨⟩H ⟶ MeCONH + C_2H_4 **6.22**

(six-centre structure) ⟶ MeC(OH)=N + C_2H_4 **6.23**

MeCONEt ⟶ MeCON + Et·   **6.24**

MeCONEt ⟶ [EtNH(CH$_2$CO)] ⟶ HC$_2$O + EtNH$_2$ **6.25**
                        $\underline{a}$

MeCONEt ⟶ [Me(EtNCO)] ⟶ NCO + C_3H_8 **6.26**
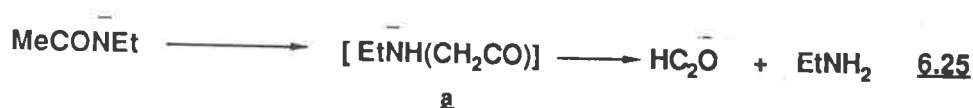
Scheme 6.7

N,N-Dimethylacetamide.

Deprotonation of N,N-dimethylacetamide ($\triangle H^\circ_{Acid}$ = 1569.5 kJ mol^{-1}[88]) can be achieved by either OH^- or H_2N^- and occurs by the removal of a proton from the acetyl group. The losses from deprotonated N,N-dimethylacetamide are, H·,
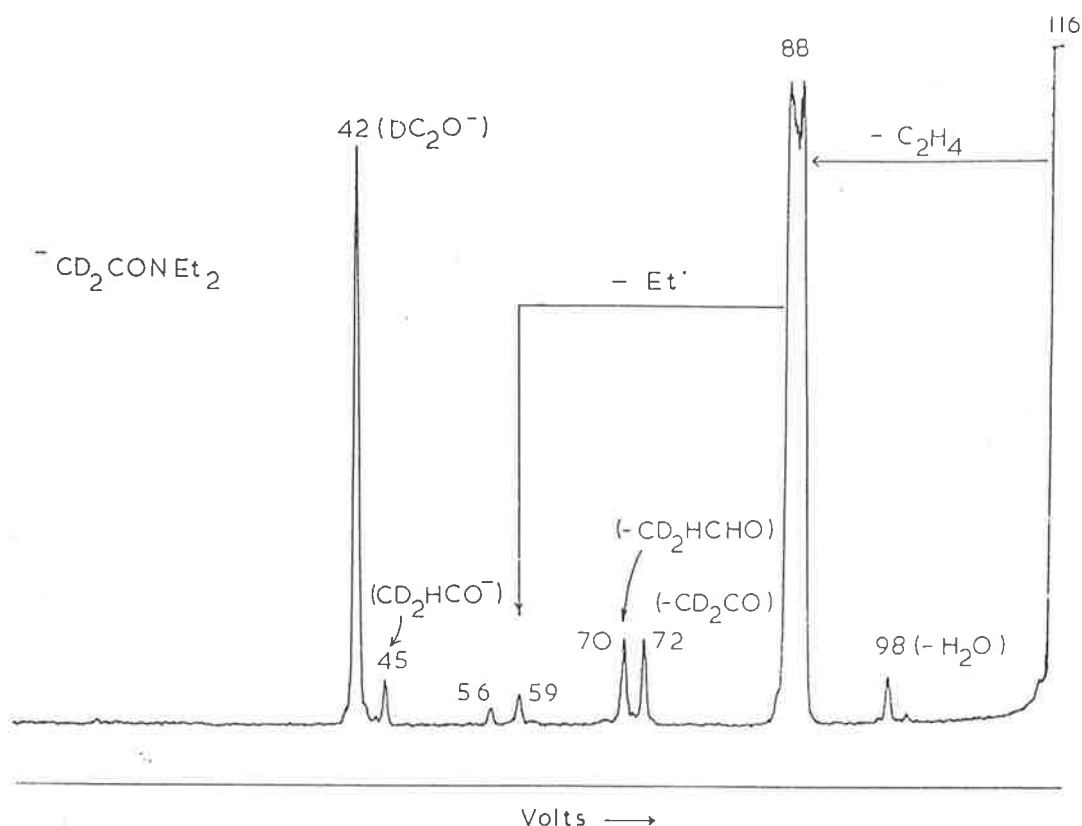
Figure 6.2: *CA Mass spectrum of the $(M-D^+)^-$ ion of CD_3CONEt_2. Width of m/z 88 at half height = 132.8 ± 0.5V.*

H_2, CH_3, CH_4, H_2O, C_2H_6 and the formation of $(CH_3)_2N^-$, CH_3CO^-, NCO^-, HC_2O^-. The fragmentations of deprotonated N,N-dimethylacetamide are analogous to those outlined for N,N-diethylacetamide below.

N,N-Diethylacetamide.

The CA mass spectra of anions derived from deprotonated N,N-diethylacetamide and its labelled derivatives are recorded in *Table 6.4* and *Figure 6.2*. Simple losses observed include CH_4, H_2O, C_2H_4, CH_2CO, CH_3CHO; in addition, ions CH_3CO^- and HC_2O^- are observed.

Deprotonation of N,N-diethylacetamide occurs by the removal of a proton on the acetyl group to form $\underline{a}$ *(Scheme 6.8)*. The most interesting fragmentation of deprotonated N,N-diethylacetamide is the loss of ethylene *(equation 6.27 or 6.28, Scheme 6.8)* which produces the base peak of the spectrum. The peak is dish shaped *(see Figure 6.2)* and the peak width at half height is 133 V, the widest peak yet observed in CA mass spectra of negative ions. Two separate mecha-

nisms can be can proposed for the loss of ethylene; both involve proton transfer through six member transition states *viz*; *i*) proton transfer to carbon *(equation 6.27, Scheme 6.8)* or *ii*) proton transfer to oxygen *(equation 6.28)*. Deuterium isotope effects were measured for this process, results are summarized beside *equations 6.27* and *6.28*. Values obtained were an average of ten measurements. The primary isotope effect of 2.5 and the secondary isotope effect of 1.09 are suggestive of a stepwise process, ie. proton transfer followed by elimination of ethylene[44,69,70] but the data do not allow differentiation of the two mechanisms shown in *equations 6.27* and *6.28*.

$$\text{MeCONEt} + \text{C}_2\text{H}_4 \quad \underline{6.27}$$

$$* \quad \text{H/D} = 2.50 \pm 0.1$$

$$\# \quad \text{H/D} = 1.09 \pm 0.02$$

$$+ \text{C}_2\text{H}_4 \quad \underline{6.28}$$

$$\overline{\text{CH}_2\text{CONEt}_2} \longrightarrow [\text{Et}_2\overline{\text{N}}(\text{CH}_2\text{CO})] \longrightarrow \text{HC}_2\overline{\text{O}} + \text{HNEt}_2 \qquad \underline{6.29}$$

$$\text{Et}_2\overline{\text{N}} + \text{CH}_2\text{CO} \qquad \underline{6.30}$$

$$\overline{\text{CH}_2\text{CONEt}_2} \longrightarrow \text{MeCON}\overset{\text{Et}}{\underset{\text{CHCH}_3}{\diagdown}} \longrightarrow [\text{MeCO(EtNCHMe)}]^{-}$$

a   b   c

$$\underline{6.32} \quad \text{MeCHNCHMe} + \text{MeCHO} \qquad \text{MeCO} + \text{EtNCHMe} \quad \underline{6.31}$$

Scheme 6.8

91
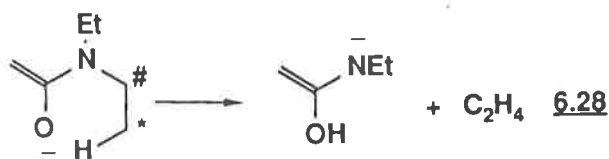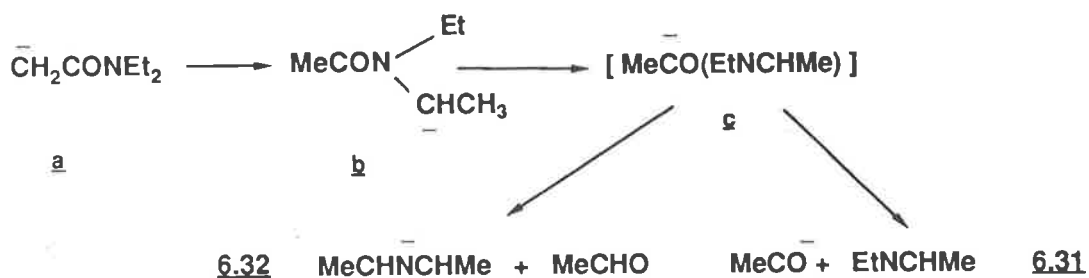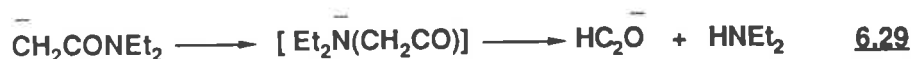
The formation of HC_2O^- and loss of CH_2CO are outlined in *equations 6.29* and *6.30 (Scheme 6.8)*. The loss of acetaldehyde and the formation of CH_3CO^- are of interest since they occur following proton transfer **a** $\longrightarrow$ **b** (*Scheme 6.8*). Fragmentation plausibly proceeds through acetyl anion complex **c** (*Scheme 6.8*) to form the acetyl anion (*equation 6.31*). Alternatively, since the acetyl anion is a powerful base (MeC$\underline{H}$O, $\Delta H^\circ_{acid} = 1632.5$ kJ mol^{-1}[90]) it can effect deprotonation as shown in *equation 6.32* with resulting elimination of acetaldehyde.

6.2.3 The CA Fragmentations of Deprotonated Higher Homologues of N-substituted and N, N-Disubstituted Acetamides.

The CA mass spectra of anions derived from the deprotonation of some higher homologues of acetamide are shown in *Table 6.5*. In general the fragmentations observed for these deprotonated species proceed *via* fragmentation pathways similar to those already described in *Schemes 6.1* to *6.8*.

6.2.4 Fragmentations of Deprotonated Analogues of Acetamide.

The CA mass spectra of some deprotonated analogues of acetamide are shown in *Table 6.6*. Replacing the methyl group adjacent to the carbonyl with ethyl, propyl or phenyl groups does not alter the major fragmentation routes. Deprotonation occurs on the nitrogen and two major pathways are the loss of H· and the formation of NCO^-.

6.2.5 Fragmentations of Deprotonated Acetanilide and Labelled Derivatives.

The CA mass spectra of deprotonated acetanilide and its labelled derivatives are summarized in *Table 6.7* and in *Figure 6.3*. Acetanilide is deprotonated by the removal of the amino hydrogen to yield **a** *(Scheme 6.9)*. The losses observed in the CA mass spectrum of deprotonated acetanilide are, H·, H_2, CH_4, H_2O, CH_2CO. In addition, ions $C_6H_5^-$, NCO^-, HC_2O^-, CN^- and CH_3^- are formed.

The base peak of the spectrum is formed by the loss of H·, labelling studies indicate there to be two distinct losses of a hydrogen radical; *i*) a major loss of H·
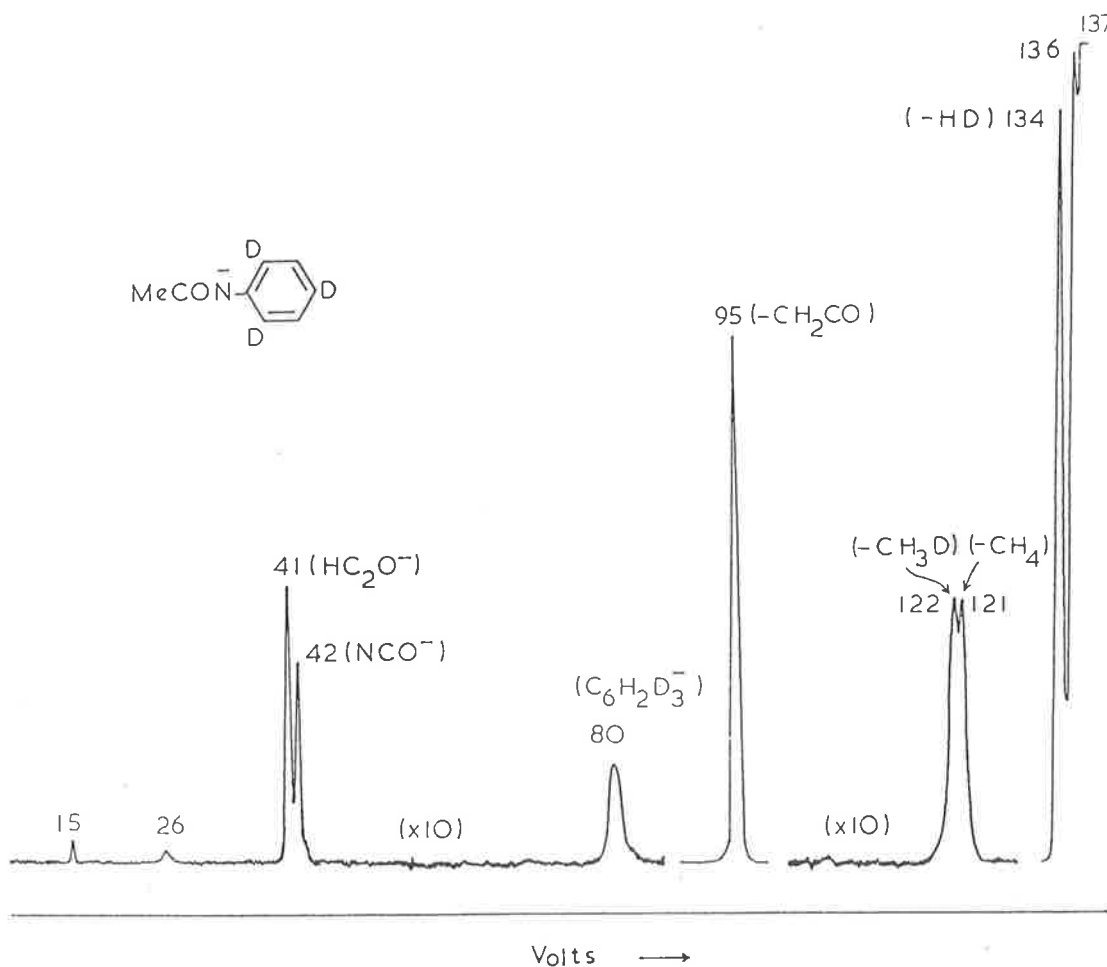
Figure 6.3: *CA Mass spectrum of Deprotonated Acetanilide D₃.*

from the acetyl group *(equation 6.33, Scheme 6.9)* and *ii*) a minor loss of H· from the aromatic ring *(equation 6.34, Scheme 6.9)*. The loss of dihydrogen is specific; one hydrogen comes from the acetyl group and the other from the aromatic ring. A possible rational is shown in *equation 6.35 (Scheme 6.9)*.

A number of fragmentations may be rationalized by the intermediacy of ion complex b *(Scheme 6.9)*. This may *i*) fragment directly to form CH_3^- and C_6H_5NCO *(equation 6.36, Scheme 6.9)*, or *ii*) form $(C_6H_4)^-NCO$ and CH_4 *(equation 6.37, Scheme 6.9)*, *iii*) the methyl anion may effect nucleophilic attack to either form $C_6H_5^-$ and CH_3NCO *(equation 6.38, Scheme 6.9)* or NCO^- and toluene *(equation 6.39, Scheme 6.9, cf. equation 6.26, Scheme 6.7)*.

93

Scheme 6.9

A series of fragmentation reactions for acetanilide derivatives.

$$C_6H_5-NH-\overset{\displaystyle O}{\overset{\|}{C}}-CH_3 \longrightarrow C_6H_5-\overset{-}{N}-\overset{\displaystyle O}{\overset{\|}{C}}-CH_3 \quad (\underline{a})$$

From **a**:

$$\longrightarrow C_6H_5-\overset{-}{N}-\overset{\displaystyle O}{\overset{\|}{C}}-\overset{\cdot}{C}H_2 + H\cdot \qquad \underline{6.33}$$

$$\longrightarrow (C_6H_4)\overset{-}{N}-\overset{\displaystyle O}{\overset{\|}{C}}-CH_3 + H\cdot \qquad \underline{6.34}$$

$$\mathbf{a} \longrightarrow \text{(indol-2-one anion)}\;-\overset{-}{O} + H_2 \qquad \underline{6.35}$$

$$\mathbf{a} \longrightarrow \left[\overset{-}{C}H_3 \left(C_6H_4NCO \right) \right]\;(\underline{b}) \longrightarrow C_6H_5CH_3 + \overset{-}{N}CO \qquad \underline{6.39}$$

From **b**:

$$\overset{-}{C}H_3 + PhNCO \qquad \underline{6.36} \qquad (C_6H_4)\overset{-}{N}CO + CH_4 \qquad \underline{6.37} \qquad C_6H_5^{-} + CH_3NCO \qquad \underline{6.38}$$
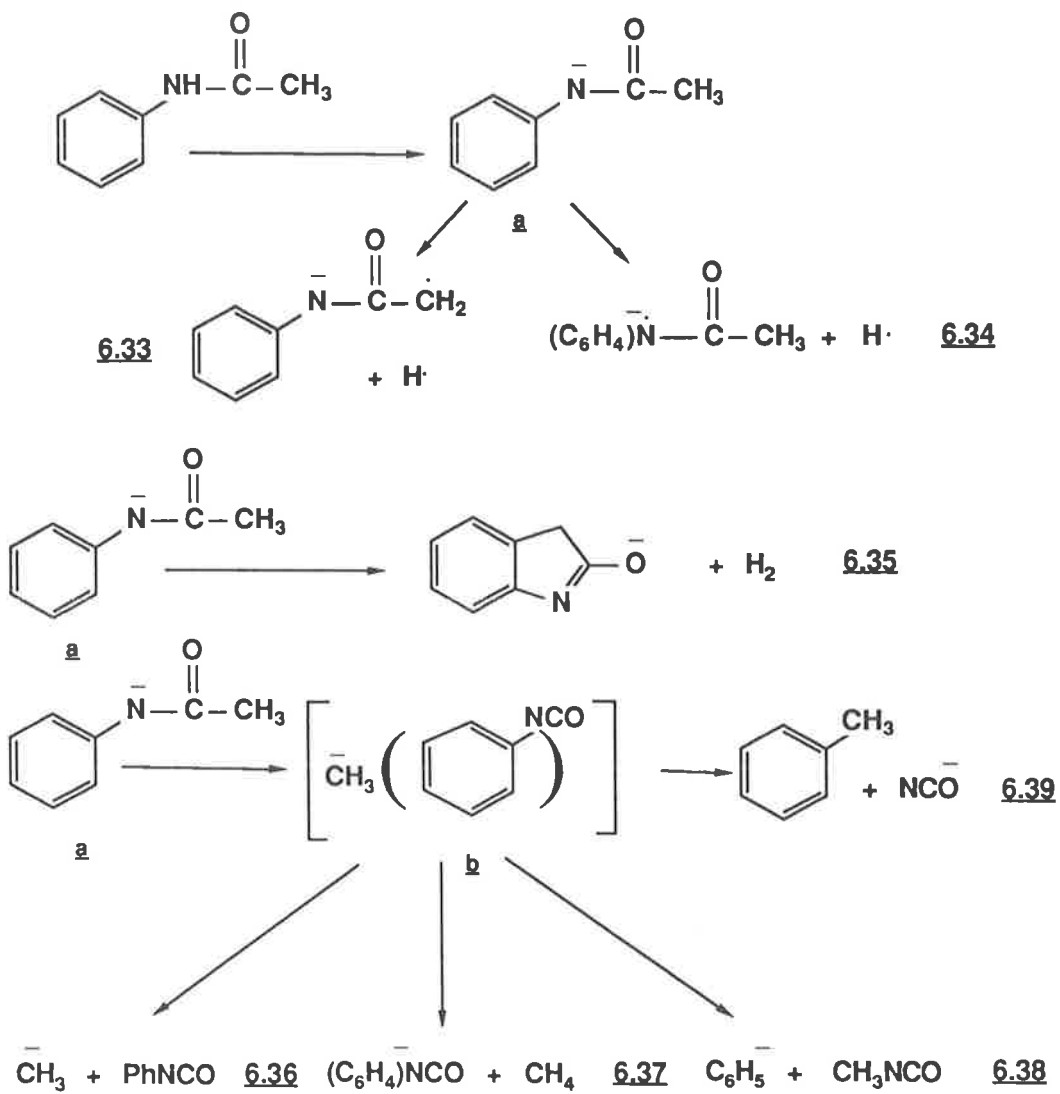
Scheme 6.9

The remaining fragmentations are analogous to those described previously.

MeCONCOC$_6$D$_5$

$-$ MeCO$_2$D

167

125

$-$ CH$_2$CO

164

42 (NCO$^-$)

106

(-CH$_3$D)

(-HOD)

(HC$_2$O$^-$)

(MeCO$_2^-$)
59

(C$_6$D$_5^-$)
82

96

148

150

41

(x 5)

(x 5)

Volts $\longrightarrow$
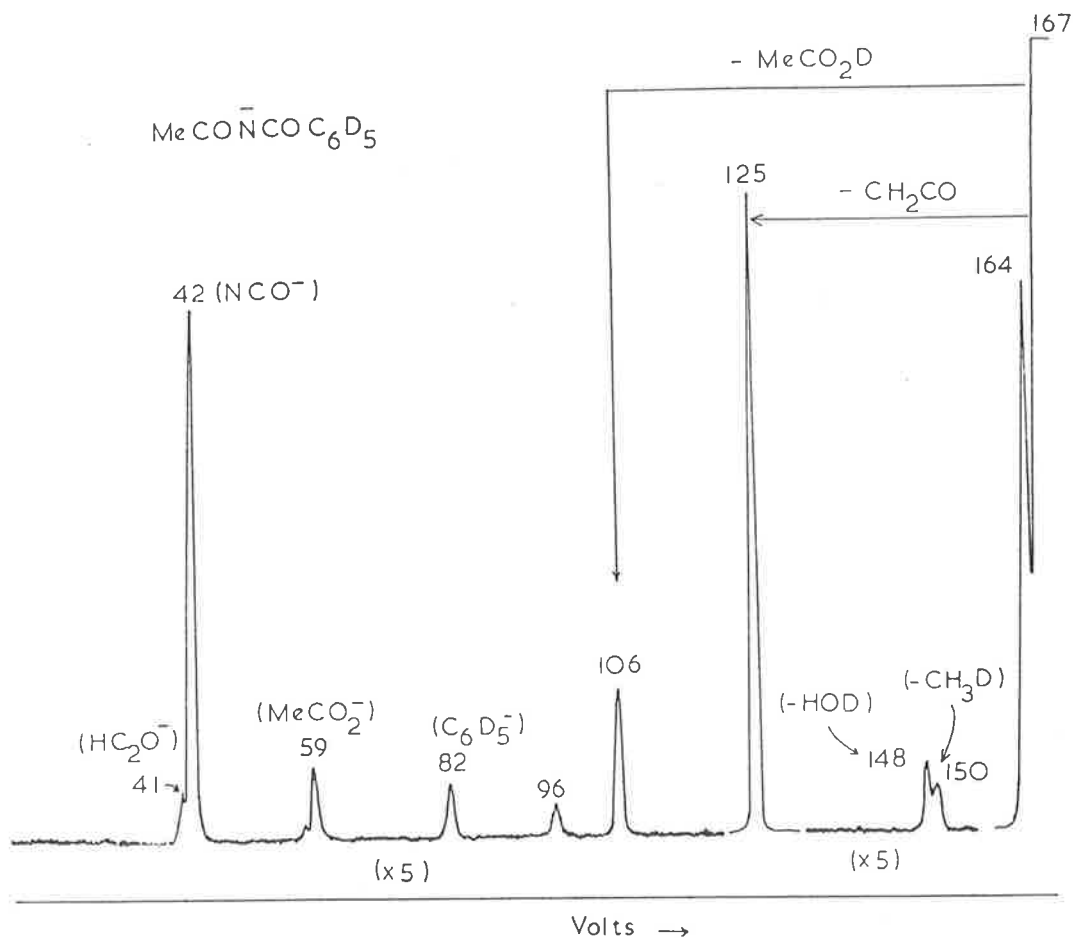
Figure 6.4: *CA Mass spectrum of Deprotonated MeCONHCOC$_6$D$_5$. When a voltage of +2000 V is applied to the collision cell, the following ratio of decompositions occurring* inside *the cell and* outside *the cell are observed: m/z (C.I.:unimolecular) - 150 (1:1), 148 (2:1), 125 (1:9), 106 (19:1), 82 (3:2), 59 (1:1) and 42 (1:2).*

6.2.6 The Fragmentations of Deprotonated Bisacetamide and Related Molecules.

The CA mass spectra of deprotonated bisacetamide analogues are shown in *Table 6.8* and *Figure 6.4*. The $\Delta H°_{Acid}$ of MeCONHCOMe[91] is 1452 kJ mol^{-1}; therefore the deprotonation of the NH moiety will occur most readily.

Most of the fragmentations outlined above also pertain to deprotonated bisacetamide and the related molecules. However there are several fragmentation processes of MeCONCOPh and PhCONCOPh that are worth describing in some detail. The interesting losses are of H$_2$, RCO$_2$H and the formation of RCO$_2^-$ from RCONCOPh (R = Me or Ph). These fragmentations are outlined in *equation 6.40-6.41 (Scheme 6.10)*. The loss of dihydrogen to form a involves a phenyl and a methyl hydrogen; the product ion may be b. Interesting decompositions of c are summarized in *equations 6.40* and *6.41*. It is proposed that rearrangement of c to d, followed by fragmentation to ion complex e, may yield the precursor of the

95

product ions shown in *equations 6.40* and *6.41*. Since the bound benzoate anion of **e** may not be able to deprotonate benzonitrile, an alternative intermediate for the products of *equation 6.41* could be the radical ion/radical complex **f**.
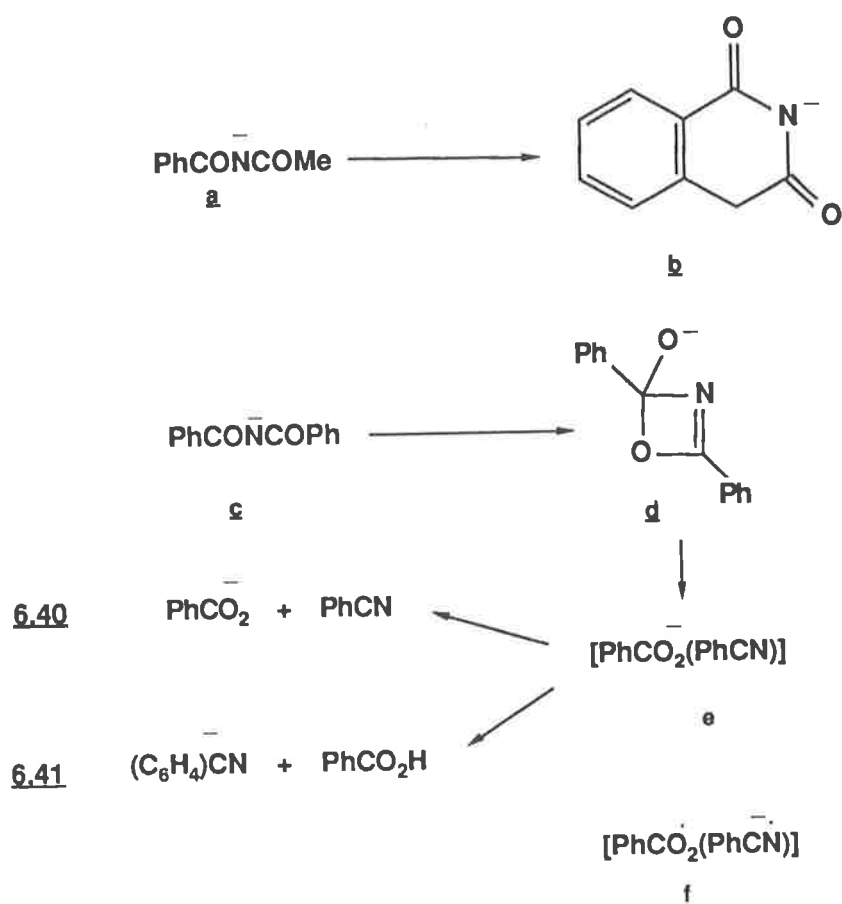
PhCONCOMe
a

b

PhCONCOPh
c

d

6.40   PhCO₂ + PhCN

[PhCO₂(PhCN)]
e

6.41   (C₆H₄)CN + PhCO₂H

[PhCO₂(PhCN)]
f

Scheme 6.10

Neutral Precursor	Anion	Loss									Formation	
		H·	H$_2$, D·	HD	Me·	CH$_4$	H$_2$O	HOD	CO	H$_2$CO	CH$_2$N$^-$	CN$^-$
HCONH$_2$	[M–H$^+$]$^-$	14	100				6					
HCOND$_2$	[M–D$^+$]$^-$		29	100				5.5				
HCONDCH$_3$	[M–D$^+$]$^-$	23	100		3.6	9.1					4.5	2.7
HCON(CH$_3$)$_2$	[M–H$^+$]$^-$						13		100	5		
DCON(CH$_3$)$_2$	[M–H$^+$]$^-$						100	26	15			
DCON(CH$_3$)$_2$	[M–D$^+$]$^-$						15		100	4		

Neutral Precursor	Anion	Loss											
		H·	H₂, D·	HD	D₂	Me·	CH₄	CH₃D	CH₂D₂ᵃ	CHD₃ᵇ	H₂Oᵃ	HODᵇ	C₂H₆
CH_3CONH_2	$[M-H^+]^-$	100											
CD_3CONH_2	$[M-H^+]^-$	31	64										
CH_3COND_2	$[M-D^+]^-$	85	75										
$CH_3CONHCH_3$	$[M-H^+]^-$	100					97				6		
$CD_3CONHCH_3$	$[M-H^+]^-$		63	7		4					100	100	
$CH_3CONHCD_3$	$[M-H^+]^-$	100	17					54	19.5		19.5	4	
$CH_3CON(CH_3)_2$	$[M-H^+]^-$	22	2			3					47		39
$CD_3CON(CH_3)_2$	$[M-D^+]^-$		12		7	4.5			26		26	16	5

Neutral Precursor	Anion	Formation									
		CH_3CO^-	CD_2HCO^-	$(CH_3)_2N^-$	HC_2O^-	DC_2O^{-c}	NCO^-c	H_2CN^-	CN^-	CH_3^-	CD_3^-
CH_3CONH_2	$[M-H^+]^-$						86				
CD_3CONH_2	$[M-H^+]^-$					100	100				
CH_3COND_2	$[M-D^+]^-$				3		100	8	4	5.5	
$CH_3CONHCH_3$	$[M-H^+]^-$				6		7	5	3		5
$CD_3CONHCH_3$	$[M-H^+]^-$						6			7	
$CH_3CONHCD_3$	$[M-H^+]^-$					13	13			13	
$CH_3CON(CH_3)_2$	$[M-H^+]^-$	38		4	100		6				
$CD_3CON(CH_3)_2$	$[M-D^+]^-$	4.5	25	7		100	100				

a. CH_2D_2 and H_2O = 18 a. m. u.

b. HOD and CD_3H = 19 a. m. u.

c. DC_2O^- and NCO^- = 42 a. m. u.

Table 6.3: CA Mass Spectra of Deprotonated N-Ethylacetamide and Labelled Derivatives.

Neutral Precursor	Anion	Loss								
		H·	H$_2$, D·	HD	CH$_4$	CH$_3$D	CD$_3$H^a	H$_2$O	HOD^a	D$_2$O
CH$_3$CONHCH$_2$CH$_3$	[M–H$^+$]$^-$	100	21		13			6		
CD$_3$CONHCH$_2$CH$_3$	[M–H$^+$]$^-$		94	100		3	11		11	4
CH$_3$CONHCD$_2$CH$_3$	[M–H$^+$]$^-$	100		16	6	7	5	11	5	
CH$_3$CONHCH$_2$CD$_3$	[M–H$^+$]$^-$	100	51	33	15		10	19	10	

Neutral Precursor	Anion	Loss						
		C$_2$H$_4$	C$_2$H$_2$D$_2$	C$_2$H$_5$	C$_2$H$_3$D$_2$	C$_2$H$_2$D$_3$	CH$_3$CHO	CH$_3$CDO
CH$_3$CONHCH$_2$CH$_3$	[M–H$^+$]$^-$	13		18				
CD$_3$CONHCH$_2$CH$_3$	[M–H$^+$]$^-$	19		43			51	
CH$_3$CONHCD$_2$CH$_3$	[M–H$^+$]$^-$		28		41		31	
CH$_3$CONHCH$_2$CD$_3$	[M–H$^+$]$^-$		24			38		

Neutral Precursor	Anion	Loss	Formation						
		CD$_3$CHO	NCO^{-b}	HC$_2$O$^-$	DC$_2$O^{-b}	CH$_2$CN$^-$	CN$^-$	CH$_3^-$	CD$_3^-$
CH$_3$CONHCH$_2$CH$_3$	[M–H$^+$]$^-$		25^c	6				4	
CD$_3$CONHCH$_2$CH$_3$	[M–H$^+$]$^-$		51		51	3	1		3
CH$_3$CONHCD$_2$CH$_3$	[M–H$^+$]$^-$		17	15			0.5	10	
CH$_3$CONHCH$_2$CD$_3$	[M–H$^+$]$^-$	84	27	21			0.7	13	

a. HOD and CD$_3$H = 19 a. m. u.

b. DC$_2$O$^-$ and NCO$^-$ = 42 a. m. u.

c. NCO$^-$ and CH$_3$CHN$^-$ = 42 a. m. u.

Table 6.4: CA Mass Spectra of Deprotonated N, N-Diethylacetamide and Labelled Derivatives.

Neutral Precursor	Anion	Loss						
		CH_4	CH_3D	$CH_2D_2^a$	H_2O^a	HOD^b	D_2O	C_2H_4
$CH_3CON(Et)_2$	$[M-H^+]^-$	2			14			100
$CD_3CON(Et)_2$	$[M-D^+]^-$			9	9			100
$CH_3CON(Et)CD_2CH_3$	$[M-H^+]^-$					3		49
$CH_3CON(Et)CH_2CD_3$	$[M-H^+]^-$		2	6	6	4		58
$CH_3CON(Et)CD_2CD_3$	$[M-H^+]^-$			2.5	2.5	2	2.5	57
$CH_3CON(CH_2CD_3)_2$	$[M-H^+]^-$					31		

Neutral Precursor	Anion	Loss						
		$C_2H_2D_2$	C_2D_4	CH_2CO	CD_2CO^c	CH_3CHO^c	CD_2HCHO	CD_3CHO
$CH_3CON(Et)_2$	$[M-H^+]^-$			21		18		
$CD_3CON(Et)_2$	$[M-D^+]^-$				11	11	14	
$CH_3CON(Et)CD_2CH_3$	$[M-H^+]^-$	45		7		8		
$CH_3CON(Et)CD_2CD_3$	$[M-H^+]^-$		22	5		8		
$CH_3CON(Et)CH_2CD_3$	$[M-H^+]^-$	24		8		9		
$CH_3CON(CH_2CD_3)_2$	$[M-H^+]^-$	55		4		21		11

a. CH_2D_2 and H_2O = 18 a. m. u.

b. HOD and CD_3H = 19 a. m. u.

c. CH_3CHO and CD_2CO = 42 a. m. u.

Neutral Precursor	Anion	Formation				
		CH_3CO^-	CH_2DCO^-	CHD_2CO^-	HC_2O^-	DC_2O^-
$CH_3CON(Et)_2$	$[M-H^+]^-$	10			100	
$CD_3CON(Et)_2$	$[M-D^+]^-$			7		82
$CH_3CON(Et)CD_2CH_3$	$[M-H^+]^-$				100	
$CH_3CON(Et)CH_2CD_3$	$[M-H^+]^-$				100	
$CH_3CON(Et)CH_2CD_3$	$[M-H^+]^-$		5		100	
$CH_3CON(CH_2CD_3)_2$	$[M-H^+]^-$		4		100	

Neutral Precursor	Anion	Loss												
		H·	H₂	H₂, H·	Me·	CH₄	H₂O	C₂H₅	C₂H₆	CH₂CO	C₃H₇	C₃H₈	(CH₃CHO+H₂)	C₄H₈
MeCONH(n-Pr)	[M–H⁺]⁻	65	9		10	12	20	57		15	43	100	35	
MeCONH(iso-Pr)	[M–H⁺]⁻	100	39	8		73	24			68	100	84		
MeCONH(n-Bu)	[M–H⁺]⁻		71			12	29		26			100	95	
MeCONH(iso-Bu)	[M–H⁺]⁻	55	37.5			78	17		100			36		
MeCONH(t-Bu)	[M–H⁺]⁻	5				100	4.5							
MeCON(n-Pr)₂	[M–H⁺]⁻					4	20	16		100		100		
MeCON(iso-Pr)₂	[M–H⁺]⁻				11					100				
MeCON(n-Bu)₂	[M–H⁺]⁻				4	12				4.2		12		100

Neutral Precursor	Anion	Loss			Formation				
		C₄H₉	C₄H₁₀	(CH₃COCH₃+H₂)	CH₃COCH₂⁻	CH₃CO⁻	NCO⁻	HC₂O⁻	CH₃⁻
MeCONH(n-Pr)	[M–H⁺]⁻						21	19	9
MeCONH(iso-Pr)	[M–H⁺]⁻						41	48	10
MeCONH(n-Bu)	[M–H⁺]⁻	58	42				19	27	9
MeCONH(iso-Bu)	[M–H⁺]⁻	65	28	28			29	31	10
MeCONH(t-Bu)	[M–H⁺]⁻	26					8	8	3
MeCON(n-Pr)₂	[M–H⁺]⁻		3.5		3.5	15.5		86	
MeCON(iso-Pr)₂	[M–H⁺]⁻		55		20	8.5		81	
MeCON(n-Bu)₂	[M–H⁺]⁻					6		22	

Table 6.5: CA Mass Spectra of Deprotonated Higher Homologues of N-substituted and N,N-disubstituted Acetamide.

Table 6.6: CA Mass Spectra of Various Deprotonated Analogues of Acetamide.

Neutral Precursor	Anion	Loss									
		H·	H$_2$, D·	HD	Me·	CH$_4$	H$_2$O	HOD	C$_2$H$_4$	C$_2$H$_5$	H$_2$CO
EtCONH$_2$	[M–H$^+$]$^-$	45	8				20				
EtCOND$_2$	[M–D$^+$]$^-$	46	15	5	5		2	7			
PrCONH$_2$	[M–H$^+$]$^-$	100	33			1	8		3		
PrCOND$_2$	[M–D$^+$]$^-$	8.9	2.6			12	4			14	
PhCONH$_2$	[M–H$^+$]$^-$	100					7		1		1
PhCOND$_2$	[M–D$^+$]$^-$	100					0.6	2			

Neutral Precursor	Anion	Loss		Formation			
		C$_2$H$_6$	C$_2$H$_5$D	C$_6$H$_5^-$	C$_6$H$_4^-$	C$_6$H$_3^-$	NCO$^-$
EtCONH$_2$	[M–H$^+$]$^-$						100
EtCOND$_2$	[M–D$^+$]$^-$						100
PrCONH$_2$	[M–H$^+$]$^-$						37
PrCOND$_2$	[M–D$^+$]$^-$						100
PhCONH$_2$	[M–H$^+$]$^-$	1		4	2	1	33
PhCOND$_2$	[M–D$^+$]$^-$		0.5	10			48

Neutral Precursor	Anion	Loss							
		H·	H$_2$, D·	HD	CH$_4$	CH$_3$D	CD$_3$H[a]	H$_2$O	HOD[a]
PhNHCOCH$_3$	[M–H$^+$]$^-$	100	74		5.5			0.6	
PhNHCOCD$_3$	[M–H$^+$]$^-$	100	38	78			20		20
C$_6$D$_5$NHCOCH$_3$	[M–H$^+$]$^-$		95	100		7			

Neutral Precursor	Anion	Loss					
		C$_2$H$_4$	C$_2$H$_3$D	C$_2$H$_2$D$_2$	C$_2$HD$_3$	CH$_2$CO	CD$_2$CO
PhNHCOCH$_3$	[M–H$^+$]$^-$					20	
PhNHCOCD$_3$	[M–H$^+$]$^-$	0.1			0.2		63
C$_6$D$_5$NHCOCH$_3$	[M–H$^+$]$^-$			1		40	

Neutral Precursor	Anion	Formation								
		C$_6$H$_5^-$	C$_6$H$_2$D$_3^-$	C$_6$D$_5^-$	NCO^{-b}	HC$_2$O$^-$	DC$_2$O^{-b}	CN$^-$	CH$_3^-$	CD$_3^-$
PhNHCOCH$_3$	[M–H$^+$]$^-$	1			1	1		0.1	0.05	
PhNHCOCD$_3$	[M–H$^+$]$^-$	0.1			7		7	0.05	0.01	
C$_6$D$_5$NHCOCH$_3$	[M–H$^+$]$^-$			1.4	2	4	2			

a. HOD and CD$_3$H = 19 a. m. u.

b. NCO$^-$ and DC$_2$O = 42 a. m. u.

Table 6.8: CA Mass Spectra of Deprotonated Bisacetamides and Labelled Derivatives.

Neutral Precursor	Anion	Loss								
		H·	H$_2$, D·	HD	CH$_3$	CH$_4$	CH$_3$D	H$_2$O	HOD	Et·
MeCONHCOMe	[M−H$^+$]$^-$	100								
MeCONHCOEt	[M−H$^+$]$^-$	100			0.2					0.4
MeCONHCOPh	[M−H$^+$]$^-$		98			5		3		
PhCONHCOPh	[M−H$^+$]$^-$	95								
C$_6$D$_5$CONHCOC$_6$D$_5$	[M−H$^+$]$^-$		88							
MeCON(Bu)COMe	[M−H$^+$]$^-$	1								
CD$_3$CON(Bu)COCD$_3$	[M−D$^+$]$^-$	1	0.5							
MeCON(C$_3$H$_5$)COMe	[M−H$^+$]$^-$	1								
MeCON(CH$_2$Ph)COMe	[M−H$^+$]$^-$	2								

Neutral Precursor	Anion	Loss							
		CH$_2$CO	CD$_2$CO	MeCCHO	C$_6$H$_6$	C$_6$D$_6$	MeCO$_2$H	PhCO$_2$H	C$_6$D$_5$CDO
MeCONHCOMe	[M−H$^+$]$^-$	59							
MeCONHCOEt	[M−H$^+$]$^-$	53		32					
MeCONHCOPh	[M−H$^+$]$^-$	100					16		
PhCONHCOPh	[M−H$^+$]$^-$				8			13	
C$_6$D$_5$CONHCOC$_6$D$_5$	[M−H$^+$]$^-$					6			10
MeCON(Bu)COMe	[M−H$^+$]$^-$	100							
CD$_3$CON(Bu)COCD$_3$	[M−D$^+$]$^-$		100						
MeCON(C$_3$H$_5$)COMe	[M−H$^+$]$^-$	100							
MeCON(CH$_2$Ph)COMe	[M−H$^+$]$^-$	100							

Neutral Precursor	Anion	Formation				
		$C_6H_5CO_2^-$	$C_6D_5CO_2^-$	$MeCO_2^-$	PhN^-	$C_6D_5N^-$
MeCONHCOMe	$[M-H^+]^-$					
MeCONHCOEt	$[M-H^+]^-$					
MeCONHCOPh	$[M-H^+]^-$			6	2	
PhCONHCOPh	$[M-H^+]^-$	100			15	
$C_6D_5CONHCOC_6D_5$	$[M-H^+]^-$		100			13
MeCON(Bu)COMe	$[M-H^+]^-$					
$CD_3CON(Bu)COCD_3$	$[M-D^+]^-$					
$MeCON(C_3H_5)COMe$	$[M-H^+]^-$					
$MeCON(CH_2Ph)COMe$	$[M-H^+]^-$					

| Neutral Precursor	Anion	Formation					
		$C_6H_5^-$	$C_6D_5^-$	NCO^-	$MeCO_2^-$	HC_2O^-	DC_2O^-
MeCONHCOMe	$[M-H^+]^-$			4		4	
MeCONHCOEt	$[M-H^+]^-$			2	1	1	
MeCONHCOPh	$[M-H^+]^-$	9		67		4	
PhCONHCOPh	$[M-H^+]^-$	29		49			
$C_6D_5CONHCOC_6D_5$	$[M-H^+]^-$		30	50			
MeCON(Bu)COMe	$[M-H^+]^-$					2	
$CD_3CON(Bu)COD_3$	$[M-D^+]^-$						2
$MeCON(C_3H_5)COMe$	$[M-H^+]^-$					5	
$MeCON(CH_2Ph)COMe$	$[M-H^+]^-$	0.1				1	

Chapter 7

CA Mass Spectra of Deprotonated Amines.

7.1 Introduction.

There has been little work done on the gas phase reactions of deprotonated amine ions; one report on the negative ions derived from electron capture of labelled and unlabelled methyl amine has appeared[87]. In this chapter, the CA fragmentations of a number of deprotonated primary and secondary amines are described to determine if: i) the major fragmentations of of deprotonated alkyl amines can be likened to those of carbanions already studied, ii) deprotonated cyclic amines undergo retro reactions of a type similar to those of deprotonated cyclohexanones *(Chapter 4)* and iii) what are the characteristic fragmentations of deprotonated aromatic amines.

The labelled amines were prepared from labelled precursors which were either commercial or prepared by standard procedures (see experimental section for complete details). The primary amines were prepared by the Gabriel synthesis; for example see *equation 7.1 (Scheme 7.1)*. The secondary amines were prepared as outlined in *equation 7.2 (Scheme 7.1)*.

$$CH_3CD_2NH_2 \xrightarrow{CH_3CD_2I} (CH_3CD_2)_2NH_2{}^+I^- \xrightarrow{KOH} (CH_3CD_2)_2NH \qquad 7.2$$

Scheme 7.1

107
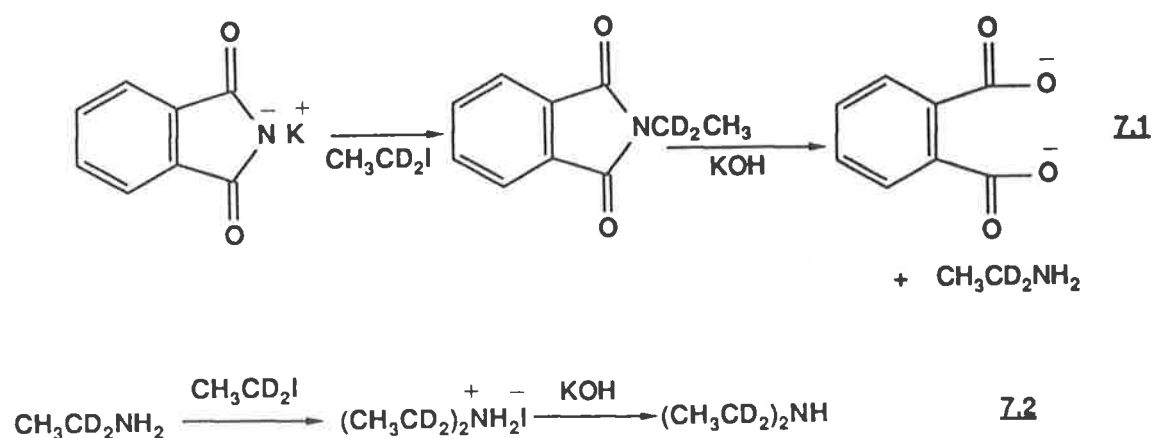
7.2 · Results and Discussion.

All amines were deprotonated with H_2N^- (ΔH_{acidNH_3}=403.5 kcal.mol^{-1})[39] formed from ammonia[47] *(equations 7.3 and 7.4)*.

$$H_3N + e^- \longrightarrow H^- + NH_2^{\cdot} \qquad\qquad (7.3)$$

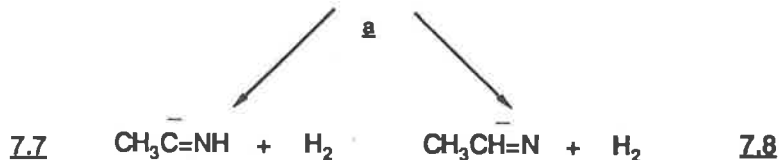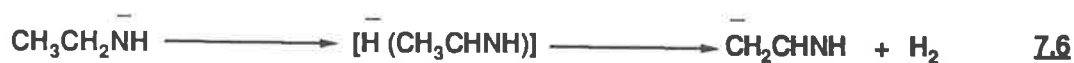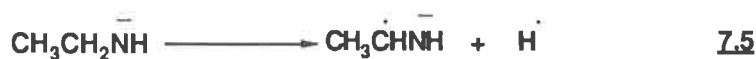$$H^- + H_3N \longrightarrow H_2 + NH_2^- \qquad\qquad (7.4)$$

7.2.1 CA Fragmentations of Deprotonated Primary Amines.

The CA mass spectra of deprotonated labelled and unlabelled primary amines are listed in *Table 7.1* and the CA mass spectra of deprotonated isopropyl-2,2,2,2′,2′,2′-D$_6$-amine shown in *Figure 7.1*. All the fragmentations observed for the deprotonated primary amines were simple and the proposed mechanisms are rationalised as proceeding through solvated ion intermediates.
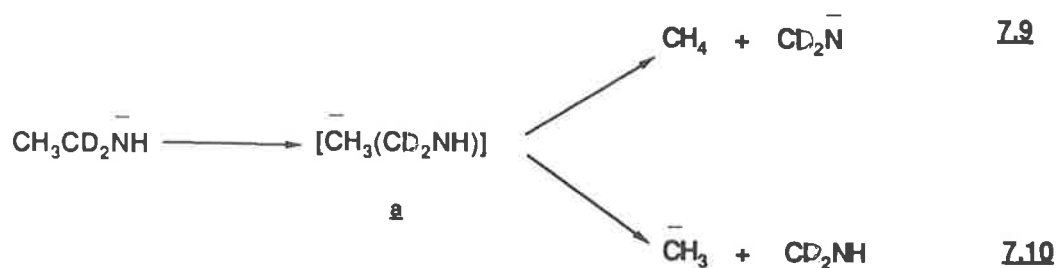
Deprotonated Ethylamine.

The major losses from deprotonated ethylamine are; H$^{\cdot}$, H$_2$ and CH$_4$. Formation of Me$^-$ is also noted. The loss of H$^{\cdot}$ occurs by loss of a hydrogen radical from the α carbon *(equation 7.5, Scheme 7.2)*. The deuterium labelling data indicate that loss of dihydrogen from deprotonated ethylamine occurs *via* three processes; in each case, the formation of hydride ion complex $\underline{a}$ *(Scheme 7.2)* is the first step. The hydride ion of $\underline{a}$ can then deprotonate at three positions; *i*) remove a hydrogen from the β carbon *(equation 7.6, Scheme 7.2)*, *ii*) remove a hydrogen from the α carbon *(equation 7.7, Scheme 7.2)* or *iii*) remove a proton from nitrogen *(equation 7.8, Scheme 7.2)*. From *Table 7.1*, it can be seen that the ion MeCD$_2$NH$^-$ loses mainly HD with a smaller amount of D$_2$; CD$_3$CH$_2$NH$^-$ loses both H$_2$ and HD and C$_2$D$_5$NH$^-$ loses mainly HD with some D$_2$. The major processes are thus those outlined in *equations 7.6* and *7.8*, it is not possible to quantify the various

losses of dihydrogen any further due to the pronounced deuterium isotope effects noted for the various losses of H_2 *(Table 7.1).*

$$CH_3CH_2\overset{-}{N}H \longrightarrow CH_3\overset{-}{C}H\overset{-}{N}H + \overset{\cdot}{H} \qquad \underline{7.5}$$

$$CH_3CH_2\overset{-}{N}H \longrightarrow [\overset{-}{H}(CH_3CHNH)] \longrightarrow \overset{-}{C}H_2CHNH + H_2 \qquad \underline{7.6}$$

$$\underline{7.7} \quad CH_3\overset{-}{C}=NH + H_2 \qquad CH_3CH=\overset{-}{N} + H_2 \qquad \underline{7.8}$$

Scheme 7.2

The loss of methane and the formation of Me^- are outlined in *equations 7.9* and *7.10 (Scheme 7.3).* The initial reaction is suggested to be the formation of solvated ion complex a *(Scheme 7.3)*; the complex can then either fragment directly to form Me^- and CH_2NH *(equation 7.10)* or the methyl anion can deprotonate CH_2NH at nitrogen [determined from the deuterium labelling *(Table 7.1)*] to form CH_2N^- and CH_4 *(equation 7.9, Scheme 7.3).*

$$CH_3CD_2\overset{-}{N}H \longrightarrow [CH_3(CD_2\overset{-}{N}H)] \quad\nearrow\quad CH_4 + CD_2\overset{-}{N} \qquad \underline{7.9}$$
$$\qquad\qquad\qquad\qquad\qquad a \qquad\qquad \searrow\quad \overset{-}{C}H_3 + CD_2NH \qquad \underline{7.10}$$

Scheme 7.3

Other Deprotonated Primary Amines.

In general, the loss of $H\cdot$ and H_2 are the predominant processes for the higher homologues. The formation of Et^- and Pr^- *(cf. equation 7.10)* are not observed since the electron affinities of $Et\cdot$ and $Pr\cdot$ are negative[92]. However, β-cleavage to
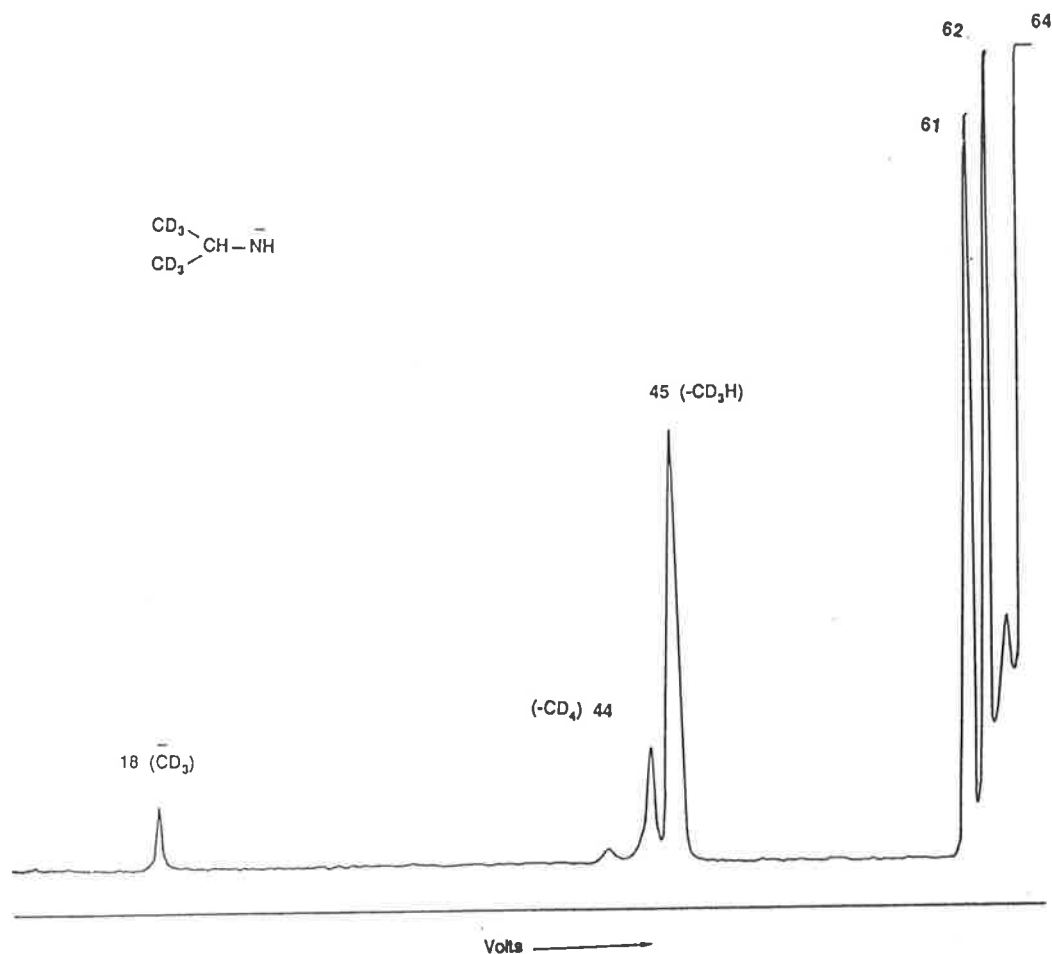
Figure 7.1: *CA Mass Spectrum of $(CD_3)_2CHNH^-$*.

nitrogen, followed by deprotonation at nitrogen *(cf. equation 7.9)* is the characteristic reaction of all compounds shown in *Table 7.1*. For example, deprotonated isopropylamine, n-propylamine and n-butylamine loss CH_4, C_2H_6 and C_3H_8 respectively.

Loss of CH_4 and formation of Me^- are major processes from deprotonated isopropylamine. These processes are analogous to the loss of CH_4 and formation of Me^- from deprotonated ethylamine *(equations 7.9 and 7.10, Scheme 7.3)*. The reaction preceding the loss of methane and formation of Me^- from deprotonated isopropylamine is again the formation of a solvated ion complex (a, *Scheme 7.4)*. This complex can either fragment directly to form Me^- and MeCHNH *(equation 7.11, Scheme 7.4)* or the methyl anion can deprotonate MeCHNH. Deprotonation can occur from two locations *(see Figure 7.1) viz; i)* from the nitrogen *(equation 7.12, Scheme 7.4)* or from the β carbon *(equation 7.13, Scheme 7.4)*. There is also a small loss of methane from deprotonated propylamine and butylamine; the labelled derivatives $PhND^-$ and $BuND^-$ *(Table 7.1)* specifically lose
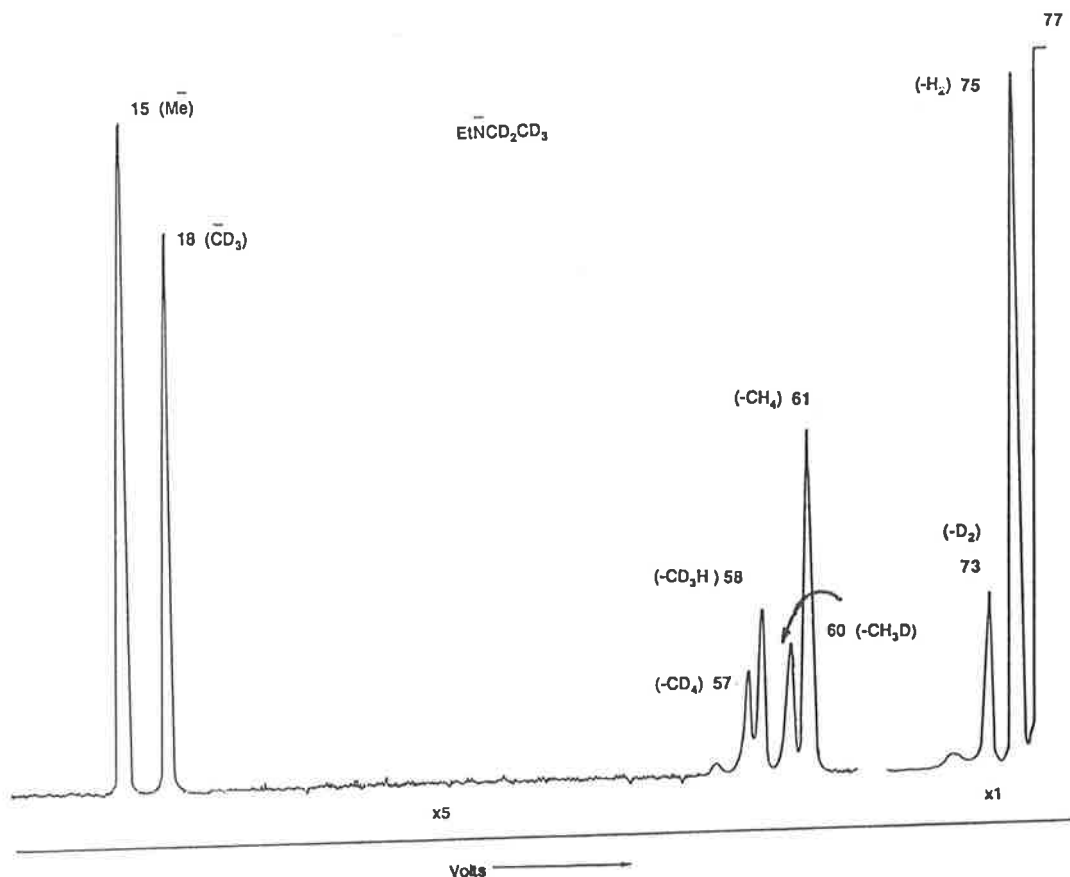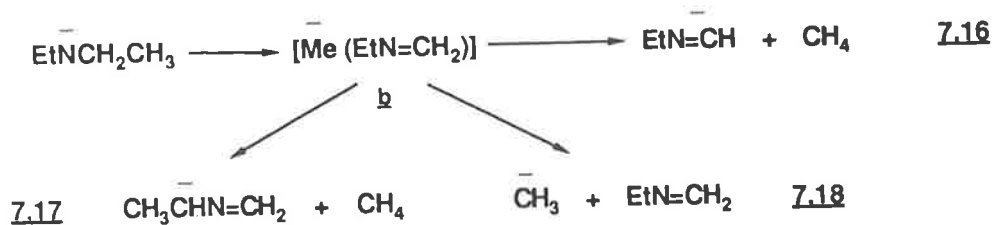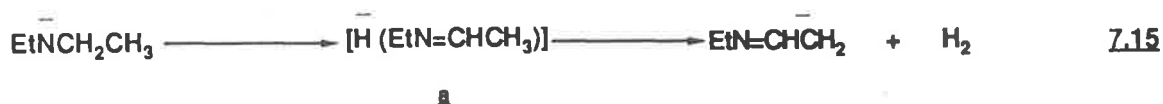
110

CH_3D. A possible mechanism involves S_Ni reactions of the type shown in *equation 7.14*.

$$CH_3CH(CH_3)-\bar{N}H \longrightarrow [CH_3(CH_3CHNH)]^- \nearrow \bar{C}H_3 + CH_3CHNH \qquad \underline{7.11}$$

a

$$\searrow CH_4 + CH_3\bar{C}HN \qquad \underline{7.12}$$

$$\downarrow$$

$$CH_4 + \bar{C}H_2CHNH \qquad \underline{7.13}$$

$$\underset{\overset{|}{HN^-}}{\overset{CH_3}{|}} \longrightarrow \left[\bar{C}H_3 \left(\boxed{}^{NH} \right) \right] \longrightarrow \boxed{}^{\bar{N}} + CH_4 \qquad \underline{7.14}$$

Scheme 7.4

7.2.2   CA Fragmentations of Deprotonated Secondary Amines.

The CA mass spectra of the deprotonated secondary amines are recorded in *Table 7.2* and in *Figure 7.2*. The fragmentations of these anions will be explained using deprotonated diethylamine (Et_2N^-) as an example.

The major fragmentations of deprotonated diethylamine are the loss of H_2 and CH_4 and the formation Me^-. The loss of dihydrogen from deprotonated diethylamine is specifically a 1,2 elimination *(equation 7.15, Scheme 7.5)*. This was determined from the deuterium labelling; specifically $(MeCD_2)_2N^-$ loses HD, while $Et(C_2D_5)N^-$ loses both H_2 and D_2. The respective loses of H_2 : HD of 100:62 and 100:36 from $Et(MeCD_2)N^-$ and $Et(CD_3CH_2)N^-$ can be interpreted in terms of deuterium isotope effects (H/D) of 1.6 for the first step and 2.7 for the second step of the reaction. Stepwise fragmentations of anions involving two kinetically significant steps have been reported previously[70,71]. The possibility of a concerted 1,2 elimination of H_2 cannot be completely discounted in this case, but such reactions are generally high energy processes[75,76].

111

Figure 7.2: *CA Mass Spectrum of* Et_2N^-.

Scheme 7.5

There are two distinct losses of methane from deprotonated diethylamine, these are both proposed to proceed through solvated ion complex **b** *(Scheme 7.5)*. Deprotonation by the methyl anion can occur from two positions: *i)* from the carbon α to the nitrogen *(equation 7.16, Scheme 7.5)*, and *ii)* from the carbon α' to the nitrogen *(equation 7.17, Scheme 7.5)*. The solvated ion complex can also fragment

112

directly to form Me⁻ and EtNCH$_2$ *(equation 7.18)*.

7.2.3   CA Fragmentations of Deprotonated Cyclic Amines.

The CA mass spectra of a number of deprotonated cycloalkylamines are shown in *Table 7.3* and in *Figure 7.3*. The spectra show a number of similarities to the deprotonated cyclohexanones described in *Chapter 4*. Deprotonated piperidine eliminates H$_2$ while the 2,6-dimethylpiperidine ion losses H$_2$, CH$_4$ and forms Me⁻. No labelling studies have been done for these particular ions but it is likely that the processes are directly analogous to that shown in *equation 4.10 (Scheme 4.4)* for cyclohexanone. No retro reactions were observed for the piperidines.
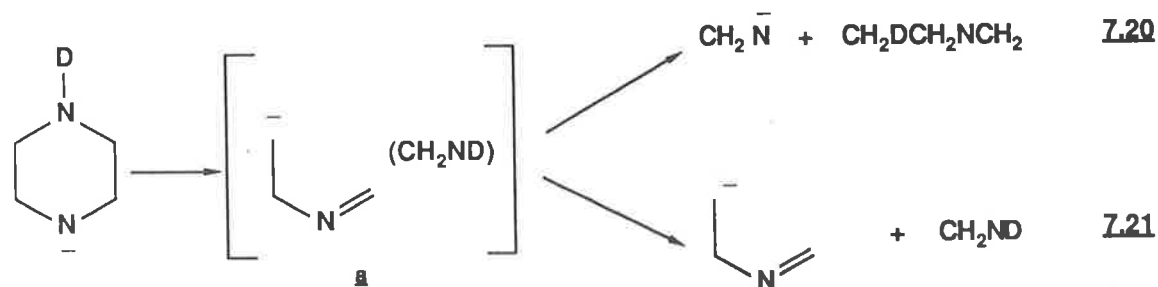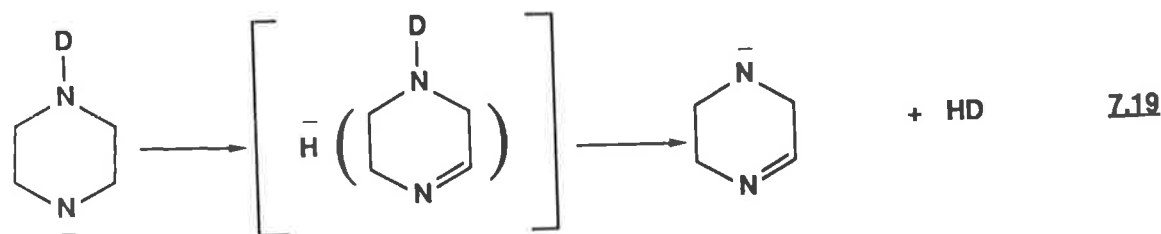
Scheme 7.6

Unlike the deprotonated piperidines the deprotonated piperizines do undergo retro reactions, but these are minor processes. The loss of dihydrogen is again the major process. There are two distinct losses of dihydrogen; the major loss is shown in *equation 7.19 (Scheme 7.6)* for the deuterated derivative. The retro reaction can be explained in terms of the formation of solvated ion complex **a** which can either *i*) form CH$_2$N⁻ and CH$_2$DCH$_2$NCH$_2$ *(equation 7.20, Scheme 7.6)* or *ii*) fragment directly to form CH$_2$NCH$_2$CH$_2^-$ and CH$_2$ND *(equation 7.21, Scheme 7.6)*.
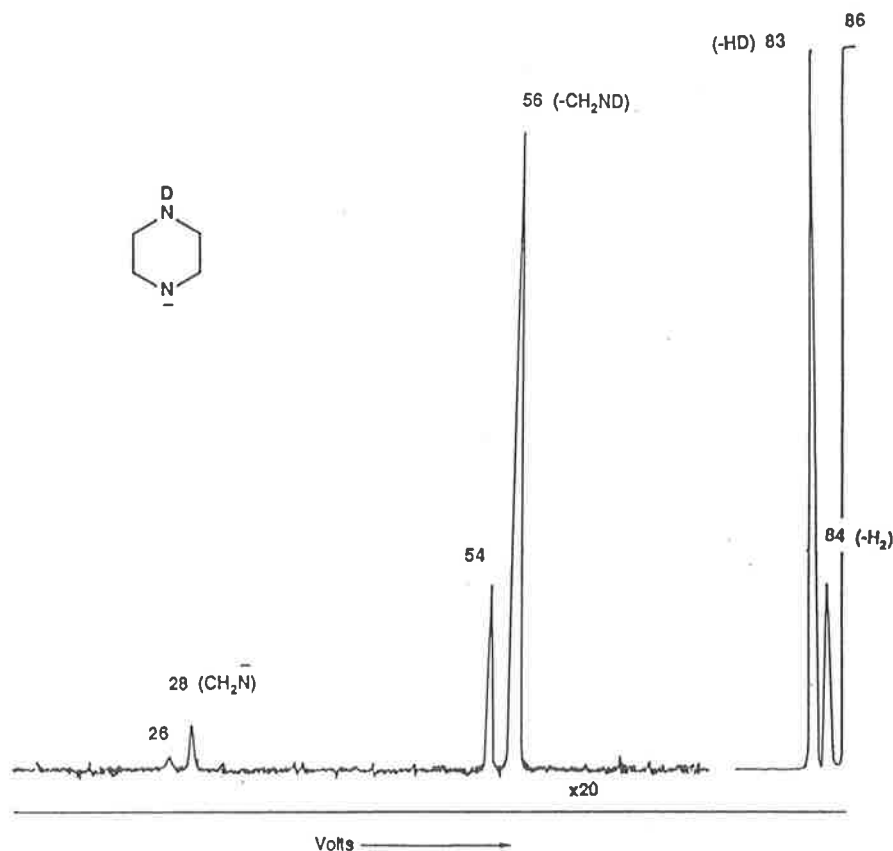
Figure 7.3: *CA Mass Spectrum of the $(M-D^+)^-$ ion from Piperazine-1.4-D_2.*

7.2.4 CA Fragmentations of Deprotonated Primary and Secondary Aromatic Amines.

The CA mass spectra of deprotonated aromatic amines are listed in *Table 7.4*. Previous work on the analogous fragmentations of the phenoxide ion (PhO$^-$) have shown losses of CO and CHO, while its labelled derivative 1-^{13}C-phenoxide loses ^{13}CO and ^{13}CHO, with phenoxide-2,4,6-D_3, losing CO and CDO[93]. The analogous thiophenoxide ion (PhS$^-$) also undergoes ring cleavage without randomization of the substituents on the ring[94]. The major fragmentation of Ph$\overline{N}$H is loss of H$^{.}$; deuterium labelling *(Table 7.4)* indicates the major loss is from the aromatic ring with a minor loss originating from the NH group. The ion Ph$\overline{N}$H also loses 27 a.m.u. and deuterium labelling indicates that the process involves the specific loss of the hydrogen attached to the nitrogen *(see Table 7.4)*. This reaction is thus analogous to the loss of CO from deprotonated phenol to form the cyclopentadienyl anion. The reaction is shown in *equation 7.22*.

114

$$PhNH^- \longrightarrow \bigcirc\hspace{-0.3em} + \ CNH \qquad \underline{7.22}$$

The major losses from deprotonated N-alkylanilines are shown in *Table 7.4*. The fragmentations of PhN̄Et are losses of; H·, H$_2$, CH$_4$, C$_2$H$_4$, Et· together with the formation of Ph$^-$ and Me$^-$. The loss of H· is outlined in *equation 7.23* and from the labelling studies *(Table 7.4)*; the hydrogen is lost exclusively from the aromatic ring. The loss of dihydrogen is interpreted in terms of formation of solvated ion complex **a**. The hydride ion of **a** can then deprotonate the allylic methyl to form PhNCHCH$_2^-$ and H$_2$ *(equation 7.24)*; this loss involves no scrambling of hydrogens. The loss of CH$_4$ and the formation of Me$^-$ are proposed to proceed through solvated ion complex **b** *(Scheme 7.7)*; deprotonation by the methyl anion will lead to C$_7$H$_6$N$^-$ and CH$_4$ *(equation 7.25)*, while direct fragmentation leads to the formation of Me$^-$ and PhNCH$_2$ *(equation 7.26)*. The formation of Ph$^-$ is interesting in that it ⁱˢ rationalized as proceeding through **d**, a species produced following proton transfer processes. From *Table 7.4* it is observed that there is partial deuterium scrambling of the phenyl and α hydrogens. This indicates that intermediate **c** is also involved in the process. Once anion **d** is formed the loss of Ph$^-$ is simply explained by direct fragmentation of solvated complex **e** *(equation 7.27)*. The loss of Et· may occur by the two step process (–H·–C$_2$H$_4$)[95]; the loss of ethane forms PhNH$^-$.

Scheme 7.7

115
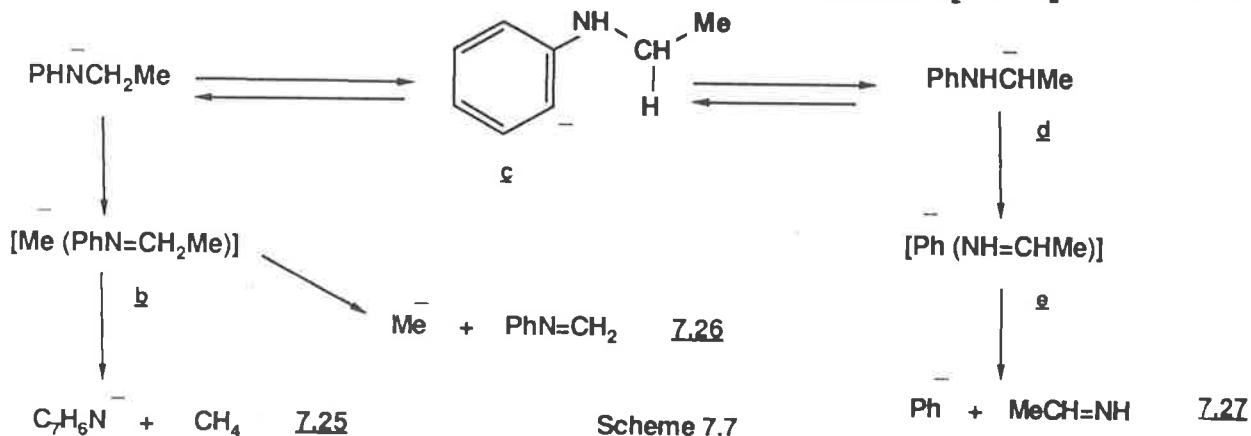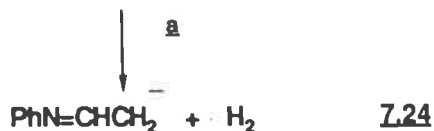
In conclusion, the major fragmentations of deprotonated primary and secondary amines are similar to those already outlined for carbanions. Most of the fragmentations can be rationalised in terms of the intermediacy of ion complexes of the type proposed throughout this thesis. There was only one proton transfer reaction *(Scheme 7.7)* preceding fragmentation. This is in marked contrast to the behaviour of carbanions, where proton transfer is quite common. The cyclic amines studied do undergo retro processes *(equations 7.20* and *7.21)*, but these are of minor importance when compared to the retro processes noted in *Chapter 4* for deprotonated cyclohexanones. The specific loss CNH is the characteristic reaction of deprotonated aniline *(equation 7.22)*.

Neutral Precursor	Anion	Loss							
		H·	H$_2$, D·	HD	(H$_2$+H$_2$)	(H$_2$+HD)	CH$_4$	CH$_3$D	CD$_3$H
CH$_3$NH$_2$	[M−H⁺]⁻	12	100						
CH$_3$CH$_2$NH$_2$	[M−H⁺]⁻	24	100		9		74		
CH$_3$CD$_2$NH$_2$	[M−H⁺]⁻		6	33	6		100		
CD$_3$CH$_2$NH$_2$	[M−H⁺]⁻	33	100	64		12			82
CD$_3$CD$_2$NH$_2$	[M−H⁺]⁻	22		100	12				61
CH$_3$CH$_2$CH$_2$NH$_2$	[M−H⁺]⁻	6	100		34		3		
CH$_3$CH$_2$CH$_2$ND$_2$	[M−D⁺]⁻		100	98		35		3	
(CH$_3$)$_2$CHNH$_2$	[M−H⁺]⁻	9	100				99		
(CH$_3$)$_2$CHND$_2$	[M−D⁺]⁻	4	100	9			42	69	
(CD$_3$)$_2$CHNH$_2$	[M−H⁺]⁻	40	100	86					
CH$_3$(CH$_2$)$_3$NH$_2$	[M−H⁺]⁻	6	100		55		3		
CH$_3$(CH$_2$)$_3$ND$_2$	[M−D⁺]⁻	12	100	82	13	86		1	

Table 7.1 cont: CA Mass Spectra of Deprotonated Primary Amines.

Neutral Precursor	Anion	Loss						Formation	
		(CH_4+H_2)	(CH_3D+H_2)	C_2H_6	C_2H_5D	C_3H_8	C_3H_7D	CH_3^-	CD_3^-
CH_3NH_2	$[M-H^+]^-$								
$CH_3CH_2NH_2$	$[M-H^+]^-$							18	
$CH_3CD_2NH_2$	$[M-H^+]^-$							21	
$CD_3CH_2NH_2$	$[M-H^+]^-$								31
$CD_3CD_2NH_2$	$[M-H^+]^-$								21
$CH_3CH_2CH_2NH_2$	$[M-H^+]^-$			8					
$CH_3CH_2CH_2ND_2$	$[M-D^+]^-$				4				
$(CH_3)_2CHNH_2$	$[M-H^+]^-$	5						6	
$(CH_3)_2CHND_2$	$[M-H^+]^-$		7	6				7	
$(CD_3)_2CHNH_2$	$[M-H^+]^-$								1
$CH_3(CH_2)_3NH_2$	$[M-H^+]^-$					26		2	
$CH_3(CH_2)_3ND_2$	$[M-D^+]^-$						72	2	

Neutral Precursor	Anion	Loss								
		H·	H$_2$, D·	HD	(H$_2$+H$_2$)	(H$_2$+HD)	CH$_4$	CH$_3$D	CD$_3$H	CD$_4$
(CH$_3$)$_2$NH	[M–H$^+$]$^-$	18	100							
(CH$_3$CH$_2$)$_2$NH	[M–H$^+$]$^-$		100		4		16			
CH$_3$CD$_2$NHEt	[M–H$^+$]$^-$		100	63		8	20	8		
CD$_3$CH$_2$NHEt	[M–H$^+$]$^-$		100	36		7	23			19
CD$_3$CD$_2$NHEt	[M–H$^+$]$^-$		100		30	4	8	4	4	4
(CH$_3$CD$_2$)$_2$NH	[M–H$^+$]$^-$			100					18	
(CH$_3$CH$_2$CH$_2$)$_2$NH	[M–H$^+$]$^-$		100		2		5			
[(CH$_3$)$_2$CH]$_2$NH	[M–H$^+$]$^-$		12				100			

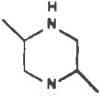| Neutral Precursor	Anion	Loss		Formation	
		(CH$_4$+H$_2$)	CH$_3$CH$_3$	CH$_3^-$	CD$_3^-$
(CH$_3$)$_2$NH	[M–H$^+$]$^-$				
(CH$_3$CH$_2$)$_2$NH	[M–H$^+$]$^-$	1		23	
CH$_3$CD$_2$NHEt	[M–H$^+$]$^-$			38	
CD$_3$CH$_2$NHEt	[M–H$^+$]$^-$			42	28
CD$_3$CD$_2$NHEt	[M–H$^+$]$^-$			23	16
(CH$_3$CD$_2$)$_2$NH	[M–H$^+$]$^-$			51	
(CH$_3$CH$_2$CH$_2$)$_2$NH	[M–H$^+$]$^-$		1.5		
[(CH$_3$)$_2$CH]$_2$NH	[M–H$^+$]$^-$	0.2		3	

Table 7.3: CA Mass Spectra of Deprotonated Cyclic Alkylamines.

Precusor Ion	Loss							
	H_2	HD	CH_4	CH_3D	CH_2NH	CH_2ND	(CH_2NH+H_2)	(CH_2ND+H_2)
	100							
	100		9					
	100				3		1	
	100		2		1		2	
	48	100		2		1		2

Table 7.3 cont: CA Mass Spectra of Deprotonated Cyclic Alkylamines.
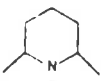
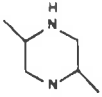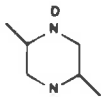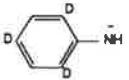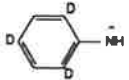| Precusor Ion	Loss						Formation		
	C_2H_3N	C_2H_2DN	$(C_2H_3N+H_2)$	$(C_2H_2DN+H_2)$	C_3H_7N	C_3H_6DN	CH_2CHN^-	CH_2N^-	CN^-
								0.5	0.1
	1		1		1		2	0.2	
		1		1		0.5	1	0.1	

Precursor Ion	Loss								
	H·	H₂	HD	H₂+H₂	Me·	CH₄	CH₃D	CD₃H	HNC
PhNH⁻	100	21							1
(ring-D₃ NH⁻ structure)	100	38	6						1
C₆D₅NH⁻	61	100	8	4					1
PhN̄Me	100	8			12	1			
PhN̄Et	100	78				12			
PhN̄CH₂CH₃	100		38					20	
C₆D₅N̄Et		100				4	4		
PhN̄Ph	100	48							

Precursor Ion	Loss				Formation					
	C₂H₄	C₂H₂D₂	Et·	C₂H₂D₃	C₆H₅⁻	C₆HD₄⁻	C₆D₅⁻	CN⁻	Me⁻	CD₃⁻
PhNH⁻								1		
(ring-D₃ NH⁻ structure)								1		
C₆D₅NH⁻								1		
PhN̄Me					28			2		
PhN̄Et	10		15		34				0.2	
PhN̄CH₂CH₃		12		13	9					0.2
C₆D₅N̄Et	a		a			3	3		0.1	
PhN̄Ph										

a. Unresolved but a linked scan showed losses of 28, 29 and 30 a.m.u.

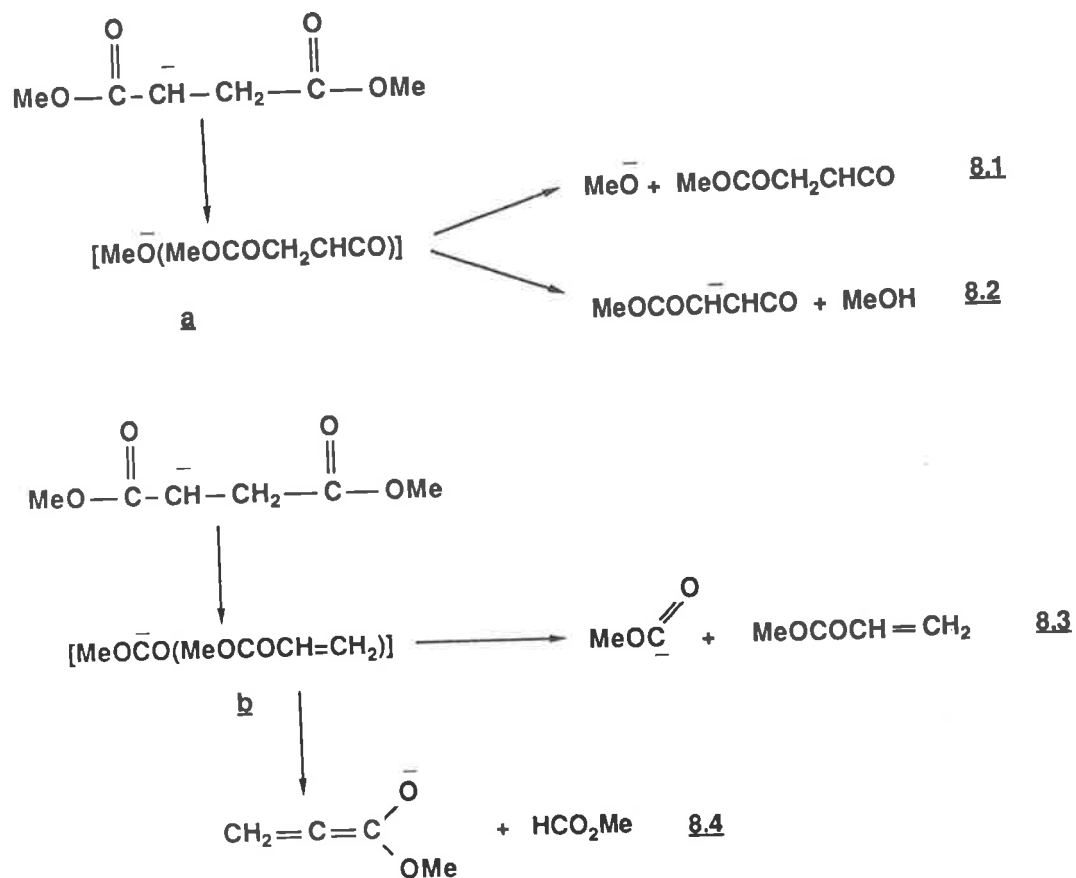Table 7.4: CA Mass Spectra of Deprotonated Aryl Amines.

Chapter 8

Summary of Reaction Types.

8.1   Introduction.

In this chapter a number of "rules" will be presented that indicate the fragmentation pathways of collisionally activated even-electron negative ions formed by chemical ionization. Many different processes have been observed, in this chapter specific examples of each type are given. The basic fragmentations can be divided in to five main types; i) formation of a solvated ion complex in which the anion initiates a number of different reactions including; a) direct displacement, b) deprotonation, c) elimination and d) nucleophilic displacement, ii) initial proton transfer to form a new anion which then can initiate a number of different reactions as above, iii) formation of a radical anion by the elimination of a radical, iv) cyclic compounds undergo a specific retro reaction with elimination of a neutral molecule, v) the anion can undergo specific rearrangement reactions which are often complex. However it should be noted that in some cases there are alternative mechanisms that cannot be excluded on the available data. These are; i) the reaction may be concerted or ii) the reaction proceeds through radical/radical ion complexes rather than anion/neutral complexes.

8.2   Formation of Solvated Ion Complexes.

A particular example of this process was shown in chapter 3, in the fragmentation of deprotonated dimethyl succinate. Here the major fragmentations were proposed to proceed through two solvated ion complexes $\underline{a}$ and $\underline{b}$ in *Scheme 8.1.* Each solvated ion complex could fragment directly to form MeO^- *(equation 8.1)* and $MeO\overset{=}{C}O$ *(equation 8.3)* or either could deprotonate the neutral molecule to give a loss of methanol *(equation 8.2)* or methyl formate *(equation 8.4)*.

123

$$MeO + MeOCOCH_2CHCO \qquad \underline{8.1}$$

$$MeOCOCHCHCO + MeOH \qquad \underline{8.2}$$

a

$$MeOC\overset{O}{\diagup} + MeOCOCH=CH_2 \qquad \underline{8.3}$$

b

$$CH_2=C=C\overset{\overline{O}}{\underset{OMe}{\diagup}} + HCO_2Me \qquad \underline{8.4}$$
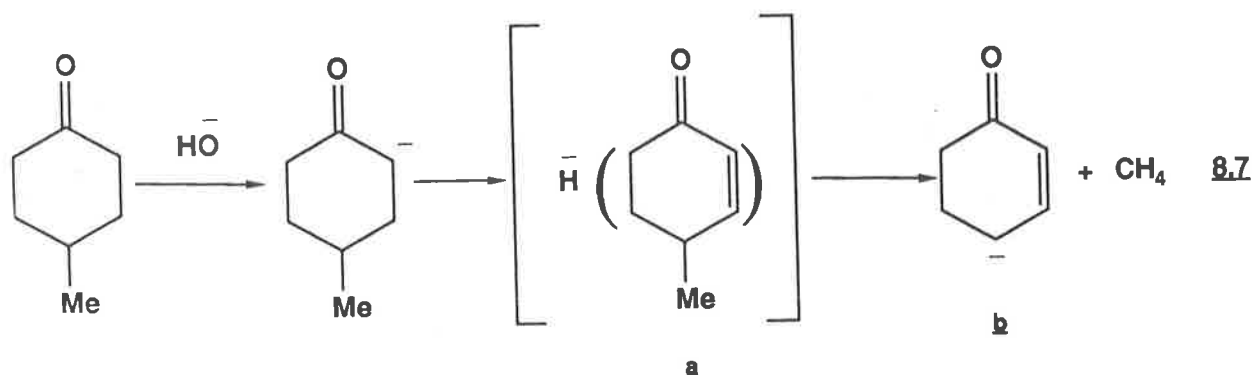
Scheme 8.1

Another example of the formation of solvated ion complex was noted in *Chapter 4*: this involved cyclohexenone solvated by a hydride ion. Deuterium labelling indicated the hydride ion could deprotonate in two positions; *i*) remove a proton from the 4 position *(equation 8.5)* or *ii*) removal of a proton from the 6 position *(equation 8.6, Scheme 8.2)*. Analogous processes were observed for the losses of methane from 3-methylcyclohexanone enolate ions.

Scheme 8.2   **a**

$$+ H_2 \qquad \underline{8.5}$$

$$+ H_2 \qquad \underline{8.6}$$

124
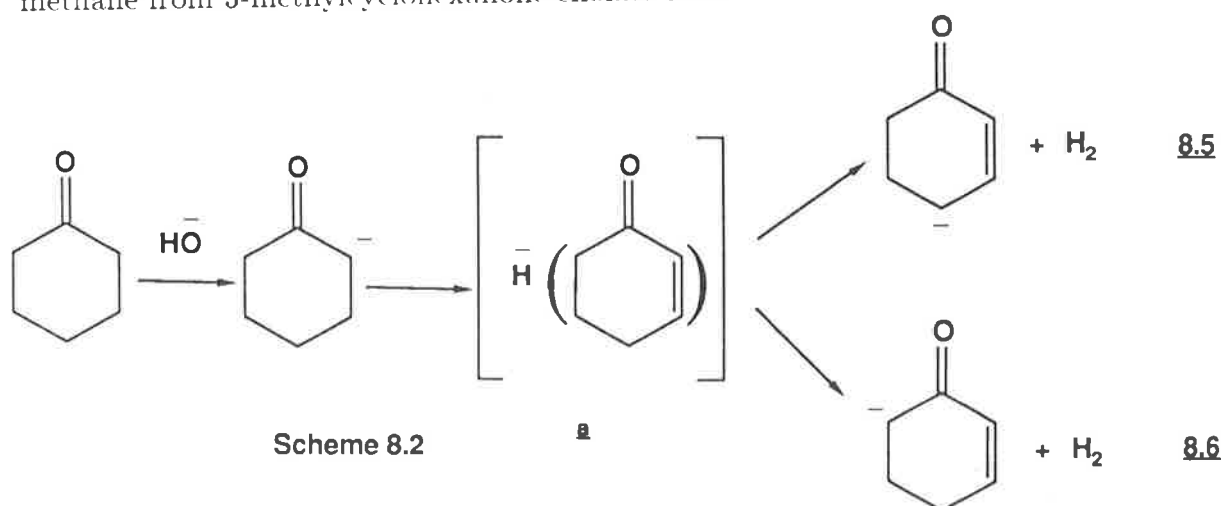
In the case of the loss of methane from 4-methylcyclohexanone it was shown by deuterium labelling that the loss of methane involved a hydrogen from the 3 position together with the 4 methyl group. A possible mechanism involves the formation of a solvated hydride ion intermediate $\underline{a}$ (*equation 8.7*), the hydride ion can then attack the methyl group *via* an S_Ni reaction to displace methane and form deprotonated cyclohexenone $\underline{b}$ (*equation 8.7*).

$$\text{O} \quad \xrightarrow{\text{H}\bar{\text{O}}} \quad \xrightarrow{} \quad \left[\bar{\text{H}} \left(\text{O} \right) \right] \quad \xrightarrow{} \quad \text{O} \; + \; CH_4 \qquad \underline{8.7}$$

$$\text{Me} \qquad\qquad \text{Me} \qquad\qquad \text{Me} \qquad\qquad \underline{b}$$

$$\underline{a}$$

A final example of the formation of a solvated ion complex was seen in *Chapter 7*. Deprotonated diethylamine eliminates methane and forms Me^-. The initial step is suggested to be the formation of methyl anion ion complex $\underline{a}$ (*Scheme 8.3*). The methyl anion of $\underline{a}$ can then either *i*) deprotonate in two different positions (*equations 8.8* and *8.9, Scheme 8.3*) or *ii*) fragment directly to form Me^- and $EtNCH_2$ (*equation 8.10, Scheme 8.3*).

$$\overline{Et}NCH_2CH_3 \longrightarrow [Me\,(Et\overline{N}CH_2)] \longrightarrow Et\overline{N}CH_2 \; + \; CH_4 \qquad \underline{8.8}$$

$$\underline{a}$$

$$\underline{8.9} \qquad CH_3CH\overline{N}CH_2 \; + \; CH_4 \qquad\qquad \overline{C}H_3 \; + \; EtNCH_2 \qquad \underline{8.10}$$
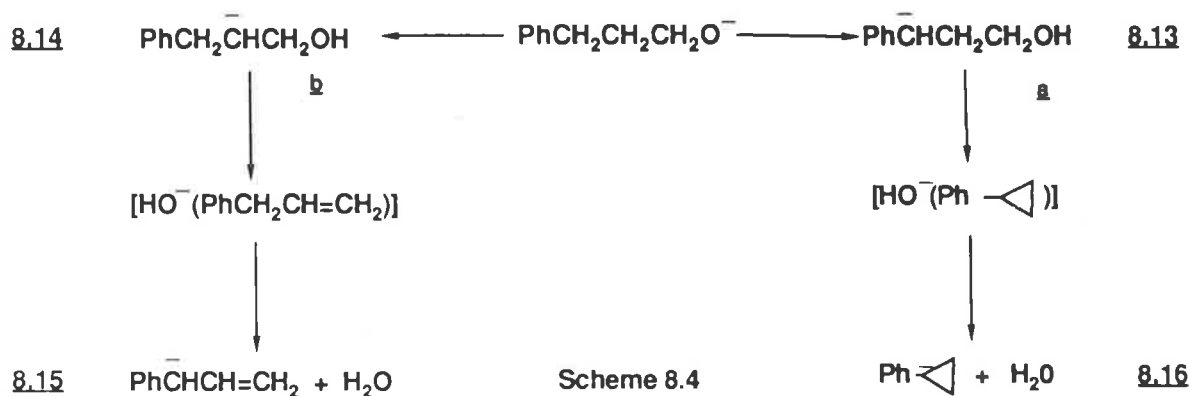
Scheme 8.3

125
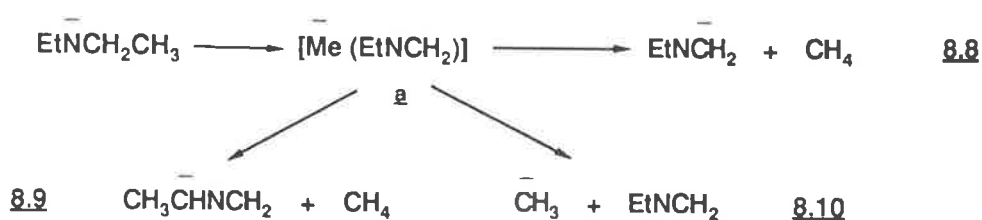
8.3   Proton Transfer.

Many examples of proton transfer occurring before fragmentation were observed; i) it is suggested that the loss of ethylene from the 2-ethylcyclohexanone enolate is a two step process involving an initial proton transfer from the terminal methyl group to the enolate anion *(equation 8.11)*. An analogous process occurs for the loss of ethylene from deprotonated diethyl acetamide *(equation 8.12)*.

8.11

+ C_2H_4

MeCONEt + C_2H_4

*   H/D = 2.50 ± 0.1

H/D = 1.09 ± 0.02

8.12
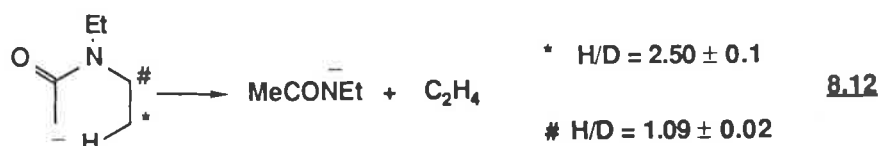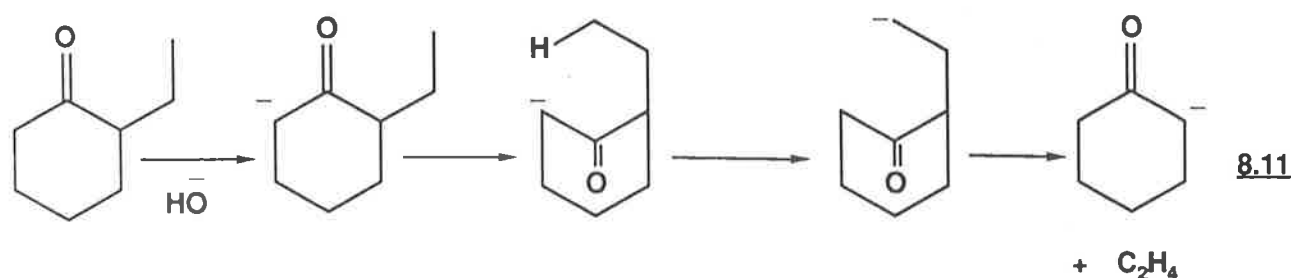
ii) The loss of water from the alkoxide ion of 3-phenylpropan-1-ol involves proton transfer. Deuterium labelling indicated the initial proton transfer could be divided into two types. in one case the proton was from the benzylic position to oxygen to form a *(equation 8.13, Scheme 8.4)*: in the other a proton is transferred from the central carbon to the oxygen to form b *(equation 8.14, Scheme 8.4)*. Two different solvated ion complexes were formed. the OH⁻ could then deprotonate either neutral *(equations 8.15 and 8.16, Scheme 8.4)*.

8.14 $PhCH_2\overset{-}{C}HCH_2OH$ ◄——— $PhCH_2CH_2CH_2O^-$ ———► $Ph\overset{-}{C}HCH_2CH_2OH$ 8.13

b

a

$[HO^-(PhCH_2CH=CH_2)]$

$[HO^-(Ph \triangleleft\,)]$

8.15 $Ph\overset{-}{C}HCH=CH_2$ + H_2O Scheme 8.4 $Ph\triangleleft$ + H_2O 8.16

iii) A specific proton transfer reaction occurring before fragmentation is observed for the loss of acetaldehyde and the formation of the acetyl anion from deprotonated diethyl acetamide. The initial deprotonation of diethyl acetamide is on the acetyl methyl group (a, *Scheme 8.5*), there is then a specific 1,4 proton transfer from one of the ethyl side chains to form a new anion b. This anion can then form a solvated acetyl ion complex which can then fragment directly *(equation 8.17, Scheme 8.5)* or the acetyl anion can deprotonate the neutral to form MeCH$\bar{\text{N}}$CHMe and acetaldehyde *(equation 8.18, Scheme 8.5)*.
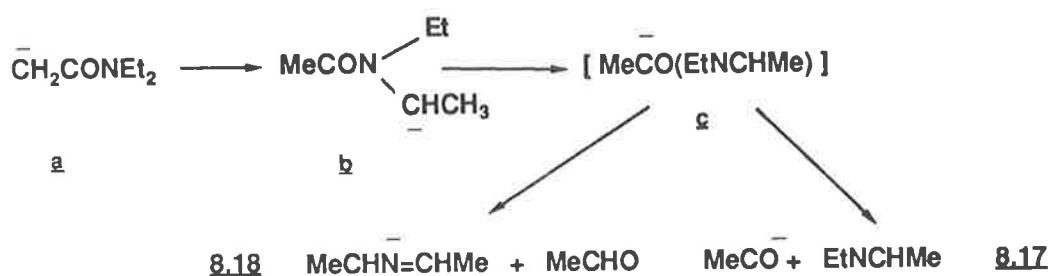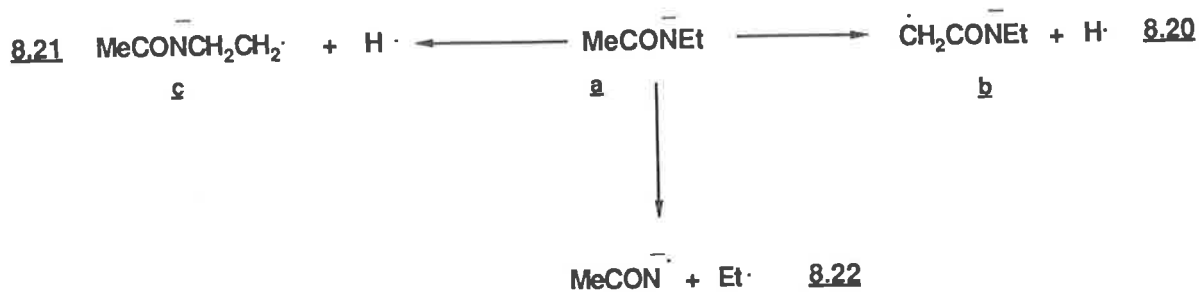

Scheme 8.5

8.4 Radical Anion Formation.

The loss of H· occurs readily from all ketone enolates studied. The loss was always α to the carbonyl group to form a stabilized radical anion (*equation 8.19*).
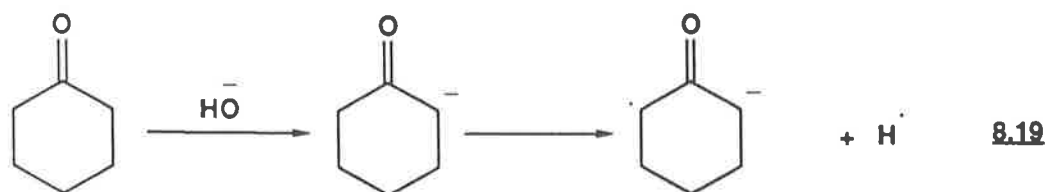
There are two separate losses of H· from N-ethyl acetamide. Initial deprotonation is from the nitrogen to form a *(Scheme 8.6)*. loss of H· can either be from the acetyl methyl group to form stabilized radical anion *(equation 8.20. Scheme 8.6)* or the H· can be eliminated from the ethyl side chain *(equation 8.21. Scheme 8.6)*. The loss of an ethyl radical is also a major process in the fragmentation of deprotonated N-ethyl acetamide *(equation 8.22. Scheme 8.6)*.

8.21 $MeCON\overline{C}H_2CH_2$· + H· ⟵——— MeCONEt ———⟶ $\overline{C}H_2CONEt$ + H· **8.20**

c   **a**   **b**

$MeCO\overline{N}$· + Et·   **8.22**

Scheme 8.6

8.5 Specific Retro Reaction.

In this thesis a number of examples of specific retro reactions were observed; *i*) the loss of ethylene from deprotonated cyclohexanones and substituted cyclohexanones. In the case of 3-substituted cyclohexanones there are two possible retro reactions that can occur, the major loss was always of the larger alkene (*equations 8.23 and 8.24, Scheme 8.7) ii*) the loss of ethylene from piperazine and the loss of ethylene and propylene from 2,5-dimethyl piperazine, again the loss of the larger alkene was the predominate process.

$+ CH_3CHCH_2$ **8.23**

$+ CH_2CH_2$ **8.24**

Scheme 8.7

128
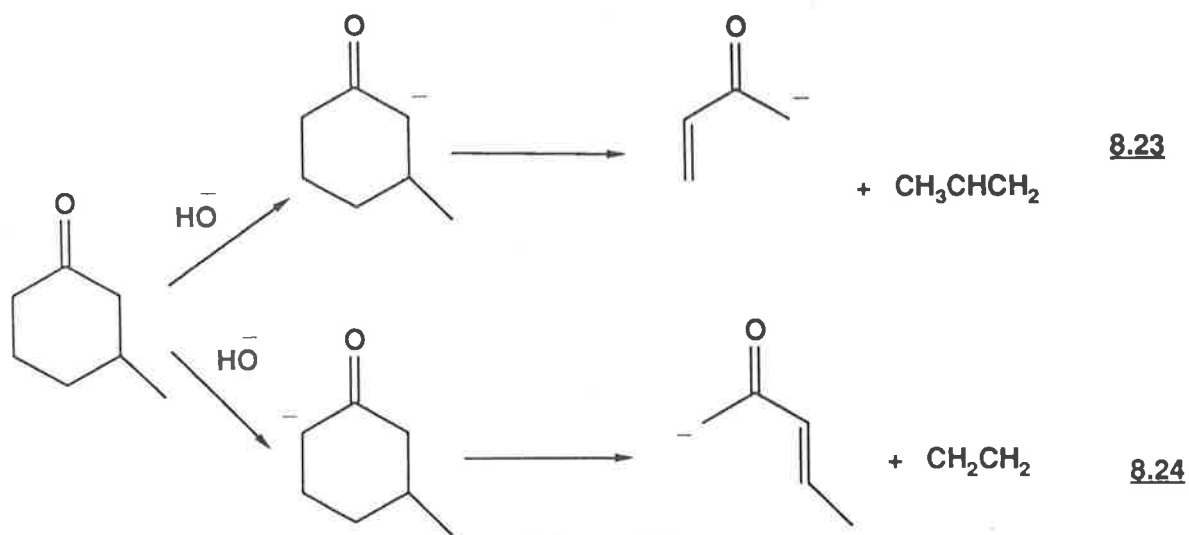
8.6   Complex Rearrangement Pathways.

The proposed Smiles intermediate <u>a</u> *(Scheme 8.8)*, fragments as shown in *equations 8.25* and *8.26*[1] *(Scheme 8.8)*. There are few other examples of complex rearrangement pathways in this thesis, however there have been a number of examples[96-100] reported recently including the Wittig rearrangement[96,97,99], and the Smiles reaction[100].

Scheme 8.8
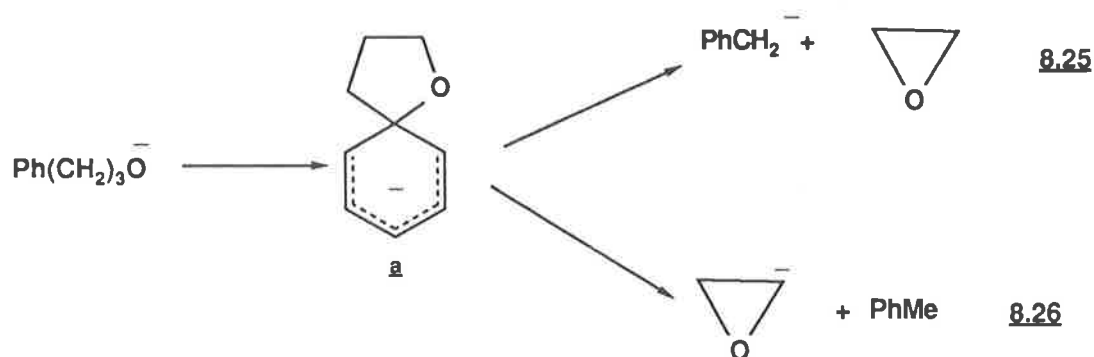
One example of the gas phase Wittig rearrangement occurs for deprotonated benzyl ethers, the CA mass spectra of ions $Ph\bar{C}HOR$ and $Ph(R)CHO^-$ (R = alkyl and phenyl) are very similar, suggesting a Wittig rearrangement[101,102,103] may be occurring in the gas phase (*equations 8.27* and *8.28, Scheme 8.9*).

Scheme 8.9
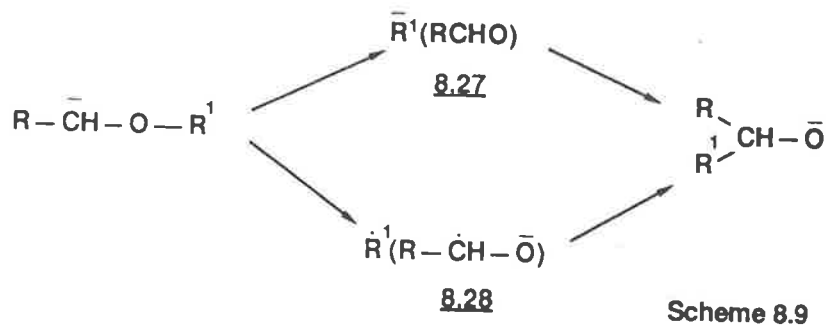
The major fragmentations can be interpreted in terms of 1,2 elimination of

---

[1]The possibility that deprotonated ethylene oxide rearranges to the acetaldehyde ion cannot be excluded on the available evidence.

groups from the Wittig product ion. For example, deuterium labelling of $Ph\bar{C}HOEt$ and $Ph(Et)CHO^-$ show that the major processes produce $MeCHCHO^- + C_6H_6$ (equation 8.29, Scheme 8.10) and $C_6H_5^-$ (equation 8.30, Scheme 8.10). An analogous process, $Ph_2CHO^- \longrightarrow (C_6H_4)^-CHO + C_6H_6$ gives the major peak in the spectrum of $Ph\bar{C}HOPh$[96].

$$Ph\bar{C}HOEt \longrightarrow \overset{Ph}{\underset{Et}{\diagdown}}CH-\bar{O} \longrightarrow [Ph(EtCHO)] \nearrow \searrow$$

$$MeCH\overset{-}{C}HO + C_6H_6 \qquad \underline{8.29}$$

$$C_6H_5^- + EtCHO \qquad \underline{8.30}$$
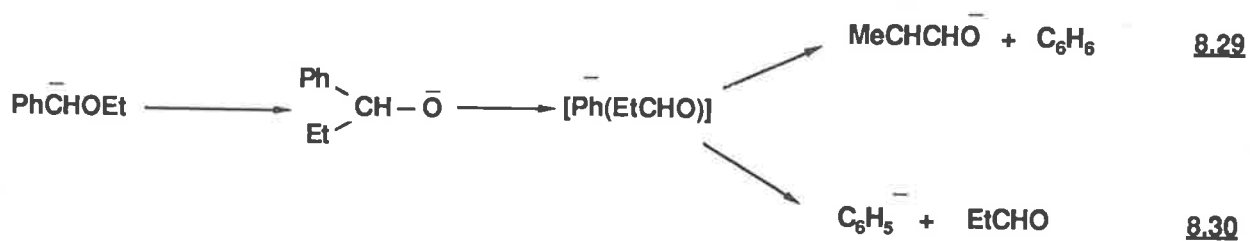
Scheme 8.10

130

Chapter 9

Experimental.

9.1   General.

Collision activation (CA) mass spectra were recorded on a VG ZAB 2HF mass spectrometer operating in the chemical ionization mode[104]. All slits were fully open to obtain maximum sensitivity and to minimize energy resolution effects[105]. The chemical ionization slit was used in the source; ionizing energy 100 eV (tungsten filament), ion source temperature 180°C, accelerating voltage –8 kV. Enolate and alkoxide negative ions were generated by H^+ abstraction by OH^- (or H^- or $O^{-\cdot}$), or by D^+ abstraction by OD^- (or by D^- or $O^{-\cdot}$)[105]. Deprotonated amines were produced by proton abstraction with H_2N^-. Reactant negative ions were generated from H_2O (or D_2O) or NH_3 by 100 eV electrons. The indicated source pressure was typically 5×10^{-5} mbar. The pressure of the substrate was approximately 5×10^{-6} mbar, The estimated total pressure in the source was 10^{-1} mbar. The pressure of helium in the second field free region collision cell was measured at 2×10^{-7} mbar, by an ion gauge situated between the electric sector and collision cell. This produced a decrease in the main beam of c.a. 10% and corresponds to essentially single collision conditions[106].

Isotope effects H/D listed in the text were determined by comparing the peak areas of the appropriate dissociations in each spectrum: listed values are a mean of ten individual measurements. Peak widths at half height are also a mean of ten individual measurements. In order to determine the collision induced : unimolecular component ratios of a particular dissociation a potential (typically 1000 V) was applied to the second collision cell: the relative areas of the shifted (collision induced) and unshifted ("unimolecular") peak give the required ratios[107].

Routine positive ion mass spectra were determined with an AEI MS 3074 double sector mass spectrometer operating at an electron energy of 70 eV. The samples were introduced into the ion source by a direct insertion probe. Infrared spectra were recorded on a Jasco A–102 infrared spectrophotometer as a nujol mull or as a liquid film. The 1602 cm^{-1} peak of polystyrene was used as the standard. ^{1}H Nuclear magnetic resonance spectra were recorded either on a Jeol PMX-60 spectrometer, a Varian T-60 operating at 60 MHz, or a Bruker WP-80 spectrometer operating at 80 MHz. ^{13}C Nuclear magnetic resonance spectra were recorded on a Bruker WP-80 spectrometer at 20.1 MHz or using a Bruker CXP-300 spectrometer operating at 75.4 MHz. All n.m.r. spectra were obtained in deuterochloroform (except where stated to the contrary), using tetramethylsilane as an internal standard. The data are given in the following order; chemical shift (δ) in p. p. m., relative intensity indicating the number of protons, multiplicity, and first order coupling constant (J) in hertz (Hz). Abbreviations: s=singlet; d=doublet; t=triplet; q=quartet; b=broad.

Melting points were determined by using a Kofler hot-stage melting point apparatus and are uncorrected. All solvents were of analytical grade or were purified according to standard procedures[108] before use. Microanalyses were performed by the Research School of Chemistry, Australian National University, Canberra, Australia.

9.2 Labelled Compounds.

The identity and deuterium incorporation of labelled compounds was routinely checked by positive ion mass spectrometry, ^{1}H n.m.r. and ^{13}C n.m.r.

The following isotopically labelled compounds were commercially available and were used without further purification: deuterium gas, deuterium oxide (>99% atom, AINSE.), methyl iodide-D$_3$ (>99% atom, Aldrich.), methanol-D$_1$ (>99% atom, Aldrich.), methanol-D$_4$ (>99% atom, Aldrich.), bromobenzene-D$_5$ (>99% atom, Aldrich.), acetic acid-D$_4$ (>99% atom, Service des molécule Marquées France.), lithium aluminium hydride-D$_4$ (>98% atom, Aldrich.), lithium hydride-D$_1$ (>99% atom, Fluka A. G.), ethanol-D$_6$ (>99% atom, Merck, Sharp and Dohme.),

sulphuric acid-D_2 (>99% atom, ICN Biomedicals, Inc.), acetone-D_6 (99% atom, Aldrich).

The following labelled compounds were prepared by standard methods; benzoyl chloride-D_5[109], acetyl chloride-D_3[110], ethanol-2,2,2,-D_3[111], ethanol-1,1-D_2[111], ethyl-iodide-1,1-D_2[112], ethyl iodide-2,2,2-D_3[112], ethyl iodide-1,1,2,2,2-D_5[112], iso-propyl-alcohol-2,2,2,2',2',2'-D_6[111], iso-propyl iodide-2,2,2,2',2',2'-D_6[112] and aniline-D_3[113]. These compounds were distilled before use.

9.3 Syntheses of the Dimethyl Succinates and related compounds.

Dimethyl succinate was a commercial sample. Di-(methyl-D_3)-succinate, dimethyl-2,3-dimethylsuccinate and dimethyl 2,2-dimethylsuccinate were prepared[114] by reaction of the appropriate bis acid chloride with methanol or methanol-D_4. Dimethyl-2,2,3-trimethylsuccinate and di-(methyl-D_3)-2,2,3-trimethylsuccinate were prepared by a standard method[115].

Dimethyl succinate-2,2,3,3,-D_4, and dimethyl 2,2-dimethyl succinate-3,3-D_2 were obtained by the reactions of dimethyl succinate and dimethyl 2,2-dimethylsuccinate as follows. A solution of the appropriate unlabelled compound (0.20 g) and sodium methoxide (0.30 g) in methanol-D_1 (1.0 ml) under nitrogen, was heated under reflux for 12 hours. Deuterium oxide (1 ml) was added and the solution extracted with diethyl ether (2×5 ml). The organic layer was concentrated and the product distilled under vacuum. Yields were 80-90% and the deuterium incorporation was greater than 95%.

Dimethyl succinate-2,3-D_2.

Dimethyl maleate (0.10 g) in toluene (10 ml) containing tris-(triphenylphosphine)-rhodium(I) chloride (0.10 g) was reduced (in a standard hydrogen apparatus) with deuterium gas for 6 hours. The toluene was removed under vacuum, diethyl ether (10 ml) was added and the solution filtered. The residue was then distilled under

vacuum to yield dimethyl succinate-2,3-D_2 [0.06 g, b.p. 95-97°C, (20 mm Hg)], yield 60%; (D_2 = 99%). The positions of the deuteriums were confirmed by n.m.r., *viz:*

^{1}H n.m.r. δ, 2.7, 2H, m; 3.6, 6H, s.

^{13}C n.m.r. δ, 28.6, t, J_{CD} = 27 Hz; 51.8, 171.8.

Dimethyl-2,2-dimethyl-3-(methyl-D_3)succinate.

Dimethyl-2,2-dimethylsuccinate (0.20 g) in tetrahydrofuran (1 ml) was added dropwise to a solution of lithium diisopropylamine [prepared from diisopropylamine (0.12 g) and n-butyllithium (1.41 mol.dm^{-1}, 1.6 ml) in tetrahydrofuran (1 ml)] at -78 °C, the mixture was stirred at that temperature for 15 minutes, methyl iodide-D_3 (0.17 g) was added, the mixture was stirred for 2 hours at -78 °C, and allowed to warm to 0°C. Aqueous ammonium chloride (saturated, 2ml) was added, the mixture extracted with diethyl ether (3×7 ml), and the combined ethereal extract was washed with aqueous sodium bisulphite (2 N, 10 ml), water (1 ml) and dried (anhydrous sodium sulphate). Vacuum distillation gave dimethyl-2,2-dimethyl-3-(methyl-D_3)succinate [b.p. 65-69°C/26 mm Hg (0.19 g, yield 90%; D_3 = 99%)].

^{1}H n.m.r. δ, 1.0, 6H, s; 2.7, 1H, b, s; 3.4, 6H, s.

Dimethyl-2,3-methyl-2(methyl-D_3)succinate.

This compound was prepared from dimethyl-2,3-dimethylsuccinate by the same method used for dimethyl 2,2-dimethyl-3-(methyl-D_3)succinate (above). Yield 85% (D_3 = 99%).

^{1}H n.m.r. δ, 1.1, 6H, m; 2.75, 1H, m; 3.6, 6H, s.

Di-(methyl-D_3)-2,2,3-trimethylsuccinate.

Hydrolysis of dimethyl-2,2,3-trimethylsuccinate, conversion into the bis acid chloride and esterification[114] with methanol-D_4 gave di-(methyl-D_3) 2,2,3-trimethylsuccinate in 80% overall yield. D_6 = 99%.

^{1}H n.m.r. δ, 1.0, 9H, m; 2.7, 1H, q, J=12 Hz.

134

9.4 Syntheses of the Dimethyl Adipates and related compounds.

Dimethyl glutarate was a commercial product. Dimethyl adipate[114], dimethyl 1,4-dimethyladipate[116] and dimethyl 1,1-dimethyladipate[117] were prepared by standard procedures. $MeOCOCD_2CH_2CD_2CO_2Me$, $MeOCOCD_2CH_2CH_2CD_2CO_2Me$, $MeOCOCD(Me)CH_2CH_2CD(Me)CO_2Me$ and $MeOCOCD_2CH_2CH_2CMe_2CO_2Me$ were prepared from the appropriate unlabelled precursor by MeOD/NaOMe exchange (see earlier) in a sealed tube at 90°C for 16 hours (incorporation > 90% D). 1-Carbomethoxycyclopentan-2-one, and 1-carbomethoxy-1,3-dimethylcyclopentan-2-one were prepared by Dieckmann condensation of the appropriate dimethyl adipates[114,117,118,119,120].

1-Carbomethoxy-3,3-dimethylcyclopentanon-2-one.

Dimethyl 1,1-dimethyladipate (2.0 g, 9.9 mmol.) in benzene (20 ml) was added slowly to sodium hydride (0.4 g, 16.7 mmol.) in benzene (30 ml). The solution was then refluxed for 18 hours. Diethylether (50 ml) was then added followed by water (10 ml) and acetic acid (10 ml). The organic layer was washed with saturated sodium bicarbonate (2×30 ml), followed by sodium chloride (2×30 ml). Concentration of the organic layer followed by vacuum distillation gave 1-carbomethoxy-3,3-dimethylcyclopentanon-2-one as a colourless liquid, b.p. 105-108°C at 18 mm Hg, yield 0.65 g (39%); C 63.34, H 8.53; $C_9H_{14}O_3$ requires C 63.51, H 8.29%. i.r. (film), ν, 3010 (C—H); 1750 (ester CO); 1720 (ketone CO); 1240 (C—O). ^1H n.m.r. δ, 0.95, 6H, s; 2.75, 2H, m; 2.1, 2H, m; 3.1, 1H, t, J = 13Hz. ^{13}C n.m.r. δ, 22.8; 23.3; 35.7; 44.9; 51.5; 53.3; 169.6; 214.9.

9.5 The Syntheses of Cyclohexanone derivatives.

Cyclohexanone, 4-methyl- and 4-ethylcyclohexanone were commercial samples. All the unlabelled 2-substituted (including 2-ethyl-4-methyl-cyclohexanone)[121], and the 3-substituted cyclohexanones[122] are known and were prepared by reported methods.

Cyclohexanone-2,2,6,6-D_4, 2-methylcyclohexanone 2,6,6-D_3, 3-methylcyclohexanone 2,2,6,6-D_4, 4-methylcyclohexanone 2,2,6,6-D_4, 2-ethylcyclohexanone 2,6,6-D_3, 3-ethylcyclohexanone 2,2,6,6-D_4, 4-ethylcyclohexanone 2,2,6,6-D_4, 2-n-propylcyclohexanone 2,6,6-D_3 and 3-n-propylcyclohexanone 2,2,6,6-D_4 were all prepared by exchange using D_2O/NaOD, in quantitative yield (D_3 or D_4 incorporation was greater than 95%). As an example, cyclohexanone (0.10 g, 1.0 mmol.) deuterium oxide (0.80 g, 40 mmol.) and sodium deuteroxide (0.01g, 0.25 mmol.) were heated in a sealed glass ampoule for 16 hours at 120°C. Extraction into diethyl ether (3×2.5 ml) followed by removal of the solvent gave quantitative recovery of deuterium labelled cyclohexanone, b.p. 49-51°C (18 mm Hg), $D_4 > 95\%$.
^{1}H n.m.r. δ, 1.7, 6H, b, s.

Cyclohexanone 3,3,5,5-D_4.

This compound was made by a synthetic sequence based on that of Green[122]. Cyclohexane dione mono-ethylene ketal (1.00 g, 6.4 mmol.) and sodium deuteroxide/deuterium oxide (2 mol.dm^{-3}, 5.1 ml) were heated in a sealed ampoule at 120°C for 16 hours. Extraction of the D_4 ketone into diethyl ether (10 ml), followed by reduction with lithium aluminium hydride (0.20 g) gave the alcohol [0.96 g (95%), D_4 = 98%], which was then converted to the tosylate by a standard method[123]. M.p. 69-71°C, yield: 0.81 g (53%); D_4 = 98%.

The tosylate (0.81 g) was heated under reflux for 48 hours with anhydrous tetrahydrofuran (10 ml) and lithium triethylborohydride[124,125] (1.76 mol.dm^{-3}, 2.9 ml). The mixture was cooled to 0°C, water (0.5 ml), then aqueous sodium hydroxide (15%, 5 ml), then aqueous hydrogen peroxide (30%, 10 ml) were added and the solution refluxed for 12 hours. Separation of the layers followed by removal of the solvent gave crude cyclohexane ethylene ketal 3,3,5,5-D_4 (0.25 g, 65%, D_4 = 98%). Hydrolysis[126] was carried out by dissolving the crude ketal in chloroform (20 ml) and stirring with aqueous oxalic acid (saturated 20 ml) for 24 hours to yield cyclohexane 3,3,5,5-D_4, b.p. 50-52°C/20 mm Hg, [0.13 g (75%), D_4 = 98%].
^{1}H n.m.r. δ, 2.3, 4H, t; 1.5, 2H, b, s.

Cyclohexanone 4,4-D_2.

The synthesis of this compound is the same as that of cyclohexanone 3,3,5,5-D_4 to the tosylate stage, except the initial deuterium exchange step is deleted and lithium aluminium deuteride replaces lithium aluminium hydride in the reduction step. The 4-tosylate-4-D_1 is treated with lithium triethylborodeuteride to give crude cyclohexanone ketal 4,4-D_2 which was hydrolysed[126] (as above) to yield cyclohexanone 4,4-D_2, b.p. 50-52°C/20 mm Hg ($D_2 = 99\%$).

^{1}H n.m.r. δ, 2.3, 4H, t; 1.8, 4H, t.

2-Methylcyclohexanone 3,3,5,5-D_4.

The standard procedure[127] of cyclohexanone 3,3,5,5-D_4 (0.35 g, 34 mmol.) and cyclohexylamine (0.36 g, 3.6 mmol.) in benzene (25 ml) gave the imine in 85% yield. The imine (0.50 g) in anhydrous tetrahydrofuran (10 ml) was added (under nitrogen) to lithium diisopropylamine (2.7 mmol.) [from n-butyllithium (1.6mol.dm^{-3}, 1.7 ml) and diisopropylamine (0.30 g, 3.0 mmol.) in anhydrous tetrahydrofuran (5 ml)] at 0°C. The mixture was allowed to stand for 5 minutes at 0°C, then methyl iodide (0.38 g, 2.7 mmol.) in anhydrous tetrahydrofuran (2 ml) was added, and the solution allowed to stir at 0°C for 45 minutes. Aqueous ammonium chloride (saturated, 10 ml) was added, the organic layer separated, the aqueous layer was extracted with diethyl ether (2×7 ml), and the combined organic phase washed with aqueous sodium bisulphite (saturated, 10 ml), aqueous sodium chloride (2×10 ml), and dried (anhydrous sodium sulphate). Removal of the solvent gave 2-methylcyclohexanone 3,3,5,5-D_4 b.p. 73-74°C, 20 mm Hg [0.2 g (59%)/$D_4 = 98\%$].

^{1}H n.m.r. δ, 1.0, 3H, d, J=11 Hz; 1.7, 2H, s, 2.35, 3H, m.

3-Methylcyclohexanone 3,3,5-D_3.

1,4-Cyclohexanedione mono-ethylene ketal (1.3 g, 8.1 mmol.) was converted into the cyclohexyl imine by a standard procedure[127] (yield: 1.5 g, 78%). Alkylation with methyl iodide (as for 2-methylcyclohexanone 3,3,5,5-D_4 above) gave 2-methyl-1,4-cyclohexanedione mono-ethylene ketal (0.61 g, 57%), which was deuterated with deuterium oxide/sodium deuteroxide (above) to yield 2-methyl-1,4-cyclohexanedione mono-ethylene ketal 2,2,6-D_3 ($D_3 = 98\%$). Reduction to the

alcohol (85% yield), conversion to the tosylate (65% yield) followed by reduction (83% yield) and removal of the protecting group (81% yield) [as outlined for cyclohexanone 3,3,5,5-D_4 (above)] gave 3-methylcyclohexanone 3,3,5-D_3, b.p. 76-78°C/18 mm Hg, [0.07 g, D_3 = 98%].

^{1}H n.m.r. δ, 1.0, 3H, b, s; 1.7, 2H, s; 2.4, 4H, s.

4-Methylcyclohexanone 3,3,5,5-D_4.

The tosylate 4-hydroxycyclohexanone ethylene ketal 3,3,5,5-D_4 (see cyclohexanone 3,3,5,5-D_4 above) was converted[128] into 4-iodocyclohexanone ethylene ketal 3,3,5,5-D_4 (78% yield).

To a suspension of copper cyanide (0.20 g, 2.2 mmol.) in tetrahydrofuran (10 ml) with methyl lithium (0.5mol.dm^{-3}, 8.9 ml) at 0°C under nitrogen, was added 4-iodocyclohexanone ethylene ketal 3,3,5,5-D_4 (0.20 g) in tetrahydrofuran (4 ml) and the mixture was stirred at 0°C for 6 hours. The temperature was increased to 5°C, whereupon aqueous ammonium chloride (saturated, 5 ml) and diethyl ether (15 ml) were added. The separated organic layer was washed with aqueous sodium bisulphite (2 N, 10 ml), aqueous sodium chloride (saturated, 10 ml), water (10 ml), then dried (anhydrous sodium sulphate). Removal of the solvent followed by vacuum distillation gave 4-methylcyclohexanone 3,3,5,5-D_4, b.p. 75-78°C/15 mm Hg, [0.065 g (73%), D_4 = 98%].

^{1}H n.m.r. δ, 1.0, 3H, d, J=11 Hz; 1.7, 1H, m; 2.4, 4H, s.

3-Methylcyclohexanone 4,4-D_2.

1,4-Cyclohexanedione mono-ethylene ketal was converted to 2-methyl-1,4-cyclohexanedione mono-ethylene ketal by the sequence outlined above for 3-methylcyclohexanone 3,5,5-D_3. This was transformed into 3-methylcyclohexanone 4,4-D_2 by the method outlined above for cyclohexanone 4,4-D_2 (D_2 = 99%).

^{1}H n.m.r. δ, 1.0, 3H, d, J=11 Hz; 1.7, 3H, m; 2.4, 4H, m.

2-Propylcyclohexanone 3,3,5,5-D_4 was made by the same procedure used for 2-methylcyclohexanone 3,3,5,5-D_4. 3-Ethyl- and 3-propylcyclohexanone 3,5,5-D_3 were made by the same procedure used for 3-methylcyclohexanone 3,5,5-D_3. 4-Ethylcyclohexanone 3,3,5,5-D_4 was made by the procedure used for 4-methylcyclo-

hexanone 3,3,5,5-D_4. 2-(Ethyl-1,1-D_2) cyclohexanone was made from ethyl iodide-1,1-D_2 by a standard procedure[112].

9.6 Syntheses of the Aromatic Alcohols.

Benzyl alcohol, 1-phenylethan-1-ol, 2-phenylethan-1-ol, 3-phenylpropan-1-ol, 4-phenylbutan-1-ol and 5-phenylpentan-1-ol were commercial samples.

Benzyl alcohol-1-D_1.

Benzaldehyde (0.20 g, 1.9 mmol.) in anhydrous diethyl ether (5 ml) was added under nitrogen to a suspension of lithium aluminium deuteride (0.10 g, 2.6 mmol.) in anhydrous diethyl ether (7 ml) and the mixture was heated under reflux for 4 hours. After cooling to 20°C, water (0.1 ml), aqueous sodium hydroxide (10%, 0.1 ml) and water (0.3 ml) were added successively. The organic layer was dried (anhydrous sodium sulphate), and distillation gave benzyl alcohol-1-D_1. b.p. 205-206°C/760 mm Hg, [0.095 g (48%), D_1 = 99%].

Benzyl alcohol-1,1-D_2.

Methyl benzoate (0.20 g, 1.9 mmol.) in anhydrous diethyl ether (5 ml) was added under nitrogen to a suspension of lithium aluminium deuteride (0.06 g, 1.6 mmol.) in anhydrous diethyl ether (5 ml), and the mixture was heated under reflux for 24 hours. Work up [as for benzyl alcohol-1-D_1 (above)] gave benzyl alcohol-D_2, b.p. 205-206°C/760 mm Hg, [0.15 g (95%), D_2 = 99%].

(Phenyl-D_5)-methanol.

(Phenyl-D_5)-methanol was made from (phenyl-D_5)magnesium bromide and para-formaldehyde by a reported method[129]. Yield 44% (D_5 = 99%).

(Phenyl-2,4,6-D_3)-methanol-1,1-D_2.

Benzoic acid 2,4,6-D_3 (0.1 g, 0.8 mmol.) [formed from bromobenzene-2,4,6-D_3[113,130] by the Grignard reaction with CO_2] in anhydrous tetrahydrofuran (2 ml) was added to a suspension of lithium aluminium deuteride (0.03 g, 0.8 mmol.) in anhydrous tetrahydrofuran (2 ml), and the mixture was heated under reflux for 24 hours.

139

Work up [as for benzyl alcohol-1-D_1, above)] gave (phenyl-2,4,6-D_3)-methanol-1,1-D_2, [0.08 g (93%), D_5 = 98%].

2-Phenylethan-1-ol-2,2-D_2.

Phenylacetic acid (1.00 g, 7.35 mmol.), deuterium oxide (5 ml) and sodium deuteroxide (0.30 g, 7.3 mmol.) were heated at 120°C in a sealed tube for 24 hours. After cooling to 20°C the solution was acidified (concentrated hydrochloric acid) and extracted with diethyl ether, dried (anhydrous sodium sulphate), the solvent removed and the exchange procedure repeated for the second time to give phenyl acetic acid-2,2-D_2 (D_2 = 98%). Phenylacetic acid-2,2-D_2 (0.9 g) in anhydrous tetrahydrofuran (10 ml) was added to a suspension of lithium aluminium hydride (0.30 g) in tetrahydrofuran (12 ml) and the mixture was heated under reflux for 16 hours. Work up (as for benzyl alcohol-1-D_1 gave 2-phenylethan-1-ol-2,2-D_2, b.p. 215-216°C/760 mm Hg; [0.55 g (62%), D_2 = 99%].

2-Phenylethan-1-ol-1,1-D_2.

Reduction of phenylacetic acid with lithium aluminium deuteride (as above) gave 2-phenylethan-1-ol-1,1-D_2. Yield 70% (D_2 = 99%).

3-(Phenyl-D_5)-propan-1-ol.

To a solution of phenyl-D_5-magnesium bromide [from bromobenzene-D_5 (0.10 g, 0.6 mmol. and magnesium (0.02g, 0.8mmol.)] in anhydrous diethyl ether (8 ml), under nitrogen, was added tetraethylene oxide[133] (0.07 g, 1.2 mmol.) in anhydrous diethyl ether (1 ml), and the solution was heated under reflux for 13 hours. Aqueous ammonium chloride (saturated, 10 ml) was added, the organic layer was separated, dried (anhydrous sodium sulphate), and the solvent removed. Vacuum distillation gave 3-phenyl-D_5)-propan-1-ol, b.p. 132-134°C/20 mm Hg, [0.09 g (52%), D_5 = 99%].

3-Phenylpropan-1-ol-3,3-D_2.

Benzyl alcohol-1,1-D_2 was converted into benzyl bromide-1,1-D_2 by a reported procedure[131] in 80% yield. The Grignard reagent from benzyl bromide-1,1-D_2 was allowed to react with ethylene oxide[132], giving 3-phenylpropan-1-ol-3,3-D_2 in 36% yield (D_2 = 99%).

3-Phenylpropan-1-ol-2,2-D_2.

2-Phenylethan-1-ol-1,1-D_2 was converted to the bromide in 53% yield by a standard procedure[131]. The Grignard reagent from 2-phenylethyl bromide-1,1-D_2 was treated with dimethyl carbonate to yield 3-phenylpropan-1-ol-2,2-D_2 in 30% overall yield ($D_2 = 99\%$).

3-Phenylpropan-1-ol-1,1-D_2.

A solution of methyl-2-phenylpropan-1-oate (0.10 g, 0.61 mmol.) in anhydrous diethyl ether (5 ml), was added under nitrogen, at 20°C, to a stirred suspension of lithium aluminium deuteride (0.05 g, 1.5 mmol.) in anhydrous diethyl ether (2 ml). The mixture was heated under reflux, then work up (as for benzyl alcohol-1-D_1 above), gave 3-phenylpropan-1-ol-1,1-D_2, [0.08 g (83%), $D_2 = 99\%$].

4-Phenylbutan-1-ol-4,4-D_2.

This compound was produced in a similar manner to 3-phenylpropan-1-ol-3,3-D_2 except that trimethylene oxide[133,134,135] was used instead of ethylene oxide. Yield 90% ($D_2 = 99\%$).

4-Phenylbutan-1-ol-1,1-D_2.

This compound was prepared by reduction of methyl 4-phenylbutanoate with lithium aluminium deuteride by the same method as was used for the formation of benzyl alcohol-1,1-D_2 (see above). Yield 90% ($D_2 = 99\%$).

5-Phenylpentanol-5,5-D_2.

This compound was made by the same procedure as was used for the preparation of 4-phenylbutanol-4,4-D_2, except that 2-phenylethylbromide-1,1-D_2 was used instead of benzyl bromide-1,1-D_2, Yield 30% ($D_2 = 98\%$).

9.7   The Syntheses of the Labelled and Unlabelled Amides.

The following compounds were either commercially available or prepared by standard procedures[114]; formamide, N-methylformamide, N,N-dimethylformamide, acetamide, N-methylacetamide, N,N-dimethylacetamide, N-ethylacetamide, N,N-di-

ethylacetamide, N-propylacetamide, N,N-propylacetamide, propionamide, butyramide, benzamide and acetanilide.

The following compounds were prepared by the procedure outlined below for the formation of N-ethylacetamide-D_1; formamide-D_2, N-methylformamide-D_1, propionamide-D_2, benzamide-D_2, N-ethylacetamide-D_1; D_1 (or D_2) incorporation $\geq 90\%$.

N-Ethylacetamide-D_1.

N-Ethylacetamide (0.1 g, 1.2 mmol.) and D_2O (0.5 g, 25 mmol.) were heated at 100 °C in a sealed tube for 12 hours. The amide was extracted from the aqueous layer with diethyl ether (3×1 ml). The organic layer was then dried with 4 Å molecular sieve powder and the solvent removed to yield N-ethylacetamide in quantitative yield [b.p. 102-104°C/15 mm Hg, $D_1 = 90\%$].

N-Isopropylacetamide, N-butylacetamide, N-sec-butylacetamide, N-t-butylacetamide, acetamide-D_3, N-methyl(acetamide-D_3), N,N-dimethyl(acetamide-D_3), N-ethyl-(acetamide-D_3), N,N-ethyl(acetamide-D_3) and acetanilide-D_3 were prepared by the general method[114] described below for the preparation of N,N-diisopropylacetamide.

N,N-diisopropylacetamide.

Acetyl chloride (0.3 g, 3.8 mmol.) in diethyl ether (1 ml) was added to N,N-diisopropylamine (0.76 g, 7.5 mmol.) in diethylether (3ml). The solid was removed by filtration. Removal of the solvent under reduced pressure gave N,N-diisopropylacetamide [0.33 g (100%), $D_1 = 99\%$].

The following compounds were also prepared by this general method except the appropriate labelled amine was added (see the next section for the synthesis of the labelled amines). (N-methyl-D_3)-acetamide, (N-ethyl-2,2-D_2)-acetamide, (N-ethyl-1,1,1-D_3)-acetamide, N-ethyl (N-ethyl-2,2-D_2)-acetamide, N-ethyl (N-ethyl-1,1,1-D_3)-acetamide, N-ethyl (N-ethyl-1,1,1,2,2-D_5)-acetamide, N-di-(ethyl-2,2-D_2)-acetamide, N-di-(ethyl-1,1,1-D_3)-acetamide, acetanilide-D_3 and acetanilide-D_5.

Dimethylformamide D_1.

Sodium cyanide (1.0 g, 20 mmol.) in deuterium oxide (1.5 ml) was added slowly to a solution of ferric sulphate (0.02 g, 0.13 mmol) in sulphuric acid D_2 (1 ml) and deuterium oxide (0.5 ml). The solution was then heated to 90°C for 1 hour and the deuterocyanide was dried by distillation through a column of anhydrous calcium chloride[136]. The labelled dimethylformamide was then prepared by the method of De Benneville[137], b.p. 77-79°C/40 mm Hg ($D_1 = 90\%$).

Bisacetamides and related compounds.

The unlabelled compounds were available from a previous study[138]. The labelled derivatives $C_6D_5CONHCOCH_3$ and $C_6H_5CONHCOCD_3$ were prepared from benzoylchloride-D_5[109] and CD_3COCl by standard procedures[139,140] ($D_3 = 99\%$, $D_5 = 99\%$).

9.8 Syntheses of the Amine derivatives.

The following compounds were commercially available: methylamine, ethylamine, n-propylamine, iso-propylamine, n-butylamine, dimethylamine, di-n-propylamine, di-iso-propylamine, aniline, aniline-D_5, N-methylaniline, N-ethylaniline, N-phenylaniline, piperidine, 2,6-dimethylpiperidine, piperazine, 2,5-dimethylpiperazine.

The following compounds were prepared by exchange with deuterium oxide in a sealed tube at 100°C for 14 hours; n-PrND$_2$, iso-PrND$_2$, n-BuND$_2$, Et$_2$ND, piperazine-1,4-D$_2$, 2,5-dimethylpiperazine-1,4-D$_2$ (D_1 or $D_2 > 95\%$).

(Ethyl-1,1-D$_2$) amine.

A mixture of ethyl iodide-1,1-D$_2$ (1.0 g, 6.3 mmol.), potassium phthalimide[141,142] (1.35 g, 7.3 mmol.) and dimethylformamide (15 ml) were heated at 90°C for 3 hours. Dichloromethane (25 ml) was added and the solution was washed with aqueous sodium hydroxide (10 %, 10 ml), aqueous sodium bisulphite (saturated, 10 ml), water (3×10 ml) and aqueous sodium chloride (saturated, 10 ml). The organic extract was dried (anhydrous sodium bicarbonate) the solvent was removed

under reduced pressure and the residue (0.72 g, 4.1 mmol.) was heated at approximately 300°C with potassium hydroxide (0.5 g, 8.9 mmol.) whereupon the labelled ethylamine distilled directly from the reaction mixture. [B.p. 17°C/760 mm Hg, 0.11 g (57%) $D_1 = 99\%$].

(Ethyl-2,2,2-D_3)-amine, (ethyl-1,1,2,2,2-D_5)-amine and (iso-propyl-2,2,2,2',2',2'-D_6) amine were prepared from the appropriately labelled ethyl- or propyl iodide by the same procedure, respective yields 48%, 52% and 32%.

Di-(ethyl-1,1-D_2) amine.

This compound was prepared by adding ethyl iodide-1,1-D_2 (0.4 g, 2.5 mmol.) to ethylamine-1,1-D_2 (0.11g, 2.3 mmol.) at 0°C. After stirring for 30 minutes, gave a quantitative yield of di-(ethyl-1,1-D_2) amine hydrochloride was obtained. The salt was then hydrolyzed by heating with potassium hydroxide at 300°C for 30 minutes, the di-(ethyl-1,1-D_2) amine distilled directly from the reaction mixture, b.p. 56°C/760 mm Hg [0.15 g (78%) $D_4 = 99\%$].

Ethyl (ethyl-1,1-D_2) amine, ethyl (ethyl-2,2,2-D_3) amine and ethyl (ethyl-1,1,2,2,2-D_5) amine were prepared similarly in respective yields 68%, 70% and 65%.

N-Ethylaniline derivatives.

N-Ethyl(aniline-D_5) and N-(ethyl-2,2,2-D_3)-aniline were prepared by a standard procedure[143] in respective yields 77% and 63%, using acetic acid/sodium borohydride/aniline-2,3,4,5,6-D_5 and acetic acid-D_4/sodium borohydride/aniline ($D_5 = 98\%$, $D_3 = 98\%$).

References.

1. Bowers, M. T. (ed.), *"Gas Phase Ion Chemistry"*, Vols. 1-3, Academic Press, New York, 1979 (Vols. 1 and 2), 1984 (Vol. 3).

2. Sweeley, C. C., Elliott, W. M., Fries, I., and Ryhage, R., *Anal. Chem.*, 1966, 38, 1549; Burlingame, A. L., Baillie, T. A., Derrick, P. J., *Anal. Chem.*, 1986, 58, 165R.

3. Aston, F. W., *Phil. Mag.*, 1919, 38, 707.

4. Dempster, A. J., *Phys. Rev.*, 1918, 11, 316

5. Farmer, J. B., 1963, in *"Mass Spectrometry"* (Ed. C. A. McDowell), p. 7, McGraw–Hill, New York.

6. Nier, A. O., *Rev. Sci. Instrum.*, 1947, 18, 398.

7. Rosenstock, H. M., Draxl, K., Steiner, B. W. and Herron, J. T., *J. Phys. Chem. Ref. Data 6,* Suppl. 1. p. 783.

8. Inghram, M. G. and Gomer, R., *J. Chem. Phys.*, 1954, 22, 1279; McReynolds, J. H. and Anbar, M., *Int. J. Mass Spectrom. Ion Proc.*, 1977, 24, 37.

9. Beynon, J. H., Cooks, R. G., Amy, J. W., Baitinger, W. E. and Ridley, T. Y., *Anal. Chem.*, 1973, 45, 1023A; Mc Lafferty, F. W., *Accts. Chem. Res.*, 1980, 13, 33.

10. VG ZAB 2HF Operating Manual, V. G. Analytical Ltd., Wythenshawe, Manchester, M239LE, England.

11. Johnson, E. G. and Nier, A. O., *Phys. Rev.,* 1953, <u>91</u>, 10; Hintenberger, H. and König, L. A., *Z. Naturforsch.,* 1957, <u>12a</u>, 773; Hintenberger, H. and König, L. A., *"Advances in Mass Spectrometry"* (Waldon, J., Ed.), Pergaman Press, 1959, New York, p. 16.

12. McLafferty, F. W., *"Tandem Mass Spectrometry",* John Wiley and Sons, 1983, New York.

13. Westheimer, F. H., *Chem. Rev.,* 1961, <u>61</u>, 265; Johnson, H. S., *Adv. Chem Phys.,* 1961, <u>3</u>, 131.

14. Rock, P. A. (Ed.), *"Isotopes and Chemical Principals",* American Chemical Society, 1975, Washington D. C.

15. More O'Ferrall, R. A., *"Proton Transfer Reactions"* (Ed. Caldin, E. and Gold, V.) Chapman Hall, 1975, London, p. 201.

16. Born, M. and Oppenheimer J. R., *Ann. Physik.,* 1927, <u>84</u>, 457.

17. Davidson, N. R., *"Statistical Mechanics",* McGraw–Hill, 1962, New York, p. 155.

18. Derrick, P. J., *Mass Spectrom. Revs.,* 1983, <u>2</u>, 285.

19. Allison, C. E., Stringer, M. B., Bowie, J. H. and Derrick, P. J., *J. Amer. Chem. Soc.,* in press.

20. Dillard, J. G., *Chem. Rev.,* 1973, <u>73</u>, 589.

21. Stafford, G. C., *Environ. Health Perspect.,* 1980, <u>36</u>, 85.

22. Harrison, A. G., *"Chemical Ionization Mass Spectrometry",* CRC Press Inc., 1983, Florida; Budzikiewicz, H., *Mass Spectrom. Revs.,* 1986, <u>5</u>, 345.

23. Barber, M., Bordoli, R. S., Elliott, G. J., Sedgwick, R. D. and Tyler, A. N., *Anal. Chem.*, 1982, 54, 645A.

24. Bowie, J. H. and Williams, B. D., In "Mass Spectrometry", In: "*Int. Rev. Sci. Phys. Chem. Ser. 2*"; Maccoll, A., Ed.; Butterworths: London, 1975, p. 89.

25. McAllister, T., *J. Chem. Soc. Chem. Commun.*, 1972, 245.

26. Bowie, J. H. and Ho, A. C., *Aust. J. Chem.*, 1973, 26, 2009.

27. Compton, R. N., Christophorou, L. G., Hurst, G. S. and Reinhardt, P. W., *J. Chem. Phys.*, 1966, 45, 4634.

28. Bowie, J. H. and Hart, S. G., *Int. J. Mass Spectrom. Ion Phys.*, 1974, 13, 319.

29. Bowie, J. H., *Aust. J. Chem.*, 1973, 26, 2719.

30. Harland, P. and Thynne, J. C. J., *J. Phys. Chem.*, 1970, 74, 52.

31. Ito, A., Matsumoto, K. and Takeuchi, T. *Org. Mass Spectrom.*, 1973, 7, 1279.

32. Bowie, J. H., Duus, F., Lawesson, S., -O., Larsson, F. C. V. and Madsen, J. Ø., *Aust. J. Chem.*, 1969, 22, 153.

33. Bowie, J. H. and White, P. Y., *Org. Mass Spectrom.*, 1972, 6, 75.

34. Brown, C. L. and Weber, W. P., *J. Amer. Chem. Soc.*, 1970, 92, 5775.

35. Bowie, J. H. Blumenthal, T. and Walsh, I., *Org. Mass Spectrom.*, 1971, 5, 777.

36. Bowie J. H., *Org. Mass Spectrom.*, 1974, 9, 304.

37. Bowie, J. H., *Org. Mass Spectrom.*, 1971, 5, 945.

38. Smit, A. L. C. and Field, F. H., *J. Amer. Chem. Soc.*, 1977, 99, 6471.

39. Bowers, M. T., "*Gas Phase Ion Chemistry*", Academic Press, 1979, Volume 2, p. 104.

40. Bowie, J. H., *Mass Spectrom. Revs.*, 1984, 3, 161.

41. Jennings, K. R., *"Mass Spectrometry Specialist Reports"*, Chem. Soc. London, 1979, 5, 203.

42. Winkler, F. J., and Stahl, D., *J. Amer. Chem. Soc.*, 1978, 100, 6779.

43. Lloyd, J.R., Agosta, W, C. and Field, F. H., *J. Org. Chem.*, 1980, 45, 3483.

44. Hunt, D. F., Shabanowitz, J. and Giordani, A. B., *Anal. Chem.*, 1980, 52, 386.

45. Hunt, D. F., Shabanowitz, J. and Giordani, A. B., *Environ. Health Perspect.*, 1980, 36, 33.

46. McClusky, G. A., Kondrat, R. W. and Cooks, R. G., *J. Amer. Chem. Soc.*, 1978, 100, 6045.

47. Grützmacher, H. F. and Grotemeyer, B., *Org. Mass Spectrom.*, 1984, 19, 135; Graul, S. T. and Squires, R. R., *Mass Spectrom. Rev.*, 1988, 7, 273.

48. Beloeil, J. C., Bertranne, M., Stahl, D. and Tabet, J. C., *J. Amer. Chem. Soc.*, 1983, 105, 1355.

49. Dreifuss, P. A., Brumley, W. C. and Sphon, J. A., *Anal. Chem.*, 1983, 55, 1036; Gower, J. I., Beaugrand, C. and Sallot, C., *Biomed. Mass Spectrom.*, 1981, 8, 36.

50. Burinsky, D. J. and Cooks, R. G., *J. Org. Chem.*, 1982, 47, 4864.

51. Crow, F. W., Bjorseth, A., Knapp, K. T. and Bennett, R., *Anal. Chem.*, 1981, 53, 619.

52. Garlard, W. A., and Miwa, B. J., *Environ. Health Perspect.*, 1980, 36, 89.

53. Miwa, B. J., Garland, W. A. and Blumenthal, P., *Anal. Chem.*, 1981, 53, 793.

54. Dougherty, R. C., Whitaker, M. J., Smith, L. M., Stalling, D. L. and Kuehl, D. W., *Environ. Health Perspect.*, 1980, 36 103.

55. Brumley, W. C., Neshiem, S., Trucksess, M. W., Trucksess, E. W., Dreifuss, P. A., Roach, J. A. G., Andrzejewski, D., Eppley, R. M., Pohland, A. E., Thorpe, C. W. and Sphon, J. A., *Anal. Chem.*, 1981, <u>53</u>, 2003.

56. Glover, W., Earley, J., Delaney, M. and Dixon, R., *J. Pharm. Sci.*, 1980, <u>69</u>, 601.

57. Surman, D. J., and Vickerman, J. C., *J. Chem. Soc. Chem. Commun.*, 1981, 324.

58. Barber, M., Bordoli, R. S., Sedgwick, R. D., and Tyler, A. N., *J. Chem. Soc. Chem. Commun.*, 1981, 325; Barber, M., Bordoli, R. S., Sedgwick, R. D., and Tyler, A. N., *Nature*, 1981, <u>293</u>, 270.

59. Biemann, K. and Martin, S., *Mass Spectrom. Rev.*, 1987, <u>6</u>, 1; Egge, H. and Peter-Katalić, M., *Mass Spectrom. Rev.*, 1987, <u>6</u>, 331.

60. Bruce, M. I. and Liddell, M. J., *App. Organomet. Chem.*, 1987, 191.

61. Rinehart, K. L., Gaudioso, L. A., Moore, M, L., Pandey, R. C., Cook, J. C., Barber, M., Sedgwick, R. D., Bordoli, R. S., Tyler, A. N. and Green, B. N., *J. Amer. Chem. Soc.*, 1981, <u>103</u>, 6517.

62. Bowie, J. H. and Benbow, J. A., *Org. Mass Spectrom.*, 1978, <u>13</u>, 103.

63. Bowie, J. H. and Blumenthal, T., *J. Amer. Chem. Soc.*, 1975, <u>97</u>, 2959.

64. Young, A. B. and Harrison, A. G., *Org. Mass Spectrom.*, 1987, <u>22</u>, 622; Hayes, R. N. and Bowie, J. H., *Org. Mass Spectrom.*, 1986, <u>21</u>, 425.

65. Hayes, R. N. and Bowie, J. H., *J. Chem. Soc. Perkin Trans. II*, 1986, 1827.

66. Bowie, J. H., White, P. Y., Wilson, F. C. V., Larsson, S. -O., Lawesson, J. Ø., Madsen, C., Nolde, C. and Schroll, G., *Org. Mass Spectrom.*, 1977, <u>12</u>, 191.

67. Szulejko, J. E., Bowie, J. H., Howe, I. and Beynon, J. H., *Int. J. Mass Spectrom. Ion Phys.*, 1980, <u>34</u>, 99

68. Stringer, M. B., Underwood, D. J., Bowie, J. H., Holmes, J. L., Mommers, A. A. and Szulejko, J. E., *Can. J. Chem.*, 1986, <u>63</u>, 764.

69. Hunt, D. F., Giordani, A. B., Shabanowitz, J. and Rhodes, G., *J. Org. Chem.*, 1982, <u>47</u>, 738.

70. Stringer, M. B., Bowie, J. H. and Holmes, J. L., *J. Amer. Chem. Soc.*, 1986, <u>108</u>, 3888; Currie, G. J., Stringer, M. B., Bowie, J. H. and Holmes, J. L., *Aust. J. Chem.*, 1987, <u>40</u>, 1365.

71. Belasco, J. G., Albery, W. J. and Knowles, J. R., *J. Amer. Chem. Soc.*, 1983, <u>105</u>, 2475.

72. Nobes, R. H., Poppinger, D., Li, W. -K., Radom, L. (in Buncel, E. and Durst, T., Eds.), *"Comprehensive Carbanion Chemistry"*, Part C, Elsevier, Amsterdam, 1987.

73. Adams, G. W., Downard, K. M., Sheldon, J. C. and Bowie, J. H., unpublished observations.

74. Hayes, R. N., Sheldon, J. C., Bowie, J. H. and Lewis, D. E., *J. Chem. Soc. Chem. Commun.*, 1984, 1431.

75. Hayes, R. N., Sheldon, J. C., Bowie, J. H. and Lewis, D. E., *Aust. J. Chem.*, 1985, <u>38</u>, 1197.

76. Sheldon, J. C., Bowie, J. H. and Lewis D. E., *Nouveau J. Chim.,* in press.

77. Mercer, R. S. and Harrison, A. G., *Org. Mass Spectrom.,* 1987, <u>22</u>, 710.

78. Eichinger, P. C. H. and Bowie, J. H., *J. Chem. Soc., Perkin Trans. II*, 1988, 497.

79. Currie, G. J., Bowie, J. H., Massy-Westropp, R. A. and Adams, G. W., *J. Chem. Soc., Perkin Trans. II*, 1988, 403.

80. Bowie, J. H. and Nussey, B., *J. Chem. Soc. Chem. Commun.*, 1970, 17.

81. Bowie, J. H. and Nussey, B., *Org. Mass Spectrom.*, 1970, 3, 933.

82. Sheldon, J. C., personal communication.

83. Binkley, J. S., Frisch, M. J., DeFrees, D. J., Raghavachari, K., Whitesides, R. A., Schlegel, H. B., Fluder, E. M. and Pople, J. A., *"Gaussian 82"*, Carnegie Mellon University.

84. Sheldon, J. C., Bowie, J. H., DePuy, C. H. and Damrauer, R., *J. Amer. Chem. Soc.*, 1986, 108, 6794.

85. Schleyer, P. v. R. and Kos, A. J., *Tetrahedron.*, 1983, 39, 1141.

86. Levy, A. A., Rains, H. C. and Smiles, S., *J. Chem. Soc.*, 1931, 3264; Evans, W. J. and Smiles, S., *J. Chem. Soc.*, 1935, 181; Bunnett, J. F. and Zahler, R. E., *Chem. Rev.*, 1951, 49, 273.

87. Hubin-Franskin, M. J. and Collin, J. E., *Bull. Chim. Soc. de Liege*, 1971, 40, 502.

88. Bartmess, J. M., *"The 1987 Gas Phase Acidity Scale"*, Department of Chemistry, University of Tennessee, July, 1987.

89. DePuy, C. H., Grabowski, J. J., Bierbaum, V. M., Ingemann, S. and Nibbering, N. M. M., *J. Amer. Chem. Soc.*, 1985, 107, 1093.

90. DePuy, C. H., Bierbaum, V. M., Damrauer, R. and Soderquist, J. A., *J. Amer. Chem. Soc.*, 1985, 107, 3385.

91. Cumming, J. B. and Kebarle, P., *Can. J. Chem.*, 1978, 56, 1.

92. Dewar, M. J. S. and Rzepa, H. S., *J. Amer. Chem. Soc.*, 1978, 100, 784; Li, W. -K., Nobes, R. H. and Radom, L., *J. Mol. Struct. Theochem.*, in press.

93. Eichinger, P. C. H., Bowie, J. H. and Hayes, R. N., unpublished observations.

94. Bowie, J. H. and Stringer, M. B., *Org. Mass Spectrom.*, 1985, 20, 138.

95. Stringer, M. B., Bowie, J. H., Eichinger, P. C. H. and Currie, G. J., *J. Chem. Soc. Perkin Trans. II*, 1987, 385.

96. Eichinger, P. C. H., Bowie, J. H. and Blumenthal, T., *J. Org. Chem.*, 1986, 51, 5078.

97. Eichinger, P. C. H. and Bowie, J. H., *J. Chem. Soc. Perkin Trans II*, 1987, 1499.

98. Rozeboom, M. D., Kiplinger, J. P. and Bartmess, J. E., *J. Amer. Chem. Soc.*, 1984, 106, 1025.

99. Eichinger, P. C. H., Bowie, J. H. and Hayes, R. N., *J. Org. Chem.*, 1987, 52, 5224.

100. Eichinger, P. C. H. and Bowie, J. H., personal communication.

101. Wittig, G. and Löhmann, L., *Ann.*, 1942, 550, 260.

102. Wittig, G., *Experientia*, 1958, 14, 389.

103. Hoffmann, R. W., *Angew. Chem. Int. Ed. Eng.*, 1979, 18, 563.

104. Terlouw, J. K., Burgers, P. C. and Hommes, H., *Org. Mass Spectrom.*, 1979, 14, 387.

105. Burgers, P. C., Holmes, J. L., Mommers, A .A. and Szulejko, J., *J. Amer. Chem. Soc.*, 1984, 106, 521.

106. Todd, P. J. and McLafferty, F. W., *Int. J. Mass Spectrom. Ion Phys.*, 1981, 38, 371.

107. Cooks, R. G., Beynon, J. H., Caprioli, R. M. and Lester, G. R., *"Metastable Ions"*, Elsevier, Amsterdam, 1973, pp. 57-70.

108. Perrin, D. D., Armarego, W. L. F. and Perrin, D. R., *"Purification of Laboratory Chemicals"*, 2nd Edition, Pergamon Press, Oxford, 1980.

109. Erlenmeyer, H., Lobeck, H. and Epprecht, A., *Helv. Chim. Acta.*, 1936, 19, 793.

110. Erlenmeyer, H. and Lobeck, H., *Helv. Chim. Acta.,* 1937, 20, 142.

111. Gaylord, N. G., *"Reductions with complex metal hydrides"*, Interscience, 1956, New York, p. 322.

112. Vogel, A., I., *"Practical Organic Chemistry"*, 3rd Ed., Longmans, Green and Co., 1948, London, p. 284.

113. Best, A. P. and Wilson, C. L., *J. Chem. Soc.,* 1946, 239.

114. Sonntag, N. O. V., *Chem. Rev.,* 1953, 52, 237.

115. Petragnani, N. and Yonashiro, M., *Synthesis,* 1980, 710.

116. Noyes, W. A. and Kyriakides, L. P., *J. Amer. Chem. Soc.,* 1910, 32, 1057.

117. Čefelin, P., Lochmann, L. and Stehliček, J., *Coll. Czech. Chem. Commun.,* 1973, 38, 1339.

118. Blatt, A. H. (Ed.), *"Organic Synthesis Collective Volume 2"*, John Wiley and Sons, 1943, New York, p. 116.

119. Best, S. R. and Thorpe, J. F., *J. Chem. Soc.,* 1909, 95, 685.

120. Schaefer, J. P. and Bloomfield, J. J. (Eds.), *"Organic Reactions"*, John Wiley and Sons, 1967, New York, 15, p. 1.

121. Stork, G. and Dowd, S. R., *J. Amer. Chem. Soc.,* 1963, 85, 2178; Harvey, W. E. and Tarbell, D. S., *J. Org. Chem.,* 1967, 32, 1679.

122. Green, M. M., Cook, R. J., Schwab, J. M. and Roy, R. B., *J. Amer. Chem. Soc.,* 1970, 92, 3076.

123. Owen, L. N. and Robins, P. A., *J. Chem. Soc.,* 1949, 320.

124. Brown, H. C., Krishnamurthy, C., and Hubbard, L., *J. Amer. Chem. Soc.,* 1978, 100, 3343.

125. Brown, H. C., Kim, S. C. and Krishnamurthy, C., *J. Org. Chem.*, 1980, 45, 1.

126. Shirley, N. and Hamon, D. P. G., personal communication.

127. Layer, R. W., *Chem. Rev.,* 1963, 63, 489.

128. Kosower, E. M., *J. Amer. Chem. Soc.,* 1955, 77, 3883; Stephenson, B, Sollié, G. and Mosher, H. S., *J. Amer. Chem. Soc.,* 1972, 94, 4184.

129. Gilman, H. (Ed). *"Organic Synthesis Collective Volume 1"*, Wiley and Sons, New York, Chapman and Sons, 1932, London., p. 182.

130. Vogel, A. I., *"Textbook of Practical Organic Chemistry"*, 4th Ed, 1978, p. 482.

131. Fieser, L. F. and Fieser, M., *"Reagents for Organic Synthesis"*, Vol. 1, John Wiley and Sons, 1967, New York.

132. Dreger, E. E., *"Organic Synthesis Collective Volume 1"*, John Wiley and Sons, 1932, London., p. 306.

133. Gaylord, N. G. and Becker, E. I., *Chem. Rev.,* 1951, 49, 413.

134. Horning E. C. (Ed), *"Organic Synthesis Collective Volume 3"*, John Wiley and Sons, 1955, New York, p. 835.

135. Searles, S., *J. Amer. Chem. Soc.,* 1951, 73, 124.

136. Brauer, G. (Ed), *"Handbook of Preparative Inorganic Chemistry"*, Academic Press, New York, 1965, 2nd edition, p. 658.

137. DeBenneville, P. L., Strong, J. S. and Elkind, V. T., *J. Org. Chem*, 1956, 21, 772.

138. Bowie, J. H., Cooks, R. G., Lawesson, S. –O. and Nolde, C., *Tetrahedron*, 1968, 24, 1051.

139. Titherley, A. W., *J. Chem. Soc.,* 1904, 85, 1673.

140. Thompson, Q. E., *J. Amer. Chem. Soc.,* 1951, 73, 5841.

141. Gilman, H. (Ed.), *"Organic Synthesis, Collective Volume 1"*, John Wiley and Sons, 1938, New York, p. 114.

142. Gibson, M. S. and Bradshore, R. W., *Angew. Chem. Int. Ed. Eng.*, 1968, 7, 919.

143. Gribble, G. W., Pierre, D. L., Skotnicki, J., Dietz, S. E., Eaton, J. T. and Johnson, J. L., *J. Amer. Chem. Soc.*, 1974, 96, 7812.

Publications.

Raftery, M. J. and Bowie, J. H., *Aust. J. Chem.*, 1987, <u>40</u>, 711;

Raftery, M. J. and Bowie, J. H., *Int. J. Mass Spectrom. and Ion Proc*, 1987, <u>79</u>, 267;

Raftery, M. J., Bowie, J. H. and Sheldon, J. C., J. *Chem. Soc. Perkin Trans. II*, 1988, 563;

Raftery, M. J. and Bowie, J. H., *Int. J. Mass Spectrom. and Ion Proc*, in press;

Raftery, M. J. and Bowie, J. H., *Org. Mass Spectrom.*, in press.

Raftery, M. J. and Bowie, J. H., *Aust. J. Chem.*, in press.

Raftery, M. J., & Bowie, J. H. (1987). Collision-induced dissociations of enolate negative ions. Deprotonated cyclohexanones. *International Journal of Mass Spectrometry and Ion Processes, 79*(3), 267-285.

Raftery, M. J., Bowie, J. H., & Sheldon, J. C. (1988). Collision-induced dissociations of aryl-substituted alkoxide ions. Losses of dihydrogen and rearrangement processes. *Journal of the Chemical Society, Perkin Transactions* 2(4), 563-569.